Economic Model Predictive Control for the Demand Side Management of Residential Microgrids

Christopher Jan Michalak

Master of Science Thesis

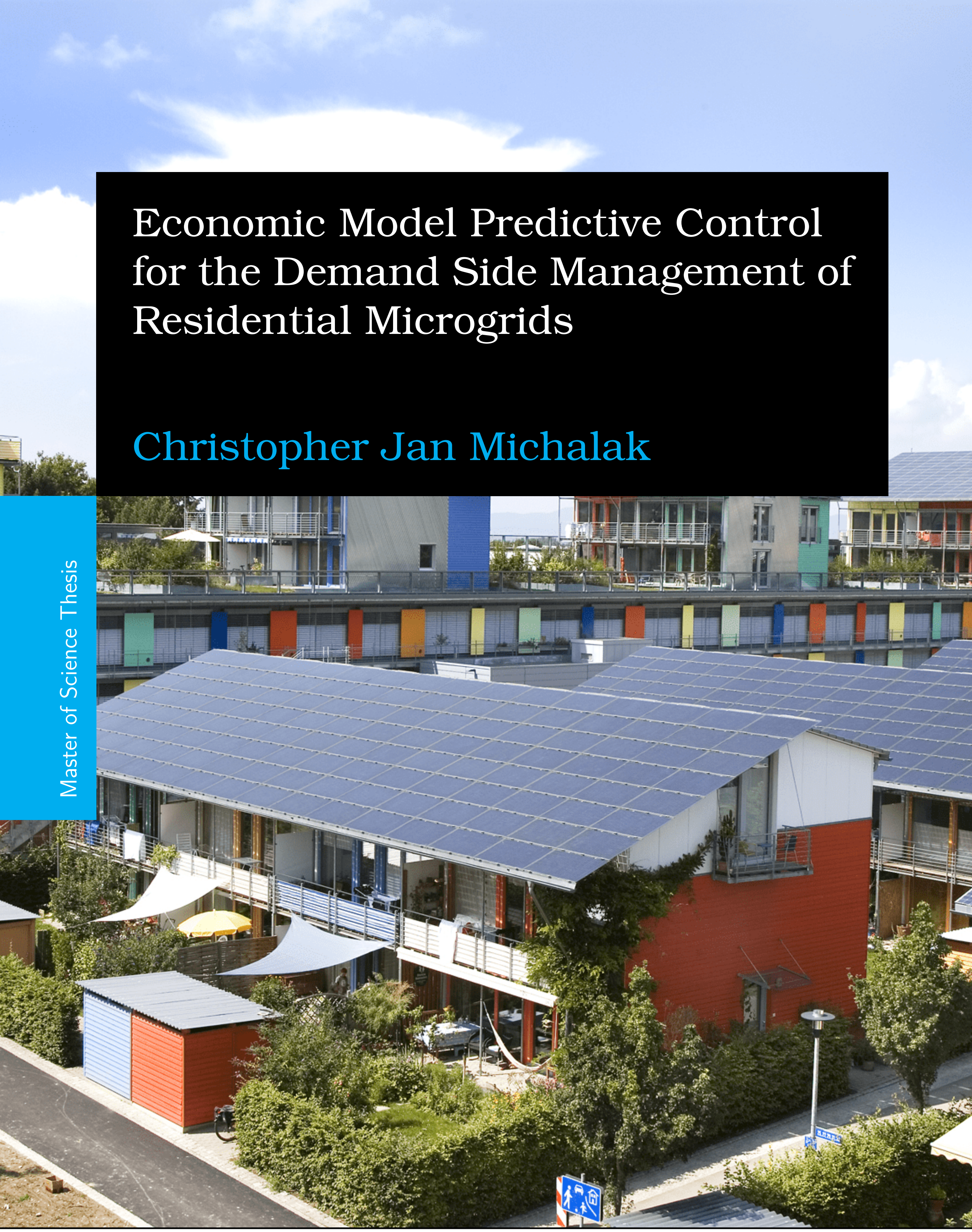

Image credit: Andrew Glaser at English Wikipedia

TU Delft Delft University of Technology

Delft Center for Systems and Control

Economic Model Predictive Control for the Demand Side Management of Residential Microgrids

Master of Science Thesis

For the degree of Master of Science in Systems and Control at Delft University of Technology

Christopher Jan Michalak

16th July 2019

Faculty of Mechanical, Maritime and Materials Engineering (3mE) · Delft University of Technology

The work in this thesis was supported by Solar Africa® (https://www.solarafrica.com).

Delft University of Technology
Department of
Delft Center for Systems and Control (dcsc)

The undersigned hereby certify that they have read and recommend to the Faculty of Mechanical, Maritime and Materials Engineering (3mE) for acceptance a thesis entitled

Economic Model Predictive Control
for the Demand Side Management of Residential Microgrids

by

Christopher Jan Michalak

in partial fulfillment of the requirements for the degree of

Master of Science in Systems and Control

Date: 16th July 2019

Supervisor(s): ____________________

Dr.ir. Tamás Keviczky

Reader(s): ____________________

Dr.ir. Sergio Grammatico

____

Dr.ir. Anahita Jamshidnejad

____

Ir. Tomas Pippia

Abstract

Traditional electric power systems with large centralized base load power plants have a limited ability to react rapidly to the high supply variability associated with the increasing deployment of variable and intermittent renewable energy sources (RESs) [1, 2]. Furthermore, with current power distribution networks primarily designed for unidirectional power flow, the introduction of reverse power flows by renewable feed-in strategies has been shown to negatively impact grid stability, security and system protection [3, 4]. For residential grid-connected microgrids (MGs) wishing to increase their renewable generation, these issues along with economic considerations often highlight that optimal operation can only be achieved through an increased self-consumption of locally generated renewable energy [5]. Recently, researchers have highlighted that these issues can be addressed by the application of demand side management (DSM). Broadly speaking, these DSM strategies can be considered as programs which attempt to modify flexible user demands in order to achieve objectives such as reduced energy costs or increased RES utilization.

To achieve these optimal energy management goals, this thesis focuses its efforts on the application of hybrid economic model predictive control (EMPC) strategies for the DSM of small to medium sized grid-connected residential MGs, containing both local photovoltaic (PV) generation capabilities and thermal energy storage (TES) devices. In particular, the investigation exploits thermal energy storage properties of switched domestic electric water heaters (DEWHs) to optimally schedule energy demand for the minimization of MG operating costs. By considering the time varying electricity tariffs, it is shown that the implementation of EMPC is able to simultaneously target reduced electricity costs while also encouraging the self-consumption of local PV generation.

Finally, to address the unavoidable presence of uncertainty in domestic hot water (DHW) user demand, the thesis additionally explores the use of stochastic and robust variants of EMPC. By explicitly considering uncertainty, these control frameworks are able to provide more robust system operation. Specifically, the work implements min-max and stochastic scenario-based frameworks, which were shown to drastically reduce the violation of user comfort constraints when compared with their deterministic counterparts.

Contents

Acknowledgements

The submission of this thesis marks the end of close to 20 years of formal education. An education that not everyone has access to, and one that I consider an extreme privilege to have received. Completing this MSc in Systems and Control has certainly been one of the most challenging endeavours I have ever undertaken. I have learnt a lot, struggled a lot, and only through the unending support of friends and family, have I finally managed to arrive at the finish line.

First, I would like to thank my supervisor Dr.ir. Tamás Keviczky for his assistance during the development and writing of this thesis. Your guidance proved invaluable, not only from a technical perspective, but also through your ability to convince me to keep moving forward.

I give thanks to all the friends and fellow students I have come to know during my time in Delft. The long days at the university campus would not have come to an end without your support. Specifically, I would like to thank Thomas, Chris, Iurie, Patrick, Rens and Folkert. To Thomas, a special thanks for the proof-reading of this work. In addition, I would also like to thank my hockey team 'Hudito H10' for providing me an opportunity to exercise, socialise, and in general to temporarily put my studies out of my thoughts.

To Hans and Ina, thank you for helping Sarah and me to transition to life in the Netherlands. We are very grateful for your generosity and support.

My deepest thanks go to my parents, you have always been there through thick and thin. Also, a special thanks to my father for meticulously proof-reading the entire thesis.

To my late grandfather, it has been a privilege to study at the same university you did so many years before. Thank you for always encouraging my inquisitive nature. I remember you fondly, particularly as my time in Delft draws to an end.

Finally, I extend my utmost gratitude to my wife, Sarah. Moving to the Netherlands with you, led to an exciting yet extremely challenging adventure. I would not have made it to this point without your unending love and support.

Chris Michalak
Delft, University of Technology
16th July 2019

"Non scholæ sed vitæ discimus."

— *Seneca the Younger*

(Niet voor school, maar voor het leven leren wij.)

Chapter 1

Introduction

In developing countries such as South Africa, there are little to no renewable generation feed-in incentives in the energy market. Consequently, an increased deployment of photovoltaic (PV) energy generation at the residential microgrid (MG) level is only economically viable provided that close to 100% of the generated energy is self-consumed[1]. Due to the uncertain, intermittent and time varying nature of PV energy generation, the problem of optimizing self-consumption and economic operation remains far from trivial, particularly when coupled with uncertain user demand profiles [6]. Current research on smart grids (SGs) and MGs has shown that the use of demand side management (DSM) and smart energy storage systems can contribute to the development of economically optimal energy management systems (EMSs) with increased renewable energy source (RES) self-consumption [7].

This thesis expands on current research through the development of optimal DSM strategies for a case-study residential MG, which is located in a residential complex near Johannesburg, South Africa. The complex consists of a number of households, each containing a controllable 150L domestic electric water heater (DEWH), with all households making use of shared roof-top PV generation. Due to the shared nature of the local PV generation, the proposed EMS is required to consider the community as a co-operative collection of energy users, all working to minimize the combined community energy operating cost.

1-1 Smart grid (SG) vision

A key enabling concept behind modern DSM strategies is the notion of the SG, which is an enhancement of the 20th century power grid. Where traditional power grids largely focused on top-down unidirectional power flows from central utilities to a large number of customers; the SG aims to make use of two-way flows of electricity and communication to create an automated and distributed energy network [8]. Table 1-1 provides a brief comparison between the existing power grid and the SG.

[1] In this work, 'self-consumption' is defined as the share of total renewable energy generation directly consumed (or locally stored and later consumed) by the producer, which often is the RES owner [5].

Table 1-1: A brief comparison between the existing power grid and the SG [9]

Existing Grid	**Smart Grid**
Electromechanical	Digital
One-way communication	Two-way communication
Centralized generation	Distributed generation
Manual monitoring	Self-monitoring
Manual restoration	Self-healing
Failures and blackouts	Adaptive and islanding
Limited control	Pervasive control
Few customer choices	Many customer choices

More specifically, SGs have been described by Gharavi et al. as:

> "...an electric system that uses information, two-way, cyber-secure communication technologies, and computational intelligence in an integrated fashion across electricity generation, transmission, substations, distribution and consumption to achieve a system that is clean, safe, secure, reliable, resilient, efficient, and sustainable. This definition covers the entire spectrum of the energy system from the generation to the end points of consumption of the electricity." [10]

They continue to describe the ultimate SG as a 'vision' rather than a system which must meet an exact specification list. In this way, a grid can be considered 'smart' even if it does not fully incorporate all the proposed features. Given the vast scope of the SG vision, it is useful to categorise the SG in to a series of separate, but interacting subsystems. To this end, this thesis briefly introduces three major subsystems of the SG as presented by Fang et. al in their extensive SG survey [8]. Namely, the:

- *Smart infrastructure system*: the energy, information, and communication infrastructure underlying of the SG that supports 1) advanced electricity generation, delivery, and consumption; 2) advanced information metering, monitoring, and management; and 3) advanced communication technologies.
- *Smart management system*: a subsystem that provides advanced management and control services.
- *Smart protection system*: a subsystem that provides advanced grid reliability analysis, failure protection, and security and privacy protection services.

This thesis is primarily concerned with the 'smart management' subsystem, wherein DSM plays a crucial role. The subsystem shows great promise to better realise management objectives such as energy efficiency improvements, supply and demand balance, emission control, operation cost reduction, and utility maximization. However, it is important to recognise that the degree to which these objectives can be achieved relies heavily on the capabilities of the underlying smart infrastructure system. To a large extent, the SG's ability to revolutionize power system management is a result of the significantly enhanced capabilities of information and communication technology (ICT) infrastructure [8].

1-2 Motivation for demand side management (DSM)

The power systems of today have historically been designed with the primary system objective of ensuring sufficient and stable energy supply to meet the worst case demand. While relatively simple to implement, this operating framework typically provides lower energy efficiencies and often leads to increased operating costs. This is due to uncertainty in the power demand of the users which fluctuates rapidly throughout the day, thereby necessitating the requirement for large standby generation and spinning reserves. These flexible grid resources result in increased costs, where the final 10% of generation capacity may only be required for 1% of the time [8]. Mitigating these issues, along with the desire to better integrate intermittent RESs with variable and uncertain generation, which further exacerbate the problem, has led to the recent surge in research focusing on so-called DSM.

Broadly speaking, DSM refers to any control system or program which attempts to modify consumer energy consumption on the customer side of the meter [11, 12]. It plays a key role in the SG vision and forms a primary component of the aforementioned 'smart management system', one of the three major SG subsystems categorised by Fang et al. in [8]. In general, the purpose of DSM is to target specific management objectives such as cost minimization, energy efficiency, emissions reduction, and/or energy security. To enact such a DSM scheme, an EMS is designed to target these desired objectives by modifying flexible user demands through mechanisms such as load shifting, peak clipping, valley filling, etc. This thesis explores the use of optimal control techniques for the implementation of DSM schemes that optimally schedule flexible energy demand in order to reduce user energy costs.

Current literature and further details on DSM are covered in the Background chapter, Section 2-1.

1-3 Residential microgrids (MGs)

This work limits its scope to the DSM of moderately sized co-operative residential communities. In this respect, it is useful to introduce the recently proposed concept of the microgrid (MG) [13]. Seen as one of the 'cornerstones' of the future SG, the organic evolution of the SG is expected to develop through the plug-and-play interaction of MGs [8].

MGs are generally defined as a localized grouping of interconnected loads and distributed energy resource (DER) units. These operate as a single controllable system that provides electricity and/or heat to its local area [13]. DERs include both distributed generation (DG) (e.g. PV, wind, diesel) and distributed storage (DS) units (e.g. battery banks, hot water tanks), all with potentially different capacities and characteristics. In principle, MGs can operate in two operating modes, namely *grid-connected* or *islanded* modes. In the majority of cases, a MG remains connected to the external utility grid (macro-grid) allowing for the import/export of excess demand/supply. In *islanded* mode the MG becomes disconnected from the utility grid at the single point of common coupling (PCC). It is then expected to remain operational as an autonomous entity, providing sufficient generation capacity and controls to supply at least a portion of the load [14]. Figure 1-1 provides an example of a MG containing these elements, which serves a variety of customers, e.g. residential buildings, commercial entities, and industrial parks.

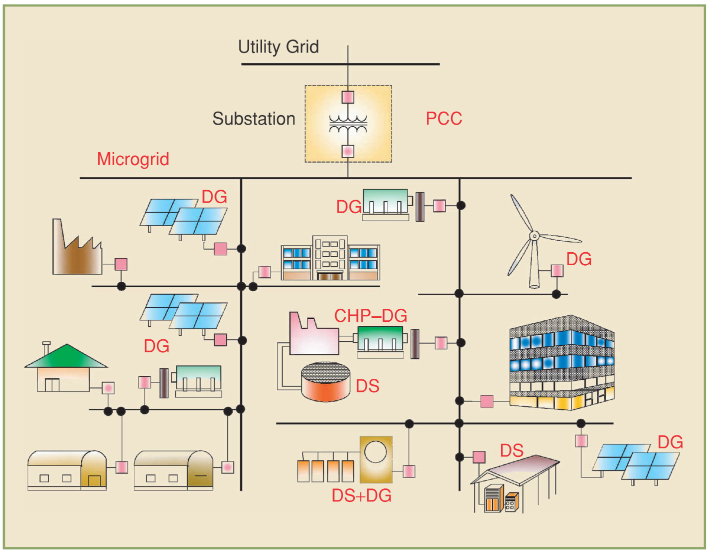

Figure 1-1: A typical MG structure including loads and DER units serviced by a distribution system [14]

For the purpose of this investigation, the aforementioned co-operative residential communities may therefore be considered as residential MGs incorporating distributed PV generation, controllable thermal energy storage (TES) (i.e. DEWH systems) and measurable uncontrollable loads. Furthermore, while general MGs can operate in *islanded* or *grid-connected* modes, this work assumes that the residential MG operates exclusively in a grid-connected mode.

1-4 Hierarchical control in power systems

In their entirety, electrical power grids arguably represent one of the largest most complex man-made systems on earth. Similar to other large-scale systems, the power grid naturally lends itself to a hierarchical operating structure. An example of this has already been discussed; through the introduction of MGs one large grid is divided into a more manageable set of sub-grids. The use of hierarchical structures is not only limited to the delineation of physical system components, it also plays a significant role in the structuring of power system controls. The principal role of MG control structures is to provide:

- Voltage and frequency regulation for both operating modes (*grid-connected* or *islanded mode*).
- Synchronization of the MG with the external utility grid.
- Power flow control within the MG as well as between the MG and the utility grid.
- Capabilities for targeting optimal economic operation.

These requirements operate within various time-scales and levels of significance, and are thus well suited to a hierarchical control structure [15]. Typically, the hierarchy consists of three levels, namely the primary, secondary and tertiary level controls, as shown in Figure 1-2. The primary control maintains voltage and frequency stability, the secondary layer compensates for any voltage and frequency deviations introduced by the primary layer. Finally, a tertiary control layer manages high level power flows and ensures optimal economic operation of the MG.

The DSM strategies investigated in this work are located in the tertiary control layer. Thus, the work will not explicitly cover the primary and secondary layer controls, under the assumption that these will be enacted elsewhere (e.g. by the external utility grid and within the PV DC-AC inverters).

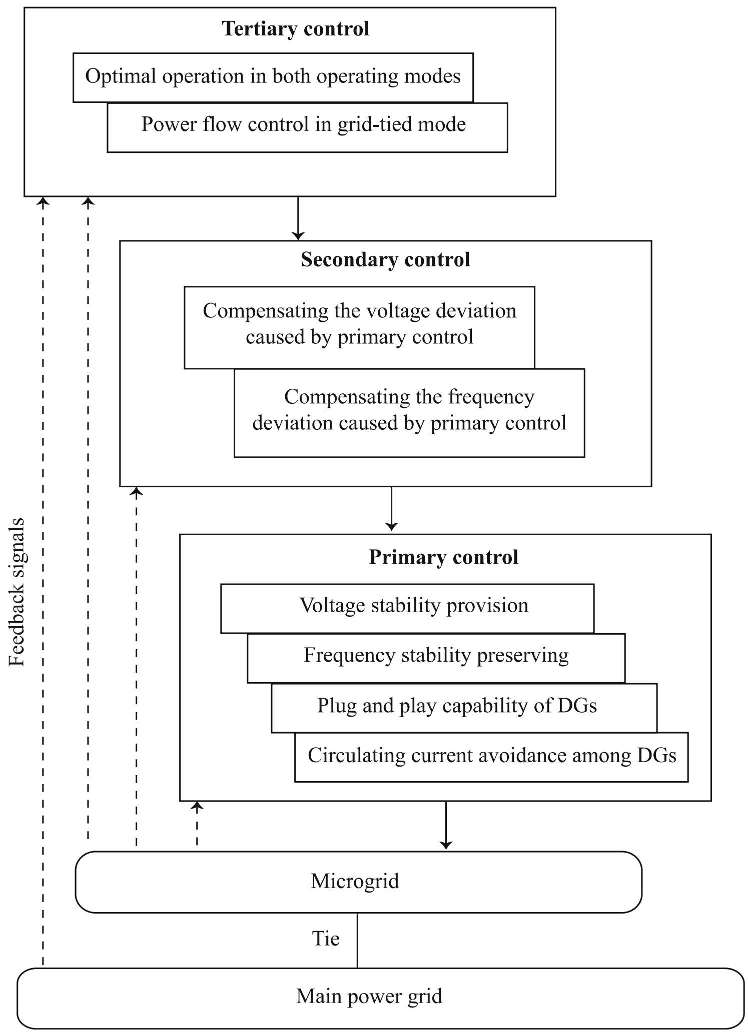

Figure 1-2: Hierarchical control levels of a microgrid [15]

1-5 Research objectives

The purpose of this thesis is to investigate the use of develop, and apply economic optimal control techniques to target the reduced economic operating costs of medium-scale grid-connected co-operative residential microgrids (MGs). Furthermore, the work explores whether the implementation of such controllers would allow for the increased deployment of local PV generation capacity by encouraging RES self-consumption.

This work focused its efforts on the development of co-operative demand side management (DSM) schemes that exploit the thermal energy storage properties of a multi-agent network of switched DEWHs. Operating under a Time-of-Use (ToU) electricity pricing, the scheme attempts to optimally schedule the heating cycles of these domestic hot water (DHW) storage units. This is done in order to shift demand to lower cost supply points, or to periods with excess PV generation. To implement these DSM schemes, this thesis makes use of model predictive control (MPC) frameworks which have recently shown great potential for directly optimizing economic performance objectives. These frameworks fall under a new subset of MPC commonly referred to as economic model predictive control (EMPC) [16, 17].

Due to the highly uncertain nature of DHW user demand, the work further explores the use of stochastic and robust variants of the aforementioned EMPC controllers. By explicitly incorporating uncertainty, these controllers are known to provide more robust system operation and, in the case of the considered MG, can be used to help ensure that DHW temperatures are maintained within acceptable operating bounds. To verify any performance gains, all the developed controllers are compared against a benchmark mechanical thermostatic controller, which represents the currently used control methodology.

1-6 Thesis contribution

The main contributions of this thesis are highlighted below:

1. Developed, implemented and tested state-of-the-art EMPC strategies on a simulated case-study MG. The case-study MG was modelled on an existing residential complex located in South Africa and represents an application not fully explored in literature. In particular, while several works have applied EMPC for the DSM of DHW storage devices (e.g. [18–23]); none of these works consider the application of stochastic MPC control frameworks in a co-operative multi-agent setting. Therefore, this work contributes to the state-of-the-art by considering an extended application of EMPC to a multi-agent system of DEWHs, with explicit consideration of user demand uncertainty.

2. Proposed, developed and evaluated the performance of a modified scenario-based EMPC formulation, herein referred to as 'scenario-based *reduced horizon* EMPC'. Instead of incorporating uncertainty scenarios over the entire prediction horizon, the proposed controller attempts to reduce conservatism by only considering uncertainty for a subset of the full prediction horizon (cf. Section 4-3-7).

3. Developed an open-source `Python` based software package which allows for the synthesis and simulation of MPC/EMPC for general multi-agent hybrid dynamic systems using

the mixed logical dynamical (MLD) modelling framework. The majority of time spent on this thesis was attributed to software development. It is hoped that future research efforts on MPC will continue to develop and distribute open-source software to reduce implementation times and to allow for validation of published results.

1-7 Thesis outline

This thesis consists of six chapters including this Introduction chapter. The remainder of the report is structured as follows:

Chapter 2 further introduces the topic of DSM and presents the reader with fundamental background knowledge to aid in the understanding of subsequent chapters. The chapter begins with a literature survey on DSM, followed by a brief coverage of the control methods applicable for its implementation, including MPC. Finally, an introduction to hybrid dynamic system modelling is presented, which describes the general MLD modelling framework used for all system models considered in this work.

Chapter 3 details the hybrid system modelling of the considered residential MG. The chapter concludes with a description of a compact MLD model that captures all MG dynamics.

Chapter 4 begins with an introduction to the recently defined EMPC control framework. Following this, it presents the components required to formulate an EMPC controller for the DSM of a case-study MG. It continues by detailing various applicable EMPC solution methodologies including deterministic, min-max and scenario-based frameworks.

Chapter 5 provides an illustrative simulation study of all the EMPC controllers presented in Chapter 4. The controllers are evaluated using various performance metrics and compared to a benchmark thermostatic rule-based (TSRB) control law.

Chapter 6 summarizes the thesis with a concluding discussion before outlining possible directions for future work.

Chapter 2

Background

In this chapter preliminary background concepts are covered to further introduce the topic. Additionally, the chapter provides readers with fundamental background knowledge to aid in the understanding of subsequent chapters. First, a broad coverage of the relevant literature on demand side management (DSM) schemes, and their classification, is presented in Section 2-1. Following this, in Section 2-2 the thesis highlights various control frameworks applicable to DSM. This section includes a preliminary introduction to model predictive control (MPC), the primary control methodology considered in this work. In Section 2-3, a brief overview of hybrid dynamic systems is presented. Importantly, the section introduces the widely applicable mixed logical dynamical (MLD) hybrid modelling class that was used to model the case-study residential microgrid (MG) and all its components. The chapter concludes with a summary discussion in Section 2-4.

2-1 Literature on demand side management (DSM)

A great deal of research has been undertaken in the area of DSM, and it is beyond the scope of this report to provide a detailed survey of all aspects and research directions currently under investigation. For detailed coverage and related references, the reader is referred to comprehensive surveys and reviews undertaken in [6, 8, 24–26]. This high level introduction to DSM is largely based on those reviews.

2-1-1 Defining DSM

While compiling this thesis it was noted that various terms have been used in literature when referring to DSM and associated programs, with some authors even suggesting that the terms are misused [25]. The most notable case of this 'misuse' is found with use of the term demand response (DR), which many authors treat as synonymous with the term DSM. For example in [6], the authors make a point to state that the terms demand response (DR), demand management, demand response management, demand side management (DSM), load control, load scheduling, and energy consumption scheduling, are all equivalent within their text.

To minimize confusion, the definitions of DR and DSM as suggested by Barbato et al. in [25] are provided as follows. In their paper the authors propose that demand management mechanisms can be separated in to two main categories, namely DR and DSM. They suggest that DR is categorised by reactive short term solutions which are designed to encourage users to shift or curtail their demand in response to signals provided by the power utility (e.g. dynamic pricing signals or emergency condition requests). Typically, the desired objective of DR is to reduce peak demand and to ensure grid stability by avoiding blackouts/brownouts during adverse operating conditions. Subsequently, they define DSM as proactive strategies in which users modify their demand profiles to achieve long term energy efficiency improvements. Ultimately, they conclude that DR and DSM are two different strategies that can be used in conjunction with each other.

In a strict sense, this thesis subscribes to the definitions of DSM and DR as proposed in [25], but only where the distinctions provide additional insight. In the majority of cases demand management mechanisms combine elements from both DSM and DR. Therefore, to simplify discussions the survey will in general refer to all demand management mechanisms as DSM, in essence branding DR as a subset of DSM (e.g. refer to Figure 2-1).

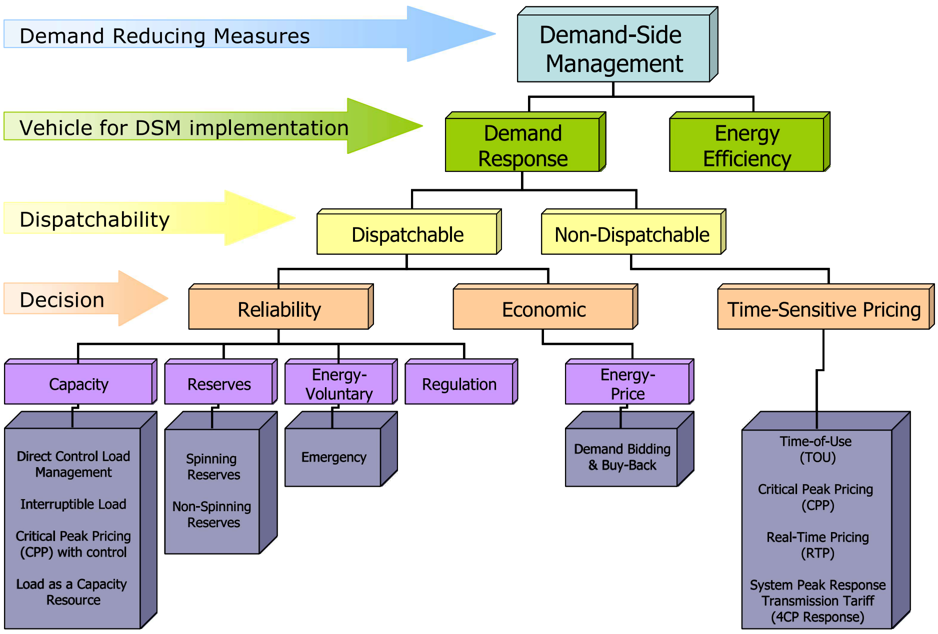

Figure 2-1: Example classification of DSM [27]

2-1-2 Management objectives of DSM

The term 'management' in DSM implies that these programs are designed to achieve some benefit or objective. These objectives can be targeted from an optimization based framework, but heuristic or sub-optimal methods are also often used. The objectives of DSM programs most widely observed in the literature, primarily focus on several key areas. These include targeting energy efficiency, cost minimization, utility maximization, emission reduction, and energy security. The objectives can complement each other but often result in conflicting targets which may be more or less desired depending on whether the objective is viewed from the utility or consumer's perspective. A brief explanation of the objectives may be summarised as follows:

- **Energy efficiency**: generally refers to programs that aim to reduce the overall system power consumption [26]. This is often achieved by so-called demand profile shaping, where demand is shifted, scheduled or reduced to achieve a flatter demand profile with less fluctuation and a lower peak-to-average ratio (PAR) [8]. Greater energy efficiency is also achieved by minimizing energy losses associated with generation, transmission, distribution, and the operation of consumer loads.
- **Cost minimization**: from the consumer perspective this translates to energy bill minimization, where all users wish to minimize the sum total cost of their energy usage. This can be achieved by reducing demand or shifting it to periods of lower energy prices [25]. The introduction of local and renewable energy generation can also reduce operating costs, either through self-consumption, temporary storage, or by selling excess capacity back to the grid. From the power utility's perspective, cost minimization would entail reducing the total cost of generating and distributing power, while meeting the demand of all consumers [6].
- **Utility maximization**: viewed from a high level social perspective, this strategy reduces the total cost of running the utility network while maximizing the sum comfort of all users [6]. Making reference to [28], an example is mentioned in [6], where the grid's social welfare is maximised by optimizing the sum total consumer utility functions minus the cost function of the power utility, all subject to the capacity constraints of the power network.
- **Emission reduction**: motivated by the desire for more sustainable energy systems, DSM strategies which target emission reduction are becoming increasingly important. As noted in [8], programs which target maximum efficiency or minimum costs will not necessarily lead to reduced emissions. Achieving significant reductions often requires an increased use of renewable energy sources (RESs), which can be more costly.
- **Energy security**: due to the increasing integration of intermittent RESs with uncertain variable generation, the task of ensuring network stability and continuity of supply has become increasingly difficult. To reduce the costs of maintaining standby generation capacity, DSM strategies can be implemented to effectively match demand with available supply and thereby minimize potential overload conditions [6, 26].

2-1-3 Classification of DSM programs

Apart from the varying target objectives which may differentiate DSM programs, other features of the program architectures have been used to classify and categorise different schemes. A number of classifications have been proposed in literature (e.g. [1, 24–26, 29]), with each dependent on the author's research focus area, and to some extent their subscribed definition of DSM/DR.

This report takes a broad view of DSM and outlines a classification based primarily on that made by Vardakas et al. in [26], but modified with components from other cited authors. Vardakas et al. propose three high level classification categories. The first category classifies DSM according to the motivation offered to consumers to participate in the program. The second classifies programs based on the operating control architecture. Finally, in the third category programs are classified by the decision variable used to implement the scheme.

DSM based on the *Offered Motivation*

The motivation methods offered to consumers typically fall within two subcategories, namely *time-based* or *incentive-based* schemes. In ***time-based*** DSM (also referred to as price-based DSM) consumers are offered time varying prices to reflect the time varying cost of supply. The intent being to motivate users to reduce or shift their demand from higher to lower priced periods. Several time-based pricing programs have been implemented in practice, or suggested in literature, and are briefly outlined below:

Flat pricing: represents the standard traditional pricing scheme, where users are charged a flat rate (e.g. $/kWh) for each unit of energy consumed. The scheme offers little motivation to modify energy consumption patterns as users can only reduce their energy costs by reducing their total consumption [26].

Time-of-Use (ToU) pricing: marginally extends on the flat pricing scheme by introducing flat prices that change at different time intervals of a day, days of a week, or seasons of a year. The scheme coarsely reflects the cost of supply, with prices higher during peak periods and lower at off-peak periods. The prices for each supply period are usually released far in advance and are typically not frequently updated [6].

Critical-peak pricing (CPP): is largely based on ToU pricing in that prices are normally fixed for different time periods [26]. However, the scheme introduces the option to change the price at critical periods where it is predicted that grid reliability will be jeopardised. By temporarily increasing prices, the utility can motivate users to curtail their demand to guarantee system stability [6].

Real-Time pricing (RTP): provides the greatest system flexibility and represents a fully dynamic pricing scheme in which prices vary continuously at discrete intervals throughout the day (e.g. every 15 minutes or hourly) [6]. RTP schemes release prices before the start of each interval, typically with a pre-determined lead time, or in some cases on a day-ahead basis (then being referred to as Day-Ahead Real-Time pricing (DA-RTP)) [26]. RTP programs allow for the most efficient and competitive energy markets as decision makers are able to act on information that most accurately reflects the current system state [29]. However, this pricing system relies heavily on the effective two-way communication capabilities of the smart grid (SG) and requires users to adopt advanced control mechanisms to enable active and mutually beneficial participation. Thus, while RTP has been successfully implemented for large industrial and commercial customers, implementation for residential customers has been limited [26].

Conversely, in ***incentive based*** (or event-based) programs, consumers are provided with fixed or time-varying payments to motivate users to modify their demand, maintain system stability, or increase operating efficiency. Enrolment in these types of programs is often voluntary, but users may be encouraged to participate through the application of penalties for non-participation [26]. Incentive based programs are further divided into classical and market based categories [29], each is briefly described as follows:

Classical: denote incentive-based programs in which consumers receive participation payments, typically in the form of bill credits or rate reductions. Examples of classical programs include:

(a) *Direct load control (DLC)*, a commonly implemented program which enables the power utility to remotely control consumer loads, through power cycling or set-point adjustment, to achieve DSM objectives. Typical examples of controllable loads include water heaters, building heating systems or air-conditioners.

(b) *Interruptible/Curtailable load* programs which provide upfront incentive payments to consumers for agreeing to curtail specific loads or reduce demand to pre-defined level, upon the receipt of utility emergency reduction requests. Penalties are often imposed for non-conformance [26].

Market based: describes schemes where participants receive economic payments based on their level of performance, contributing to the achievement of DSM objectives. Market based programs include:

(a) *Demand bidding* is a program usually only applied to large consumers which allows a user to place curtailment capacity bids in the wholesale market. If a bid is accepted by the market, the user must curtail their demand in accordance with the bid capacity, or otherwise risk facing penalties.

(b) *Emergency DR* provides participants with incentive payments for measured load reductions during emergency grid conditions where the stability of the grid is jeopardised. Consumers can choose not to curtail their loads and forgo the incentive payments [26].

(c) *Capacity market* programs function in a similar fashion to the emergency DR schemes, but are not implemented with the primary function of mitigating emergency grid conditions. Instead, the program aims to provide participants with payments for pre-defined load reductions to replace the need for conventional standby generation and spinning reserves [29].

DSM based on the ***Control Architecture***

Vardakas et al. [26] further classify DSM methods based on their control architecture. In their paper the authors use this category to classify programs as either centralised or distributed in nature. This thesis extends the classification through the consideration of additional characteristics of the control architecture, as outlined by Barbato et al. in [25].

Before presenting the classification extensions, the control architectures are first considered based on whether control actions are determined using a centralised or distributed controller structure, here referred to as the ***control topology***.

Centralised topology: signifies a control system where the control actions of all users or agents are computed by a single central controller. Centralised control topologies require all sensor and state information to be collected and transmitted to a central location to enable globally optimal decision making. With a growing number of users, this topology increases the demand on centralised computational resources, and presents the need for networks with higher bandwidths and lower latencies. In addition to the scalability issues, these large networks introduce security and privacy concerns as sensitive user information is shared with the central controllers [25].

Distributed topology: presents an alternative to traditional centralised topologies and instead allows agents to make local control decisions based on externally provided information indicating the overall system state [26]. The topology allows for increased scalability while limiting the requirement to centrally collect sensitive user information. However, the distributed nature of the system often reduces the ability for the system to achieve global optimum performance because decisions made by individual agents based on limited information may not positively contribute to the global system objectives [25]. Hence, efficiently achieving global optimal (or near optimal) performance in a distributed setting remains an active research area.

Extending on this is a related characteristic as discussed by Barbato et al. in [25], where DSM control architectures are classified by the nature of their ***users' interactions***. Here the distinction is made between schemes with selfish individual users vs co-operative users:

Individual users: define programs where each user or agent is individually and separately managed. From an optimization perspective, this results in agents which optimize their own objectives without co-operating with other agents, or considering their impact on the overall system performance.

Co-operative users: here users communicate and collaborate with one another by defining control actions to optimize a shared utility function. This can lead to increased global performance as users are able ensure that their actions do not negatively impact global system objectives.

Next, the authors go on to further classify DSM methods by the characteristics of their ***optimization approach*** [25]. While many features could be used to classify various optimization approaches, the authors focus primarily on whether the proposed programs consider problem data in a stochastic or deterministic manner.

Deterministic optimization: classifies DSM control methods which treat all model parameters, system measurements, exogenous signals and predicted signals, as deterministic quantities. These methods ignore any uncertainty, such as those inherent to user demand and RES generation predictions, and instead make an assumption that these values will exactly match the predictions. Consequently, deterministic approaches may lead to poor or infeasible solutions if signals deviate significantly from their expected values.

Stochastic/Robust optimization: where deterministic approaches ignore prediction and model errors, stochastic methods attempt to capture these uncertainties by representing data as random variables. By explicitly considering these unavoidable uncertainties, the optimization methods lead to more robust solutions, which in theory are able to improve average long term performance. Stochastic methods are typically separated into two categories, namely stochastic or robust optimization. In stochastic optimization uncertain data is represented through a probabilistic model with known or estimated statistical properties; the optimization problem is formulated such that the expected value of the cost function is optimized. On the other hand, robust optimization is more suited to problems where the uncertainty does not have a well-defined statistical distribution or cannot be modelled by probabilistic model. In robust optimization uncertain data is typically modelled by a (in)finite deterministic uncertainty set, with the optimization objective to guaranty solution feasibility for all uncertainty realisations, while achieving some measure of robust solution performance.

Finally, Barabato et al. categorise DSM control architectures based on the ***time scale*** considered for determining control actions. Here the authors distinguish between real-time and day-ahead methods:

Day-ahead: refers to DSM frameworks where users' control actions or operating plans are determined and fixed for a finite future time horizon. In the day-ahead case this would be 24 hours, but other time horizons are also possible. From a control theory perspective these scheduling methods typically correspond to open-loop constrained finite time optimal control problems, which obtain optimal performance under the assumption that all data and predictions are deterministic without any uncertainty [30].

Real-time: specifies methods which update users' control actions on a (near) real-time basis. These methods enable the control system to react to real-time events and data which may not have been accurately predicted when the operating plans were initially computed. Real-time DSM strategies often resemble MPC or receding horizon control frameworks [30]. Alternatively, real-time strategies can be implemented using classical control theory or rule-based control, which do not rely on data predictions [31].

DSM based on the *Decision Variable*

The third and final category explored by Vardakas et al. [26] was to classify DSM programs by the characteristics of the decision variable used for determining control actions. The authors identify two main groups, the first schedules loads by determining when these should be activated (either on or off), and the second makes control decisions by determining the amount of energy to be allocated to each load during each time period. Respectively these are referred to as ***task based*** or ***energy based*** DSM methods.

Task based: describe DSM schemes where the controller is responsible for scheduling the activation time of controllable loads. Task based methods consider two types of loads: fixed must-run loads which are non-manageable (e.g. TV, lights), and schedulable loads which may either be shifted to other time slots (e.g. dishwashers, washing machines) and/or interrupted (e.g. pool pumps). From an optimization perspective the decision variable for task based scheduling is time rather than load energy.

Energy based: represent methods that allow for the control of devices with controllable energy demand/supply (e.g. water heaters, space heating, air conditioners, battery storage systems). Energy based methods formulate the problem with the decision variable representing the quantity of energy consumed/supplied at each time instant.

Remark 2.1: It should be noted that problems suited to a task based framework can be reformulated in an energy based framework to allow for the consideration of both time scheduled loads and energy controllable loads.

2-2 Control methods for DSM

A high level overview of the fundamental characteristics of DSM programs was outlined in Section 2-1. The purpose of this section is to provide an introduction to the control methods that are typically applied in DSM systems. It does not intend to exhaustively cover the details of all DSM control frameworks, but rather aims to provide the reader a general appreciation of the overarching operating principles. Chapter 4 provides a detailed description of economic model predictive control (EMPC) based methods for DSM, which form the primary focus of this thesis research. For a detailed review of other methods mentioned below, the reader is referred to comprehensive surveys and related references found in [6, 8, 26, 31–33].

2-2-1 Rule-based and classical control

Rule-based and classical control techniques are currently the most widely used methods for the control of consumer loads and storage devices. These controllers rely on "if-then" type decision logic and proportional-integral-derivative (PID) type control loops, allowing system designers to define static decision mappings which determine control actions based on the current system state [31].

For example, in the case of domestic hot water (DHW) heaters, the traditional thermostatic control switch can be taken as the most basic implementation of a rule-based controller. Here the control actions are governed by a simple hybrid systems model (see (3-7)) where the heating element is activated when the temperature drops below a minimum set-point and is deactivated after reaching a maximum set-point [34]. From a DSM objectives perspective, a thermostatic switch with fixed set-points offers limited control flexibility for targeting cost minimization or energy efficiency [31]. The same can be said for well-known classical techniques such as PID control for temperature set-point tracking.

Many power utilities around the world use rule-based control methods to implement simple load shifting DSM schemes. For example, Australian utilities offer a ToU rate based DSM service where the power supply to loads such as water heaters and pool pumps are only activated at off-peak times. The method can only be applied to flexible interruptible loads and in the case of domestic electric water heaters (DEWHs), the storage tank must be of sufficient capacity to allow for hot water delivery during on-peak hours.

2-2-2 Optimization based control

In recent times, researchers and practitioners have turned to optimization based control methods to allow for more flexible systems which are better able to realize DSM performance objectives. Optimization based controllers often incorporate predictions of controllable state trajectories along with forecasts of exogenous system signals (e.g. photovoltaic (PV) generation, energy demand, weather, etc.). Then, by defining a performance cost which reflects the management objective, the controller is able to determine optimal control actions to minimize this cost through the application of various mathematical optimization techniques. Optimization based controllers for DSM can either operate in a single or co-operative multi-agent MPC based framework, where agents work co-operatively to optimize a global system objective. Or alternatively, they can operate in a framework of non-cooperative game theoretic control where selfish agents compete with each other to optimize their own individual objectives while possibly neglecting global system performance [33].

Model predictive control (MPC)

MPC, also known as receding-horizon control (RHC), has a long development and application history, with origins dating back to the introduction of linear-quadratic-Gaussian (LQG) controllers in the early 1960's. Coupled with the ever advancing capabilities and reduced costs of information and communication technologies (ICTs), increasing interest in applying MPC for DSM has been motivated by its extensive successful deployment in industrial process control applications [35].

In addition to incorporating dynamic system predictions in the optimal decision making process; a key strength of MPC is its ability to explicitly consider real-world system state and input constraints [36]. In principal, MPC therefore provides a well suited control methodology for maximizing DSM performance objectives. The most basic form of MPC is implemented by repeatedly solving a shifting finite horizon open-loop optimal control problem. At each sampling time, the problem is re-solved using updated system state information with the optimal control signal only applied during the next time interval. The solution process is repeated indefinitely with a constantly receding or rolling finite optimization horizon [30, 36].

The constrained open-loop optimal control problem that underpins MPC[1] is compactly captured by [17]:

$$\min_{\tilde{u}(k)} \quad J(k) = \sum_{k=0}^{N_p-1} l(k, x(k), u(k), w(k)) \tag{2-1a}$$

$$\text{s.t.} \quad x(k+1) = f(x(k), u(k), w(k)) \tag{2-1b}$$

$$x(k) \in \mathcal{X}, \quad u(k) \in \mathcal{U}, \quad w(k) \in \Omega \tag{2-1c}$$

$$x(0) = x(t), \quad \omega(0) = \omega(t), \tag{2-1d}$$

where $\tilde{\boldsymbol{u}}(k)$ is the optimal control input sequence[2] that minimizes the cumulative performance cost $J(k)$ over the set of future time instants included in the optimization horizon, N_p.

[1] MPC mathematical framework is further explored in Chapter 4.
[2] Refer to (4-5) for definition of tilde notation.

Performance cost $J(k)$ is composed of stage costs $l(\cdot)$ which represent a positive deviation from a desired objective at each time instant k. The optimization problem is undertaken subject to the system dynamics (2-1b), and state, input and disturbance constraints (2-1c), with descriptions given in (2-2) and (2-3).

In Chapter 4 a detailed description of MPC is presented from an economic DSM perspective. Interested readers who desire further coverage of details related to classical MPC are referred to extensive and highly cited surveys undertaken by Mayne et al. in [36], and by Qin et al. in [35].

Game theoretic control

Game theory is the study of rational decision makers operating in an interactive environment, each with the desire to maximize a desired strategic outcome. The well-established field has lead to the development of a broad reaching analytical and conceptual framework, which together with a set of mathematical tools, enable the analysis of complex multi-agent systems. The systems are said to be comprised of 'players', each of which are required to determine and deploy strategies, often with partially or fully conflicting objectives [33].

The application of game theory to multi-agent control systems often results in a problem formulation that is solved through the use of distributed optimization techniques [37]. Thus, while the study of game theory is not primarily concerned with optimization based control; it has been shown that concepts arising from game theory can be used to analyse multi-agent systems and design controllers for use in DSM. In particular, dynamic and/or differential game theory has received an increasing interest for application in DSM and power system control [38]. Dynamic games offer an alternative modelling and analysis framework for the optimal control of complex systems and share many conceptual similarities with classical optimal control and MPC. However, where classical optimal control and MPC have traditionally only been studied for single agent systems or a system of fully co-operative agents; game theory provides analytical frameworks well suited to studying non-cooperative multi-agent systems with partially or fully conflicting interests and restricted information exchange [39, Section 1.1].

In general all games consist of three fundamental components:

1. Individual player's i, belonging to the set of players $\mathcal{N}$.
2. Strategies x_i belonging to the set of strategies $\{\mathcal{X}_i\}_{i\in\mathcal{N}}$.
3. Utilities u_i belonging to the utility set $\{u_i\}_{i\in\mathcal{N}}$.

Non-cooperative games denote a class of problems where each selfish player $i \in \mathcal{N}$ independently selects a strategy $x_i \in \mathcal{X}_i$ to maximize their utility $u_i(x_i, \boldsymbol{x}_{-i})$, which is also dependent on the other players' strategies $\boldsymbol{x}_{-i}$ [6]. In non-cooperative games players wish not to share their decision strategies or other private information, but are sometimes persuaded to 'co-operate' with other players through self-enforcing incentive mechanisms. These incentives can be used to encourage selfish players to deploy strategies which, while continuing to maximize the player's own utility, also contributes to improved global system performance [33].

A key concept in the analysis of non-cooperative games is the notion of the Nash equilibrium. Named after J. Nash, the foundational solution concept characterises a stable state in a non-cooperative game where no player $i \in \mathcal{N}$ is able to unilaterally improve their strategy x_i, given the strategies of all other players $\boldsymbol{x}_{-i}$ [33]. Making use of this solution concept, Mohsenian-Rad et al. propose a game theoretic control scheme for optimal DSM [12]. By adopting a suitable adaptive real-time pricing scheme, they show that a utility can incentivise selfish players to individually adopt cost optimal consumption schedules, which in turn converge to a global optimum cost at the Nash equilibrium.

While game theoretic control offers an extensive analysis and design framework for DSM, it was not further explored for the research problem under consideration. This work investigates a residential MG where all agents cooperate fully to achieve a globally defined management objective. From a game-theoretic perspective the problem would therefore be considered as a cooperative, as opposed to a non-cooperative game; and as stated by Basar et al. in [39, Ch. 1.2], "cooperative games can, in general be reduced to optimal control problems by determining a single cost function to be optimized by all players, which suppresses the 'game' aspects of the problem". Therefore, instead of turning to game theory, the problem is approached using tools from optimal control and MPC.

For a detailed coverage on the theory of dynamic non-cooperative game theory, the reader is referred to the book by Basar et al. [39]. For surveys and related references on game theory applied to DSM and power system control, refer to works [6, 33, 38].

2-3 Hybrid system modelling

Dynamic system models form a central component in almost all control frameworks, they are required both for controller synthesis and system simulation. These models can take on a wide variety of forms with various structures, and incorporate a number of simplifying assumptions. The choice of modelling structure is primarily influenced by the physical system properties and dynamic behaviour, coupled with consideration of the intended control application. Many components in the MG contain switched or hybrid system dynamics, which need to be explicitly considered to achieve high performance control outcomes. As such, it is important to briefly introduce several modelling concepts from hybrid systems theory, which can provide further structure to the control problem formulation and allow for the application of more general solution frameworks. The hybrid system models described in this section, in particular MLD models, form the base modelling framework for the control problem formulations investigated in this thesis.

Hybrid systems: denote a class of dynamic systems that contain both time-driven and event-driven dynamics [40, Section 1.3.5]. In other words, they are dynamic processes of a mixed continuous and discrete nature, that evolve both according to dynamic equations (i.e. differential or difference equations), and according to logic rules (e.g. if/else statements) [30].

Hybrid systems theory presents one of the broadest modelling frameworks for real-world dynamic processes. Therefore, it is no surprise that research into these systems has generated numerous model structures, each with different properties and areas of application. The choice of suitable modelling structure is characterised by a trade-off between two conflicting criteria: the so-called ‘modelling power’ and ‘decisive power’ [41]. Broad-based frameworks, such as the hybrid automata[3], provide an extremely general modelling structure for hybrid systems and are thus said to have a high modelling power. Unfortunately, modelling structures that are too broad almost certainly have a low decisive power, making it difficult to prove quantitative and qualitative properties of individual systems in the framework [41]. Roughly speaking, the use of models with low decisive power translates into control problem formulations that are likely undecidable or intractable.

Given the modelling trade-offs and characteristics of the MG devices under consideration, it was decided to limit the discussion to the relevant subclasses of hybrid systems. In particular, it is worth exploring two specific subclasses, namely piecewise affine (PWA) and MLD systems. These frameworks provide formal modelling structures which can accurately capture the dynamics and constraints of these switched DEWHs. More importantly, a considerable amount of research has been undertaken for the optimal control of systems described by these models, with the MLD model initially proposed with this exact objective in mind [42].

2-3-1 Dynamic system models

Before introducing specific hybrid system modelling frameworks, it is useful to introduce generic dynamic models that are able to compactly represent the dynamic state evolution of the systems treated in this work. These generic models will be used as stand-in representations of the specific detailed component models, to allow for simplified mathematical descriptions of the control methods under discussion. The work will primarily be concerned with state-space based models with time invariant dynamics captured either by continuous-time differential or discrete-time difference equations.

The generic continuous-time state-space model is given by:

$$\dot{x}(t) = f(x(t), u(t), \omega(t)) \tag{2-2a}$$

$$y(t) = g(x(t), u(t), \omega(t)), \tag{2-2b}$$

where $x(t) \in \mathcal{X} \subseteq \mathbb{R}^{n^x}$ is the system state vector, $y(t) \in \mathcal{Y} \subseteq \mathbb{R}^{n^y}$ is the output vector, $u(t) \in \mathcal{U} \subset \mathbb{R}^{n^u}$ is the manipulated input vector, $\omega(t) \in \Omega \subset \mathbb{R}^{n^\omega}$ is the disturbance vector, and the notation $\dot{x}$ denotes the time derivative of the state. The set $\mathcal{X}$ denotes the set of admissible system states. The input vector $u(t)$ is typically constrained by the available control energy with bounds governed by the admissible input set $\mathcal{U}$. The disturbance vector may include uncontrollable exogenous inputs, unknown external forces and modelling errors, which may be subject to uncertainty. The disturbance vector is assumed to be bounded in the disturbance set Ω [17].

Real-world physical systems are almost always governed by continuous time dynamics, operating within a continuous and/or discrete state-space. However, given that computer-based control systems are now ubiquitously deployed and form the primary tool for complex system control, it is often more useful to consider discrete-time system models. The generic

[3] For a detailed description of hybrid automata refer to [40]

discrete-time state-space model is governed by general difference equations of the form:

$$x(k+1) = f(x(k), u(k), \omega(k)) \tag{2-3a}$$
$$y(k) = g(x(k), u(k), \omega(k))), \tag{2-3b}$$

where $x(k) \in \mathcal{X} \subseteq \mathbb{R}^{n^x}$, $y(k) \in \mathcal{Y} \subseteq \mathbb{R}^{n^y}$, $u(k) \in \mathcal{U} \subset \mathbb{R}^{n^u}$ and $\omega(k) \in \Omega \subset \mathbb{R}^{n^\omega}$, denote the discrete-time equivalents of the continuous-time states, outputs, inputs and disturbances as described in (2-2). Additionally, $k \in \mathbb{Z}$ is introduced to represent the current discrete time instant, typically incremented with a constant sampling interval, t_s.

Remark 2.2: The thesis exclusively considers digital control techniques, where all continuous-time models are first discretized, in this case by a zero-order hold (ZOH), before being used by the computer-based control system. The main reason for focusing on discrete-time models stems from the need to solve optimal control or scheduling problems, for which the continuous-time counterpart would be intractable or very difficult to solve [30]. Continuous-time differential equations can be discretized using ZOH sampling or differentiation approximations, with procedures detailed in e.g. [43, Chapter 2 and 8].

2-3-2 Piecewise affine (PWA) systems

PWA systems [44] provide a general modelling framework for a subclass of hybrid dynamical systems that are capable of describing a large number of physical processes. Among others, these include discrete-time linear systems with static piecewise linearities, or switching systems where the dynamics can be described by a finite number of discrete-time linear models with switching governed by a set of logic rules [45].

The PWA framework has received considerable research interest as it provides the "simplest" extension of linear systems that in addition to capturing hybrid phenomena, is able to model many non-linear and non-smooth processes with arbitrary accuracy [46]. A system can be considered as PWA, provided that the dynamics may be described by region specific affine dynamics for each defined polyhedral partition of the state/input/disturbance space. A general formulation of the discrete-time PWA model structure, similar to that described in [41, 45], is given by:

$$x(k+1) = A_q x(k) + B_{1,q} u(k) + B_{4,q} \omega(k) + b_{5,q} \tag{2-4a}$$
$$y(k) = C_q x(k) + D_{1,q} u(k) + D_{4,q} \omega(k) + d_{5,q} \tag{2-4b}$$

for,

$$\begin{bmatrix} x(k) \\ u(k) \\ \omega(k) \end{bmatrix} \in \mathbf{\Pi}_q,$$

where the state and output vectors $x(k) \in \mathbb{R}^{n^{x,c}} \times \{0,1\}^{n^{x,l}}$ and $y(k) \in \mathbb{R}^{n^{y,c}} \times \{0,1\}^{n^{y,l}}$ can contain both real and binary variables. Similarly for the input and disturbance vectors, $u(k) \in \mathbb{R}^{n^{u,c}} \times \{0,1\}^{n^{u,l}}$ and $\omega(k) \in \mathbb{R}^{n^{\omega,c}} \times \{0,1\}^{n^{\omega,l}}$ respectively. The system of equations are defined for operation modes $q = 1, \ldots, n_q$, where $\mathbf{\Pi}_q$ are convex polyhedra (i.e. defined by a finite number of linear inequalities) in the state/input/disturbance space with non-overlapping interiors. A_q, $B_{[\cdot],q}$, C_q and $D_{[\cdot],q}$ are region specific matrices with appropriate dimensions, and $b_{5,q}$ and $d_{5,q}$ are region specific real vectors.

2-3-3 Mixed logical dynamical (MLD) systems

The MLD system modelling framework was initially proposed by Bemporad et al. in their seminal work for the control of hybrid systems integrating logic, dynamics and constraints [42]. The modelling framework is able to capture the evolution of a number of hybrid system subclasses, including:

- Linear hybrid systems.
- Sequential logical systems (Finite state machines and Automata).
- Nonlinear dynamic systems, where the nonlinearity can be expressed through combinational logic.
- Some classes of discrete event systems.
- Constrained linear systems.
- Linear systems.

The modelling approach results in the following system description:

$$x(k+1) = Ax(k) + B_1u(k) + B_2\delta(k) + B_3z(k) + B_4\omega(k) + b_5 \tag{2-5a}$$
$$y(k) = Cx(k) + D_1u(k) + D_2\delta(k) + D_3z(k) + D_4\omega(k) + d_5 \tag{2-5b}$$
$$Ex(k) + F_1u(k) + F_2\delta(k) + F_3z(k) + F_4\omega(k) + Gy(k) \leq f_5 + \Psi\mu(k), \tag{2-5c}$$

where $x(k) \in \mathbb{R}^{n^{x,c}} \times \{0,1\}^{n^{x,l}}$, $u(k) \in \mathbb{R}^{n^{u,c}} \times \{0,1\}^{n^{u,l}}$ and $\omega(k) \in \mathbb{R}^{n^{\omega,c}} \times \{0,1\}^{n^{\omega,l}}$ are defined with a similar structure to PWA systems in (2-4). In addition, the model utilizes binary and continuous auxiliary variables, respectively $\delta(k) \in \{0,1\}^{n^{\delta}}$ and $z(k) \in \mathbb{R}^{n^{z}}$, which are introduced to capture logic relations as mixed-integer linear inequalities. Finally, non-negative slack variables $\mu(k) \in \mathbb{R}^{n^{\mu}}_{\geq 0}$ may be included to allow constraints to be relaxed (i.e. soft-constraints), subject to a slack penalty function. $\{A,\, B_{1-4}\}$, $\{C,\, D_{1-4}\}$ and $\{E,\, F_{1-4},\, G,\, \Psi\}$ are state, output and constraint equation matrices respectively, and b_5, d_5 and f_5 are vectors, all of appropriate dimensions. The inequalities in (2-5c) are interpreted component-wise and may be subject to time-varying constraint matrices and vectors (not explicitly shown).

Remark 2.3: The slack variables, $\mu(k) \in \mathbb{R}^{n^{\mu}}_{\geq 0}$, have been explicitly added to the MLD model description because it provides designers with a clear insight of where slack has been introduced. These slack variables can always be removed or constrained to $\mu(k) \equiv \mathbf{0}$, in order to enforce hard-constraints.

The MLD framework is characterised by the key notion of embedding propositional or Boolean logic within the state equations. This is achieved by transforming Boolean variables into 0-1 integers, and expressing the relations as mixed-integer linear inequalities [30]. The exact mechanics of this transformation are explicitly covered in [30, 42, 47], and for the sake of brevity will not be expanded on here.

2-3-4 Equivalence of hybrid dynamic models

After the development of PWA, MLD and several other[4] hybrid modelling classes, it was later proven that under mild assumptions the discrete-time versions of these systems are all equivalent [46, 47]. Proving the equivalence of these models was extremely useful as each of these modelling frameworks has its own advantages and areas of applicability. Thus, the equivalence proofs allow one to easily transfer properties and tools from one modelling framework to another [30].

The equivalence of certain hybrid dynamic models is particularly relevant for the application of optimization based control to residential MGs. For example, the dynamics of the switched DEWH ((3-2) with (3-7)) can naturally be captured using a constrained PWA model. Yet, while the PWA structure is suitable for accurately capturing system dynamics, it is difficult to directly incorporate PWA models into compact optimization based control formulations. On the other hand, the MLD framework has been developed with this specific purpose in mind; through equivalence it has been shown that MLD models can be used to recast hybrid dynamical optimization problems into mixed-integer linear (MILP) and quadratic (MIQP) programs, solvable using branch and bound techniques [30].

2-4 Summary discussion

This chapter provides a broad-based introduction to DSM concepts and operating principles, all of which are applicable to residential MGs. Subsequent chapters investigate the application of these concepts to a specific case-study MG. In particular, this thesis develops suitable centralised DSM strategies for the optimal co-operative control of small to medium-sized residential MGs. To allow for an economical integration of uncertain renewable PV generation, the strategies need to consider the dynamics and constraints of controllable DEWHs together with uncertain user energy demands. Of all the control methods discussed in Section 2-2, the optimization based MPC schemes show the greatest potential to incorporate these aspects and achieve the desired MG operating objectives. As a result, the remainder of thesis will be used to provide a detailed account on the application of MPC schemes, within the context of optimal economic control for DSM.

[4] i.e. linear complementarity (LC) systems, extended linear complementarity (ELC) systems, max-min-plus-scaling (MMPS) systems - refer to [46] for their descriptions.

Chapter 3

Modelling Residential Microgrids

In this chapter the report outlines the system modelling structures that were used to model the case-study residential microgrid (MG). First, a high-level description of the case-study MG is presented in Section 3-1. Next, Section 3-2 outlines the modelling of the domestic electric water heaters (DEWHs). Following this, Section 3-3 describes the modelling and forecasting methodologies used for exogenous system signals, including photovoltaic (PV) generation, uncontrollable electrical loads, and domestic hot water (DHW) demand. Finally, Section 3-4 combines all system components to form a compact mixed logical dynamical (MLD) model of the overall MG.

The application of model predictive control (MPC) schemes for the demand side management (DSM) of residential MGs requires the development of problem specific dynamic system models. Within the MPC framework, these models allow the controller to predict future system states for the determination of state dependent optimal control input sequences. The selection of suitable system models directly influences the computational complexity of the resultant optimal control problems. While elaborate non-linear system models may provide more accurate state predictions, these models are often not suitable for MPC. Consequently, this thesis limits its scope to the development simplified hybrid MLD models, for which solvable MPC problems can be developed.

3-1 Case-study residential microgrid (MG)

In general, residential MGs may include any number of devices, likely of different types, and each subject to device specific dynamics and constraints. This work only considers a simplified MG model based on an actual residential community located near Johannesburg, South Africa. The community grid-connected MG consists of a number of individual households each containing one controllable thermal energy storage (TES) unit (i.e. a DEWH), all with shared access to a communal renewable energy source (RES) (i.e. rooftop PV generation).

Figure 3-1 depicts such a MG, where:

- N_h - number of DEWHs for households $i \in \{1, \dots, N_h\}$ with,
  - $P_{h,i}(k)$ [W] - DEWH electric input power
  - $\omega_{h,i}(k)$ [L/s] - household DEWH hot water demand
- $P_g(k)$ [W] - the utility grid import/export power ($P_g(k) \geq 0 \Rightarrow$ power imported)
- $P_{\text{pv}}(k)$ [W] - aggregate shared communal rooftop PV generation power
- $P_r(k)$ [W] - aggregate residual (uncontrollable) electrical power demand

Remark 3.1: The specific MG configuration considered in this work only represents a very simple example of a residential MG (i.e. only one controllable device type). Even though this may seem restrictive, readers should note that the MPC control methodologies discussed in Chapter 4 are equally applicable to more complex configurations and can be easily expanded to incorporate devices such as battery energy storage (BESS) systems, heating, ventilation, and air conditioning (HVAC) systems, diesel generators, etc. In fact, the exact same control structure and tool-set may be applied, provided that the devices can be modelled by the widely applicable MLD modelling framework (2-5).

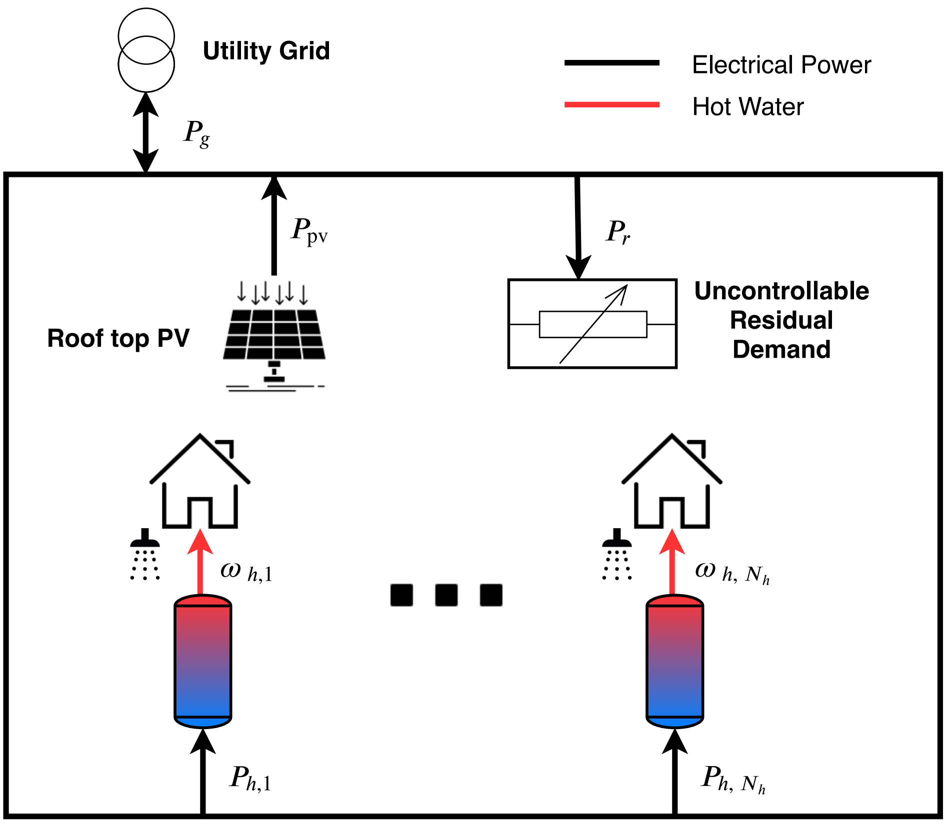

Figure 3-1: Diagram of MG considered in this thesis.

3-2 Domestic electric water heater (DEWH) modelling

Modelling of TES devices for control by energy management systems (EMSs), and in particular modelling of tank based DEWHs, has been covered extensively in literature [19, 23, 34, 48–52]. The physically based storage models are formulated by making various simplifying assumptions to enable the development of models that are suitable for computationally efficient simulation and tractable control problem formulations. These models are typically formulated based on thermal and electric energy balance as outlined in [19, 48];

$$\dot{Q}_{\text{tank}} = \dot{Q}_{\text{inflow}} + \dot{Q}_{\text{heater}} - \dot{Q}_{\text{demand}} - \dot{Q}_{\text{loss}}, \tag{3-1}$$

where $\dot{Q}_j$ [W] represents the heat flow rate attributed to component j.

3-2-1 Fully mixed DEWH model

The fully mixed (FM) storage or homogeneous thermal capacity model provides one of the most widely used and simple models for application in optimization based control for DSM [51]. The one-dimensional model assumes a homogeneously distributed temperature profile exists within the tank and that all water entering the tank mixes perfectly with the existing tank contents [51, 52]. Thus, the model ignores thermal stratification and other non-linear fluid/thermal dynamic effects. This allows the DEWH to be modelled with a single temperature variable (i.e. state), as presented in Figure 3-2.

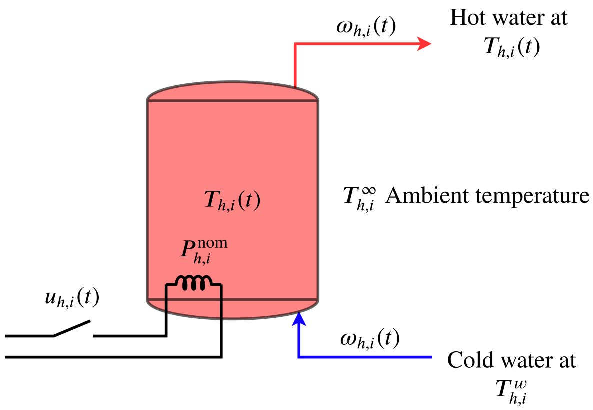

Figure 3-2: Diagram of a DEWH

Based on the energy balance given in (3-1), the continuous-state dynamics for the FM model are given by a simple first order differential equation [23, 50],

$$\underbrace{m_{h,i} \cdot C_w \frac{dT_{h,i}(t)}{dt}}_{\dot{Q}_{\text{tank}}} = \underbrace{\omega_{h,i}(t) \cdot C_w(T_{h,i}^{w} - T_{h,i}(t))}_{\dot{Q}_{\text{inflow}} - \dot{Q}_{\text{demand}}} + \underbrace{P_{h,i}^{\text{nom}} u_{h,i}(t)}_{\dot{Q}_{\text{heater}}} - \underbrace{U_{h,i} A_{h,i}^{s}(T_{h,i}(t) - T_{h,i}^{\infty})}_{\dot{Q}_{\text{loss}}}, \tag{3-2}$$

where $m_{h,i}$ [kg] is the total mass of water in the tank and C_w [J/(kg K)] is the thermal capacity of water, both assumed to be constant[1]. $T_{h,i}(t)$ [°C] is the average water temperature in the

[1] Assuming constant $m_{h,i}$ and C_w, implies that the stored energy in the tank is directly proportional to the average tank temperature, $T_{h,i}(t)$.

heater, $\omega_{h,i}(t)$ [L/s] is the water demand mass flow rate at the inlet, $T^{w}_{h,i}$ [°C] is the inlet water temperature, $P^{\mathrm{nom}}_{h,i}$ [W] is the nominal electric power of the resistive heating element, $u_{h,i}(t)$ is the on-off (binary) switched heating element input, $U_{h,i}$ [W/(m^2 K)] is the overall standing heat loss co-efficient across the tank insulation, $A^{s}_{h,i}$ [m^2] is the surface area of the tank, and $T^{\infty}_{h,i}$ [°C] is the ambient temperature surrounding the tank.

Linear parameter-varying (LPV) model

Notice that (3-2) is not a linear system due to the '$D_{h,i}(t)T_{h,i}(t)$' term. However, it can be considered as a linear parameter-varying (LPV) system [53], re-written in a standard form as follows:

$$\dot{x}_{h,i}(t) = A^{c}_{h,i}(\omega_{h,i}(t))x_{h,i}(t) + B^{c}_{h1,i}u_{h,i}(t) + B^{c}_{h4,i}\omega_{h,i}(t) + b^{c}_{h5,i}, \tag{3-3}$$

with the state and disturbance input defined respectively as tank temperature and hot-water demand, i.e.:

$$x_{h,i}(t) \coloneqq T_{h,i}(t), \quad \omega_{h,i}(t) \coloneqq D_{h,i}(t),$$

and,

$$A^{c}_{h,i}(\omega_{h,i}(t)) = \frac{-U_{h,i}A^{s}_{h,i} - C_w\omega_{h,i}(t)}{m_{h,i}C_w}, \qquad B^{c}_{h1,i} = \frac{P^{\mathrm{nom}}_{h,i}}{m_{h,i}C_w},$$

$$B^{c}_{h4,i} = \frac{C_wT^{w}_{h,i}}{m_{h,i}C_w}, \qquad b^{c}_{h5,i} = \frac{U_{h,i}A^{s}_{h,i}T^{\infty}_{h,i}}{m_{h,i}C_w}.$$

Written in this form it is clear that the continuous state matrix, $A^{c}_{h,i}(\cdot)$, is dependent on the time-varying hot-water disturbance variable (or parameter), $\omega_{h,i}(t)$.

3-2-2 Linearised DEWH model

Directly using the DEWH LPV model (3-3) for controller synthesis would lead to increased complexity of the resultant controllers. This is especially true for the stochastic or scenario based controllers, which are investigated in subsequent chapters to better handle the uncertain DHW demands, $\omega_{h,i}(t)$. Consequently, it was decided that the MPC controllers developed in this work would be designed using a linearised control model. Thus, the work makes use of two separate models, a linearised model (3-4) for computing control actions and the LPV model (3-3) for closed-loop simulation. The linearised continuous-time DEWH model is computed by Taylor expansion of (3-3) about the operating point $(x_{h,i}, u_{h,i}, \omega_{h,i}) = (T^{\mathrm{nom}}_{h,i}, 0, 0)$, leading to the following linear system approximation:

$$\dot{x}_{h,i}(t) \approx \bar{A}^{c}_{h,i}x_{h,i}(t) + \bar{B}^{c}_{h1,i}u_{h,i}(t) + \bar{B}^{c}_{h4,i}\omega^{\mathrm{nom}}_{h,i}(t) + \bar{b}^{c}_{h5,i}, \tag{3-4}$$

with $T^{\mathrm{nom}}_{h,i}$ [°C] the nominal DEWH tank and hot-water demand withdrawal temperature and,

$$\bar{A}^{c}_{h,i} = \frac{-U_{h,i}A^{s}_{h,i}}{m_{h,i}C_w}, \qquad \bar{B}^{c}_{h1,i} = \frac{P^{\mathrm{nom}}_{h,i}}{m_{h,i}C_w},$$

$$\bar{B}^{c}_{h4,i} = \frac{C_w(T^{w}_{h,i} - T^{\mathrm{nom}}_{h,i})}{m_{h,i}C_w}, \qquad \bar{b}^{c}_{h5,i} = \frac{U_{h,i}A^{s}_{h,i}T^{\infty}_{h,i}}{m_{h,i}C_w}.$$

To enable the use of the linearised system model (3-4), it is assumed that all DHW volume demand sequences, $\omega_{h,i}(t)$, are scaled for withdrawal at a constant temperature, $T_{h,i}^{\text{nom}}$. In other words, rather than assuming that users demand a certain volume of hot-water at the current tank temperature, it is assumed that the users will demand a certain amount of heat energy with the volume of water determined by the required heat demand. Therefore, $\omega_{h,i}^{\text{nom}}(t)$ [L/s] is the DHW demand volume required to deliver the requested heat demand at temperature, $T_{h,i}^{\text{nom}}$.

However, as mentioned, the controllers designed using the linearised control model (3-4) are later simulated with the LPV model (3-3) in closed-loop. The LPV model does not assume that the water demand is extracted at a constant temperature. Thus, in order to compute the physical volume of water that is extracted when using the LPV model, $\omega_{h,i}(t)$, it is necessary to make use of the following relation:

$$\omega_{h,i}(t) = \left[\frac{T_{h,i}^{\text{nom}} - T_{h,i}^{w}}{x_{h,i}(t) - T_{h,i}^{w}}\right] \omega_{h,i}^{\text{nom}}(t). \tag{3-5}$$

3-2-3 Control inputs and switched dynamics

DEWHs have historically been actuated using mechanical thermostatic (rule-based) controllers, which introduce switched hybrid system dynamics. A discrete-time model representing the classic thermostatic control law is given by [34]:

$$P_{h,i}(k) = P_{h,i}^{\text{nom}} \cdot u_{h,i}(k), \quad u_{h,i}(k) \in \{0,\, 1\}, \tag{3-6}$$

with,

$$u_{h,i}(k) = \begin{cases} 1, & \text{if } x_{h,i}(k) \leq T_{h,i}^{\text{on}} \text{ (heating element on)} \\ 0, & \text{if } x_{h,i}(k) \geq T_{h,i}^{\text{off}} \text{ (heating element off)} \\ u_{h,i}(k-1), & \text{if } T_{h,i}^{\text{on}} < x_{h,i}(k) < T_{h,i}^{\text{off}} \text{ (maintain previous input),} \end{cases} \tag{3-7}$$

where for each DEWH agent $i \in \{1, \ldots, N_h\}$, $P_{h,i}(k)$ [W] is the electrical input power and $(T_{h,i}^{\text{on}}, T_{h,i}^{\text{off}})$ are the minimum and maximum temperature set-points respectively. Implementing this classical control approach only requires the use of very simple and inexpensive actuation hardware, with binary control input $u_h(k) \in \{0,\, 1\}$ dictating the on-off switching dynamics.

To reduce costs and maintain the simplicity of the actuation hardware, it is often a requirement that advanced management schemes continue to utilise switched on-off control laws, as opposed to the use of a continuously variable input power. While reducing hardware costs, this requirement complicates the application of optimization based control with binary decision variables leading to an increased computation complexity. Fortunately, significant advances in integer based optimization algorithms and hybrid control theory continue to increase the number of tractable applications, with promising results obtained for similar system configurations (e.g. [23, 54–57]).

3-2-4 DEWH MLD model

In a domestic residential setting, the average tank temperatures are normally bounded within an operating range for system safety and to ensure consumer comfort. These temperature constraints can be captured by the following inequalities:

$$T_h^{\min} \leq x_h(t) \leq T_h^{\max}. \tag{3-8}$$

Then, considering the linearised continuous-time FM DEWH model (3-4), subject to switched control inputs (3-6), and state/input constraints (3-8). For each individual DEWH agent, $i \in \{1, \ldots, N_h\}$, this model can be discretized, using zero-order hold (ZOH) (cf. Remark 2.2), and by following reference procedures in [42], recast into the standard MLD framework (2-5), resulting in:

$$x_{h,i}(k+1) = A_{h,i}x_{h,i}(k) + B_{h1,i}u_{h,i}(k) + B_{h4,i}\omega_{h,i}^{\mathrm{nom}}(k) + b_{h5,i} \tag{3-9a}$$

$$y_{h,i}(k) = x_{h,i}(k) \tag{3-9b}$$

$$E_{h1,i}x_{h,i}(k) \leq f_{h5,i} + \Psi_{h,i}\mu_{h,i}(k), \tag{3-9c}$$

with tank temperature state $x_{h,i}(k) \in \mathbb{R}$, binary power switching input signal $u_{h,i}(k) \in \{0, 1\}$, DHW demand $\omega_{h,i}^{\mathrm{nom}}(k) \in \mathbb{R}$, and temperature constraint slack variable $\mu_{h,i}(k) \in \mathbb{R}^2_{\geq 0}$. $A_{h,i}$, $B_{h1,i}$, $B_{h4,i}$, $E_{h1,i}$, and $\Psi_{h,i}$ are DEWH state equation and constraint matrices, $b_{h5,i}$ and $f_{h5,i}$ are vectors, all of appropriate dimensions. Refer to Appendix A-1 for a detailed description.

3-3 Exogenous RES generation and demand modelling

To successfully implement MPC for DSM, in addition to utilizing dynamic models of the controllable DEWHs, the EMS is also required to compute predictions of all exogenous uncontrollable inputs (or disturbances). For the MG under consideration, this includes the prediction of DHW demand for all DEWH agents, $\hat{\omega}_{h,i}(k)$, the aggregate uncontrollable residual electrical power demand, $\hat{P}_r(k)$, and the aggregate PV power generation, $\hat{P}_{\mathrm{pv}}(k)$ (ref. Figure 3-1). The accuracy of these forecasts directly impacts the feasibility and optimality of optimization based predictive control techniques. Controllers making use of predictions with large errors or uncertainties often have to accept reduced or poor close-loop system performance. Fortunately, many techniques have been proposed for the forecasting of RES generation and user demand profiles, with the development and improvement of such methods remaining a topic of continued research interest.

Before detailing the disturbance forecast and modelling framework utilised for this thesis investigation, Section 3-3-1 provides an overview of forecasting for DSM.

3-3-1 Background on generation and demand forecasting

Predictive control strategies for DSM typically operate with prediction horizons in the order of hours to days, with sampling times of minutes to hours (e.g. [19, 55, 58]) Consequently, the forecast methods used for these strategies should be optimized for similar horizons and sampling resolutions. In literature, relevant methods are commonly referred to as 'short term forecasts' with forecast horizons of 1 h to 1 day/week, ahead [59].

The underlying mathematical and computational methods for the forecasting of generation and demand signals are often very similar, if not exactly the same. This is clearly seen when comparing for example [60] and [61]. In all cases, the forecasting models rely on input signals and/or model training data to make predictions of future signal values. Models can make use of endogenous (internal) input data, typically formed as current and/or lagged (i.e. historical) time-series records of the generation/demand, or they can use exogenous (external) input data such as local environment measurements (temperature, humidity, wind speed, etc.), satellite images, or Numerical Weather Predictions (NWPs) (temperature, irradiance, cloud cover, wind speed, etc.) [60].

In general the approaches for forecasting generation and demand can be broadly classified into four categories [60–62]:

Statistical approach: denote data-driven methods that are able to extract relations in past data to predict future behaviour. They generally base predictions solely on historical measured data, but may make use of exogenous input signals. Among others, statistical approaches include the use of:

- Persistence models: simple and naive predictors that assume future signal realizations remain equal to the latest measurement.
- Linear stationary models: used to predict time series that fluctuate around a static mean, including;
  - Auto-Regressive (AR) models
  - Moving Average (MA) models
  - Auto-Regressive Moving Average (ARMA) models
  - Auto-Regressive eXogenous (ARX) models
  - Auto-Regressive Moving Average with eXogenous variables (ARMAX) models
- Linear non-stationary models: used to predict time series that do not exhibit a static mean, including;
  - Auto-Regressive Integrated Moving Average (ARIMA) models
  - Seasonal ARIMA (SARIMA) models
- Non-linear stationary models: such as the Non-linear AR-eXogenous (NARMAX) model.

Artificial Intelligence (AI) approach: make use of AI techniques such as artificial neural networks (ANNs) to forecast generation and demand signals.

Physical approach: while technically not a stand-alone forecasting technique, these approaches make use of external forecasts such as NWPs to make predictions using physical system models. An example would be the use solar irradiation and temperature predictions to determine PV generation forecasts by using PV model (3-11).

Hybrid approach: includes any combination of the aforementioned approaches.

Each of these methods have their own merits and drawbacks. Ultimately, the selection of suitable forecasting techniques needs to consider many factors such as the required forecasting accuracy, the available input data, the development budget (time and cost), and the associated computational resources.

Relevant forecasting literature for DSM

A detailed coverage, or implementation, of the numerous applicable forecasting methods is beyond the scope of this thesis. Further information on how each of these approaches have been applied to the forecasting of PV generation, residual load and DHW demand, can be found in the surveys and reviews referenced below:

- **PV generation**: for a recent and detailed coverage of techniques for the forecasting of PV power generation, refer to the reviews undertaken by Antonanzas et al. [60], Wan et al. [62], and Inman et al. [63]. These provide details on all the aforementioned forecasting approaches applicable to PV generation.
- **Electrical demand**: literature reviews on electrical load forecasting have been undertaken by Khan et al. [61] and Suganthi et al. [64]. For a detailed overview of AI based techniques, readers are referred to the work by Raza et al. [59].
- **DHW demand**: extensive reviews specifically related to DHW demand forecasting do not exist, but readers may refer to a paper by Gelažanskas et al. [65] which briefly outlines relevant works before implementing and comparing forecasting techniques for the DHW demand of residential houses.

3-3-2 Persistence forecasting

Although many forecasting methodologies and frameworks exist, all with varying levels of accuracy and implementation complexity, it was decided that this work would only make use of a very simple naive persistence forecast. To capture temporal trends, the forecasts are made by assuming that today's forecast is equal to a 24 h lagged historical measurement (i.e. assume "today will be the same as yesterday"):

$$\hat{\omega}(k) = \omega\left(k - \frac{24\,\mathrm{h}}{t_s}\right), \tag{3-10}$$

where t_s [s] is the discrete control system sampling time.

Remark 3.2: The decision to limit the scope to the use of naive persistence based forecasting was made as it represents the most basic methodology that could be implemented for controller simulation. Even though more advanced forecasting methodologies may likely lead to reduced prediction errors, and potentially increased controller performance; their implementation was not required to show the feasibility and benefits of MPC strategies for DSM. Incorporating more advanced forecasting methodologies (e.g. building on works referenced in Section 3-3-1) is left as an exercise to be considered for future work.

3-3-3 PV generation and residual electrical demand modelling

To enable DSM strategies which optimize the economic utilization of PV generation, it was necessary to incorporate predictions (or forecasts) of future generation capacity and residual electrical demand into the decision making process [62, 66]. These forecasts can be generated in a number of ways as highlighted in Section 3-3-1. Some of these methods incorporate physical system models while others are primarily formulated using data-driven techniques.

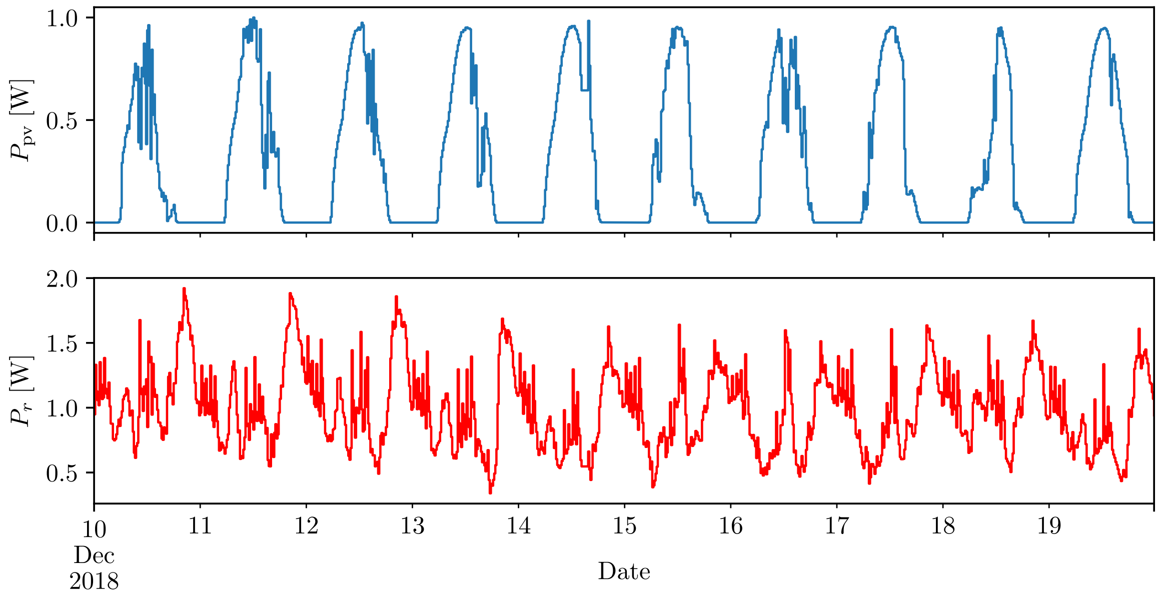

Figure 3-3: 10 day normalized subset of historical data for PV generation, $P_{\rm PV}(k)$, and residual MG electrical demand, $P_r(k)$, obtained from a site managed by Solar Africa®. Top plot: PV generation normalized to maximum capacity of $1\mathrm{W}$. Bottom plot: MG aggregate residual uncontrollable load power normalised to long-term mean of $1\mathrm{W}$.

PV generation

The output power of PV generation is affected by a wide variety of factors, such as the local solar irradiance, reflectivity, PV cell temperatures, and inverter efficiency. An example of a highly simplified PV model similar to that described in [67]:

$$P_{\rm pv}(k) = \eta_{\rm pv}(k) \cdot A_{\rm pv} \cdot G_c(k) \left[1 - \alpha_{\rm pv}(T^c_{\rm pv}(k) - T^{\rm STC}_{\rm pv})\right], \tag{3-11}$$

where $P_{\rm pv}(k)$ [W] is the aggregate system PV generation[2], $\eta_{\rm pv}(k)$ [%] denotes the conversion efficiency of the PV cell array, $A_{\rm pv}$ [m^2] is the array surface area, $G_c(k)$ [W/m^2] is the incident solar irradiance acting on the array, $\alpha_{\rm pv}$ is a power temperature co-efficient, $T^c_{\rm pv}$ [°C] solar cell operating temperature, and $T^{\rm STC}_{\rm pv}$ [°C] is the cell array reference temperature under standard test conditions.

[2] Here, $P_{\rm pv}(k) > 0$ reflects the power generated by the array. Henceforth, unless otherwise stated a convention is adopted such that $P_{[\cdot]} \geq 0$ implies a load power, and $P_{[\cdot]} < 0$ implies a generated power.

While making use of such models may allow for more accurate forecasts; as mentioned in Remark 3.2, the use of such models or advanced forecasting techniques is beyond the scope this work. Instead, the PV generation predictions, $\hat{P}_{\text{pv}}(k)$, were determined using the previously stated naive data-driven persistence forecast method (3-10). To enable this, representative historical PV generation data was obtained from Solar Africa® for use in simulations. For reference, the first 10 days of the normalized PV generation data are presented in the upper plot of Figure 3-3. The normalized PV data was scaled depending on the maximum PV generation capacity selected for the case-study simulations.

Residual electrical demand

In the same manner, residual electrical demand sequences $P_r(k)$, are also based on historical data recordings from Solar Africa®, with required predictions, $\hat{P}_r(k)$, again made using a persistence forecast (3-10). The historical demand sequences were obtained from a community MG with several hundred households. The data was normalized with unity mean and scaled depending on the number of households considered in the case-study simulation. The first 10 days of the normalized historical residual demand data are presented in the lower plot of Figure 3-3.

3-3-4 Domestic hot water (DHW) demand modelling

In an ideal case the thesis would also have made use of actual historical DHW demand data for forecasting, scenario generation (cf. Section 4-3-6) and control simulation. Unfortunately, it was not possible to reliably extract realistic DHW demand profiles from the data provided by Solar Africa®. Consequently, this thesis makes use of stochastic synthetically generated DHW demand data based on the work of Jordan and Vajen in [68].

In [68], the authors describe a software tool, `DHWcalc`, which they developed to generate realistic DHW demand profiles for both single and multi-user scenarios. The software considers several different draw-off categories (showers, baths, etc.) and distributes these throughout the year with user-defined statistical means, according to an associated daily draw-off probability distribution function. The draw-off categories are each defined by minimum and maximum draw-off flow rates, which vary around a provided mean according to a Gaussian distribution. The software ensures that for each household, a long term user defined daily mean DHW demand rate is maintained. Additionally, users are able to apportion the demands to vary based on seasonal changes (e.g. weekday vs weekend, winter vs summer).

For the thesis work, the `DHWcalc` tool was used to generate demand profiles with the following main characteristics and assumptions:

- A long-term daily mean DHW usage, $\mathbb{E}\left[\omega_{h,i}^{\text{Nom}}\right] = 200\text{L/d}$, per household (the software default).
- All seasonal variations were ignored. Thus, the DHW demand profiles were generated by assuming equal probability distributions for all days of the year. This was done to simplify the simulation implementation, particularly when applying scenario-based MPC (cf. Section 4-3-6).

- The DHW draw-off categories were apportioned as follows:
  - 75% for showers
  - 19% for small and medium ancillary draw-offs
  - 6% for baths.

Figure 3-4 provides an illustration of example daily DHW demand scenarios, along with a box and whisker plot to demonstrate how demand is distributed throughout a day. The box plot was created by generating synthetic data for 22,000 days and highlights that the majority of demand occurs in the mornings and evenings. The ends of the whiskers depict upper and lower limits of the demand across all 22,000 daily realizations.

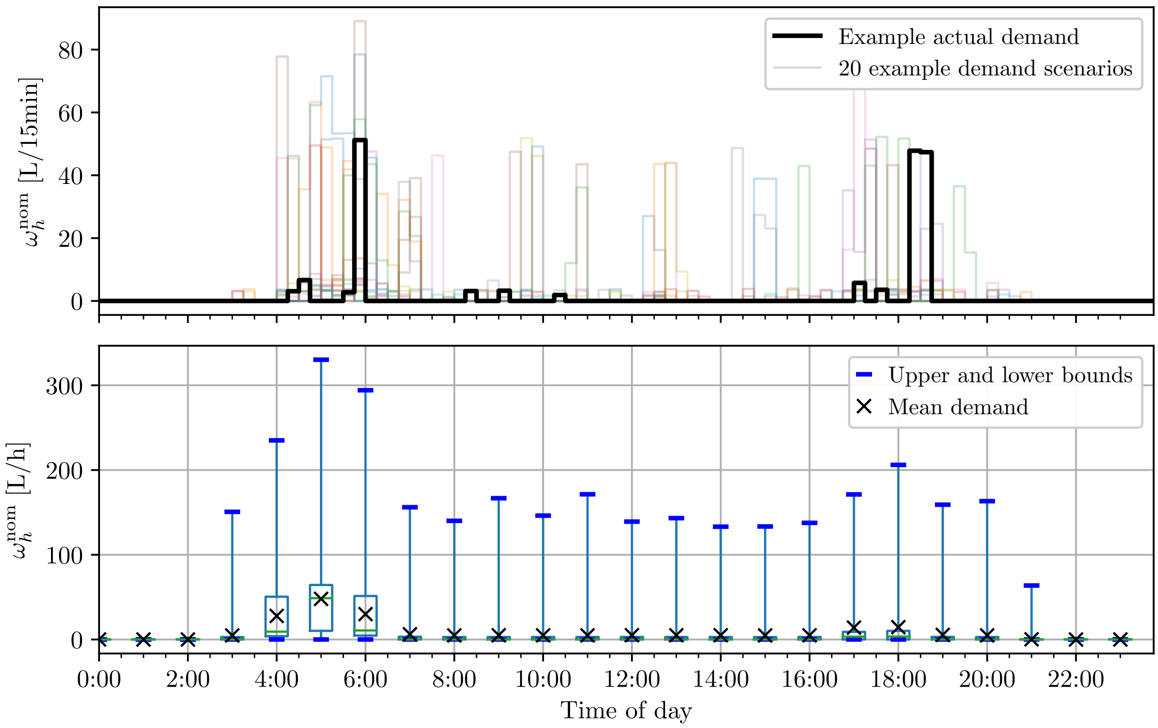

Figure 3-4: Synthetic data for DHW demand, $\omega_{h,i}^{\mathrm{nom}}(k)$. Top plot: depicts a synthetic actual DHW demand realization surrounded by 20 possible predicted stochastic daily scenarios. Bottom plot: hourly distribution of demand over 22,000 daily synthetic demand scenarios.

3-4 Combined overall MG system dynamics

Having discussed physically based system models for individual DEWHs, the ability to forecast uncertain exogenous system inputs, and the generic MLD hybrid modelling structure; it is now possible to briefly describe the combined overall MG model which forms the basis of this work's optimal control problem formulations. The thesis limits its scope to the control of grid connected residential MGs with shared RESs, where each household contains a controllable DEWH. To this end, the following subsection presents the overall MG model with N_h DEWHs (see Figure 3-1).

3-4-1 Interaction with the utility grid

The problems considered in this work assume that the MG operates exclusively in a grid connected mode, thus it will always be possible to exchange energy with the external utility grid. Moreover, for all practical purposes it is assumed that this utility can be considered as a 'quasi-infinite' bus which is always able to supply all future MG demand, even without the support of local RES capacity. Under a general modelling framework, such a connection allows deficit electric demand energy to be bought from the utility, and vice versa excess generation can be sold back for profit. To capture these dynamics, and to allow for different import and export tariffs, required the construction of a logic constrained model similar to that described in [58].

First, auxiliary variables $\delta_g(k) \in \{0, 1\}$ and $z_g(k) \in \mathbb{R}$ are defined such that:

$$z_g(k) := P_{g,\mathrm{imp}}(k) = P_g(k)\delta_g(k), \tag{3-12}$$

and that the following logic relations hold,

$$\begin{cases} [P_g(k) \geq 0] \Leftrightarrow [\delta_g(k) = 1] \\ [\delta_g(k) = 1] \Rightarrow [z_g(k) = P_g(k)] \\ [\delta_g(k) = 0] \Rightarrow [z_g(k) = 0], \end{cases} \tag{3-13}$$

where $P_g(k) >= 0$ [W] denotes the power imported from the utility grid, $P_{g,\mathrm{imp}}(k)$ [W]. If these logic statements are satisfied, the power exported from the grid $P_{g,\mathrm{exp}}(k)$ [W] is computed as:

$$P_{g,\mathrm{exp}}(k) = P_g(k) - z_g(k). \tag{3-14}$$

Logic statements (3-13) cannot be directly incorporated into the optimal control problems. However, by using transformational procedures outlined in [42], they can be equivalently expressed by standard form MLD mixed-integer linear inequalities. By applying these procedures, (3-13) is equivalent to:

$$F_{g2}\delta_g(k) + F_{g3}z_g(k) + G_g P_g(k) \leq f_{g5}, \tag{3-15}$$

with,

$$F_{g2} = \begin{bmatrix} -P_g^{\min} \\ -P_g^{\max} - \epsilon \\ -P_g^{\max} \\ P_g^{\min} \\ -P_g^{\min} \\ P_g^{\max} \end{bmatrix}, \qquad F_{g3} = \begin{bmatrix} 0 \\ 0 \\ 1 \\ -1 \\ 1 \\ -1 \end{bmatrix}, \qquad G_g = \begin{bmatrix} -1 \\ 1 \\ 0 \\ 0 \\ -1 \\ 1 \end{bmatrix}, \qquad f_{g5} = \begin{bmatrix} -P_g^{\min} \\ -\epsilon \\ 0 \\ 0 \\ -P_g^{\min} \\ P_g^{\max} \end{bmatrix},$$

where $P_g^{\min}$ [W] and $P_g^{\max}$ [W] are the minimum and maximum MG export/import operating power bounds, and ϵ a properly small scalar tolerance (typically the machine precision) which is introduced to allow strict inequalities to be approximated as non-strict inequalities.

Power balance in the MG

To ensure stable MG operation, a balance between energy supply and demand must be met at each time instant k. This requirement is enforced by introducing the following equality constraint:

$$P_g(k) = \underbrace{\sum_{i=1}^{N_h} P_{h,i}(k)}_{\text{controllable}} + \underbrace{P_r(k) + P_{\text{pv}}(k)}_{\text{uncontrollable}} \quad \forall k, \tag{3-16}$$

where $P_r(k)$ is the aggregate residual power demand (i.e. all uncontrollable loads) in the MG, $P_{h,i}(k)$ reflects the electrical input power of the i^{th} DEWH agent, and $P_{\text{pv}}(k)$ the aggregate PV generation in the MG.

To capture the power balance constraint (3-16) in a standard compact MLD form, it is re-written as:

$$y_g(k) := P_g(k) = D_{g4}\boldsymbol{\omega}_g(k), \tag{3-17}$$

where,

$$\boldsymbol{\omega}_g(k) = \left[\begin{array}{c} \boldsymbol{\omega}_g^{\text{con}}(k) \\ \hline \boldsymbol{\omega}_g^{\text{exo}}(k) \end{array}\right] = \left[\begin{array}{c} P_{h,1}(k) \\ \vdots \\ P_{h,N_h}(k) \\ \hline P_r(k) \\ P_{\text{pv}}(k) \end{array}\right], \quad D_{g4} = \mathbf{1}^\top := \begin{bmatrix} 1 \\ \vdots \\ 1 \\ 1 \\ 1 \end{bmatrix}^\top .$$

For later descriptions, note that $\boldsymbol{\omega}_g(k)$ has been partitioned with $\boldsymbol{\omega}_g^{\text{con}}(k)$ the deterministic controllable DEWH power inputs and $\boldsymbol{\omega}_g^{\text{exo}}(k)$ the uncertain exogenous residual demand and PV generation.

3-4-2 Overall system MLD model

By combining all the grid device models and grid interaction dynamics, it is possible to present a compact overall MLD model representation of the case-study MG (cf. Figure 3-1). For time step, k, the system is defined by[3]:

$$\text{DEWH dynamics and constraints } \forall i \in \{1,\dots,N_h\} \begin{cases} x_{h,i}^{k+1} = A_{h,i}x_{h,i}^k + B_{h1,i}u_{h,i}^k + B_{h4,i}\omega_{h,i}^{\text{nom},k} + b_{h5,i}\,, & \text{(3-18aa)} \\ E_{h,i}x_{h,i}^k \leq f_{h5,i} + \Psi_{h,i}\mu_{h,i}^k\,, & \text{(3-18ab)} \\ \mu_{h,i}^k \geq \mathbf{0}, & \text{(3-18ac)} \\ x_{h,i}(0) = x_{h,i}(t), \quad \omega_{h,i}^{\text{nom}}(0) = \omega_{h,i}^{\text{nom}}(t), & \text{(3-18ad)} \end{cases}$$

[3] The superscript time index, k, is used reduce notational clutter, e.g. x^k is therefore equivalent to $x(k)$.

Grid power balance and constraints

$$
\begin{cases}
P_g^k = D_{g4}\boldsymbol{\omega}_g^k, & \text{(3-18ba)} \\
P_{g,\text{imp}}^k = z_g^k, \quad P_{g,\text{exp}}^k = P_g^k - z_g^k, & \text{(3-18bb)} \\
F_{g2}\delta_g^k + F_{g3}z_g^k + G_g P_g^k \leq f_{g5}, & \text{(3-18bc)} \\
P_r(0) = P_r(t), \quad P_{\text{pv}}(0) = P_{\text{pv}}(t). & \text{(3-18bd)}
\end{cases}
$$

The overall system MLD model collectively captures the dynamics and constraints of N_h DEWHs (3-9), along with the grid power balance (3-17) and logic constraints (3-15).

The development of the overall MG system model marks the end of the system modelling chapter. With all system dynamics compactly captured using the MLD modelling framework, it is then possible to explore the associated MPC control problem formulations. In Chapter 4, this thesis details the MPC frameworks that were developed to optimize the economic operation of the overall MG model (3-18).

Chapter 4

Economic Model Predictive Control for Demand Side Management

Various high level concepts and control methods for demand side management (DSM) were presented in Chapter 2. Of particular interest is the application of model predictive control (MPC), briefly introduced in Section 2-2. Applying MPC and associated control techniques to DSM has so far shown promising results, with many studies (e.g. [23, 58]) indicating an improved operating performance over more traditional DSM implementations. This chapter expands on the initial introduction by providing a detailed coverage of the MPC problem formulations, within the context of economic optimal control for DSM. All control problem formulations presented in this chapter are developed for the overall residential microgrid (MG) model as defined in Section 3-4. In Chapter 5 these formulations are simulated in an illustrative study to evaluate their performance on the considered case-study MG.

First, Section 4-1 provides a broad introduction to the recently coined MPC control framework, 'economic model predictive control (EMPC)'. Section 4-2 then presents the components required to formulate an EMPC controller for the DSM of a case-study MG. Following this, Section 4-3 details various EMPC solution frameworks developed and applied in this work; including, deterministic, stochastic and robust methodologies. The chapter concludes with a brief analysis of optimization methods and complexity considerations, followed by a concluding discussion.

4-1 Introducing economic model predictive control (EMPC)

The development of so-called *standard* MPC has primarily been driven by its application in large scale industrial process industries. As with any other component of a commercial enterprise, the ultimate high level objective of control systems incorporating MPC, is to positively contribute to the attainment of optimal economic performance. In the process control industry this goal has traditionally been targeted by deploying a multi-level hierarchical control architecture, typically partitioned into two distinct layers. The first layer, referred to as the real-time optimization (RTO) layer, is responsible for optimizing an operating economic performance metric by determining the optimal steady-state process set-points of continuously updated steady-state operating models. Updating on the time scale of hours to days, the RTO passes these optimal set-points to the second control layer commonly referred to as the *advanced process control system*. This lower layer is responsible for driving the physical system states to the provided optimal set-points, and upon reaching these, reject any dynamic disturbances that enter the system. Reacting in the order of seconds to minutes, this layer is often implemented using a reference tracking MPC framework, here referred to as *standard* MPC. Recently, researchers have found that this classical two-layer approach may not always be suitable when targeting optimal economic performance. Consequently, this has led to the development of a newly defined optimal control framework referred to as *economic* MPC (EMPC) [16, 17]. This section provides a brief overview of the classic two-layer hierarchical control structure followed by a formal introduction to EMPC.

Classic two-layer hierarchical control

To formalise the aforementioned two-layer hierarchical structure, simplified high-level problem formulations for the RTO and *standard* MPC are briefly introduced below:

RTO problem: real-time optimization typically operates with a much longer sampling period than the lower level control layers, and is primarily concerned with solving optimization problems of the form shown in (4-1) [17]:

$$\min_{x_s,\, u_s} \quad l_e(x_s, u_s) \tag{4-1a}$$

$$\text{s.t.} \quad x(k+1) = f(x_s, u_s) = x_s, \tag{4-1b}$$

$$x_s \in \mathcal{X}, \quad u_s \in \mathcal{U}, \tag{4-1c}$$

where the objective function $l_e(\cdot)$, referred to as the economic cost function (or economic stage cost), is constructed to reflect the cumulative instantaneous process operating costs and is often based on metrics such as the net instantaneous operating profit or deviation from the desired production rates. As previously mentioned, RTO is traditionally only concerned with the optimization of economic performance under the condition that the plant must operate at a steady-state. Thus, in addition to process state and input constraints denoted in (4-1c); the problem is formulated subject to the steady-state system evolution constraint given by (4-1b).

Without loss of generality, the optimal steady-state solution of the RTO problem (4-1), denoted by $(x_s^*,\, u_s^*)$, is assumed to be unique and located at the origin of (2-3)[1] (i.e., $f(x_s^*,\, u_s^*) = f(0,0) = 0$) [17]. This simplifies the definition of lower level control layers, in that they need only target the system origin as the reference set-point to reach the economic optimum.

Standard MPC problem: operating within the second control layer as part of the advanced process control system, the *standard* MPC is deployed to asymptotically track the optimal steady-state set-points, $(x_s^*,\, u_s^*)$, as determined by the RTO layer [16].

[1] To simplify the explanation, here the disturbance vector $\omega(k)$ is neglected, i.e. $\omega(k) \equiv 0$.

Recapping on the initial overview given in Section 2-2-2, MPC attempts to approximate infinite horizon optimal control by, at each time instant, solving a constrained finite horizon open-loop optimal control problem of the form given by:

$$\min_{\underline{u}(k)} \quad J_{\text{MPC}} = \sum_{k=0}^{N_p-1} l_m(x(k), u(k)) \tag{4-2a}$$

$$\text{s.t.} \quad x(k+1) = f(x(k), u(k)), \tag{4-2b}$$

$$x(k) \in \mathcal{X}, \quad u(k) \in \mathcal{U}, \tag{4-2c}$$

$$x(0) = x(t), \tag{4-2d}$$

with an objective function J_{MPC}, the sum of MPC stage costs $l_m(\cdot)$ over the finite horizon $\mathcal{N}$. The objective is optimised subject to system dynamics (4-2b), and state/input constraints given by (4-2c) with ($\mathcal{X}$,$\mathcal{U}$), the set of admissible states and inputs respectively.

Ensuring asymptotic stability of the targeted steady-states is the primary objective of the *standard* MPC framework. To accomplish this, the stage cost $l_m(\cdot)$, typically a quadratic performance criterion, is chosen as a non-negative real valued function such that the minimum value is realised at the optimal/desired set-points, (x_s^*, u_s^*) [16], i.e. it is assumed that:

$$0 = l_m(x_s^*, u_s^*) \leq l_m(x(k), u(k)), \quad \forall (x(k), u(k)). \tag{4-3}$$

Using the system's current state $x(t)$ as the initial state, problem (4-2) is solved in a receding horizon fashion with only the first control action of the determined optimal control sequence, $\underline{u}(k)$, applied to the plant. This on-line solution process is repeated indefinitely with a constantly shifting prediction horizon, leading to a so-called implicit optimal control law. The requirement for on-line optimization constitutes the main distinguishing feature of MPC, as opposed to conventional controllers, which use pre-computed control laws that directly map a current system state to a required control action [36].

Remark 4.1: Although the notion of stability forms an overriding requirement of MPC frameworks and control systems in general, early versions of MPC were implemented without any stability guarantees. Instead practitioners resorted to the tuning of cost and horizon parameters, and thorough testing regimes to provide stability assurances. With increasing deployment, researchers devoted considerable attention to the topic, and the theory of MPC stability has now reached a relatively mature stage. Subject to further conditions, such as minimum prediction horizons, or the addition of terminal constraints and/or terminal penalties; the *standard* MPC formulation has guaranteed stability properties, with proofs mainly based on Lyapunov stability theory. Detail coverage on the stability of MPC is beyond the scope of this thesis, instead interested readers are referred to a seminal review undertaken by Mayne et al. in [36].

Economic model predictive control

While the classical hierarchical two-layer approach forms the backbone of many industrial process control systems and often achieves good performance; the separation of economic optimization and dynamic process control has been shown to be inefficient or inappropriate for many processes where dynamic economic performance is crucial. In these instances, researchers have turned their attention to control frameworks where the MPC layer is modified to directly and dynamically optimize an economic performance criteria without reference to an economically optimized steady-state. In effect this renders the RTO layer redundant, with economic optimization now directly captured in the plant control layer. This modified control framework, referred to as *economic* MPC, is no longer subject to the assumption that optimal economic performance is realised at a steady-state. Thus, (4-3) does not hold in general and it may happen that $l_e(x(k), u(k)) < l_e(x_s^*, u_s^*)$ for some feasible pair $(x(k), u(k))$ that is not a steady-state [16].

In contrast with the two-layer hierarchical approach, the general problem formulation for EMPC is provided below:

EMPC problem: specifies a dynamic receding horizon model predictive control methodology that directly optimizes an economic performance criteria. The problem formulation closely resembles that of *standard* MPC with the tracking stage cost, $l_m(\cdot)$ replaced by an economic stage cost, $l_e(\cdot)$, similar to that used in RTO. The optimal control problem underpinning EMPC takes the form given in (4-4).

$$\min_{\underset{\sim}{u}(k)} \quad J_{\text{EMPC}} = \sum_{k=0}^{N_p-1} l_e(x(k), u(k)) \tag{4-4a}$$

$$\begin{aligned} \text{s.t.} \quad & x(k+1) = f(x(k), u(k)), && \text{(4-4b)} \\ & x(k) \in \mathcal{X}, \quad u(k) \in \mathcal{U}, && \text{(4-4c)} \\ & x(0) = x(t), && \text{(4-4d)} \end{aligned}$$

with an objective function J_{EMPC}, the sum of EMPC stage costs $l_e(\cdot)$ over the finite horizon N_p. The objective is optimised subject to constraints which remain the same as, or at least very similar to, those defined for the *standard* MPC problem (4-2).

Remark 4.2: In general, the stability proofs for *standard* MPC formulations, referred to in Remark 4.1, do not apply to EMPC. For one, the Lyapunov arguments used to prove asymptotic stability of *standard* MPC often rely on the assumption that (4-3) holds, which as discussed earlier is not necessarily true for EMPC [16]. More importantly, because the EMPC framework can be applied to non-linear systems, or objectives which result in feasible pairs $(x(k), u(k))$ with costs less than the best steady-state, i.e. $l_e(x(k), u(k)) < l_e(x_s^*, u_s^*)$, asymptotic stability of an equilibrium state cannot be expected in general [69]. As a result of these differences, researchers have devised alternative stability analysis frameworks for EMPC. Similar to *standard* MPC, these methods typically rely on the addition of terminal penalties, stability constraints or sufficiently large prediction horizons, in order to provide stability guarantees [16, 17, 69]. However, as with many other practical implementations of MPC/EMPC, this work does not aim to provide formal stability guarantees. Instead, the presented controllers rely on simulation based validation, where stable operation is managed through the selection of sufficiently large prediction horizons.

This section provides only a general introduction to EMPC, a framework which shows great potential for the optimal economic control of residential MGs. Research on EMPC and model based predictive control in general is extensive and continues to be developed. For further in-depth theoretical coverage of EMPC research from a global perspective, readers are referred to excellent reviews recently undertaken in [16, 17]. The sections that follow will instead extend on this brief introduction to EMPC by focusing on the specific formulations that were applied for the DSM of residential MGs.

4-2 EMPC problem formulation for DSM

Having introduced the general EMPC methodology in Section 4-1, the following sections aim to detail various mathematical components and solution frameworks that are required to effectively apply EMPC for the DSM of residential MGs. Here the discussions are particularly concerned with EMPC schemes that target operating cost minimization through the optimization-based predictive control of residential loads (e.g. domestic electric water heaters (DEWHs)). Later in Chapter 5, these control problem formulations are simulated and compared with the standard mechanical thermostatic rule-based (TSRB) controller (3-7), currently used for temperature control.

Notational simplification

Before continuing, it is useful to introduce a simplifying mathematical notation, similar to that in [55, 70]. Any bold variable with a tilde accent underneath represents the stacked version of that variable in the prediction horizon, e.g.:

$$\underset{\sim}{\boldsymbol{u}}_h(k) \coloneqq \begin{bmatrix} u_h^\top(k) & \dots & u_h^\top(k+N_p) \end{bmatrix}^\top. \tag{4-5}$$

To enable compact representations when using this notation, time index k may also be discarded (unless required), i.e. $\underset{\sim}{\boldsymbol{u}}_h \equiv \underset{\sim}{\boldsymbol{u}}_h(k)$.

Furthermore, note that (4-5) includes a terminal horizon element (e.g. $u_h(k+N_p)$ in $\underset{\sim}{\boldsymbol{u}}_h(k)$), for all system variables, including inputs. It is included here, because for general mixed logical dynamical (MLD) systems the state constraints at time k may depend on the input at time k. Therefore, to ensure that terminal state-constraints are satisfied a feasible terminal input would need to exist. The terminal input can be excluded if not required for this purpose.

4-2-1 Decision variables

The decision variables for the MG EMPC problem include all controllable device inputs, constraint slack variables and auxiliary MLD logic variables, of the overall MG system model (3-18). By defining $V_{[\cdot]}(k)$ as the stacked version of an MLD model's decision variables, for all k, the variables specific to the case-study are given by:

$$V_{h,i}(k) = \begin{bmatrix} u_{h,i}^\top(k) & \mu_{h,i}^\top(k) \end{bmatrix}^\top \quad \forall i \in \{1, \cdots, N_h\} \tag{4-6}$$

$$V_g(k) = \begin{bmatrix} \delta_g^\top(k) & z_g^\top(k) \end{bmatrix}^\top. \tag{4-7}$$

4-2-2 System constraints

For optimal economic control of the MG, the selected EMPC objective is optimized subject to the MG system dynamics and state/input/logic constraints. For this work, these evolution dynamics were captured in the combined overall MG model (3-18). Direct utilisation of this model structure for the EMPC optimization problem formulation is not always convenient due to the implicit iterative nature of the state evolution equations (cf. (3-18ab)). This implicit structure requires the optimization problem to optimize over not only the system inputs, but also the state predictions. To accomplish this requires the use of additional optimization variables for each state, which are then subject to evolution equality constraints. Alternatively, it is possible to reformulate the implicit model to allow for an EMPC formulation which makes use of explicit state predictions, thus removing the requirement for equality constraints.

The evolution of MG model (3-18) over the prediction horizon, is given in the explicit form:

$$\begin{array}{c}\text{DEWH dynamics}\\ \text{and constraints}\\ \forall i \in \{1,\dots,N_h\}\end{array}\left\{\begin{aligned}
&\underset{\sim}{\boldsymbol{x}}_{h,i} = \Phi_{hx,i}x_{h,i}(0) + \Gamma_{hv,i}\underset{\sim}{\boldsymbol{V}}_{h,i} + \Gamma_{h\omega,i}\underset{\sim}{\boldsymbol{\omega}}_{h,i}^{\text{nom}} + \Gamma_{h5,i}\,, && \text{(4-8aa)}\\
&H_{hv,i}\underset{\sim}{\boldsymbol{V}}_{h,i} \le H_{hx,i}x_{h,i}(0) + H_{h\omega,i}\underset{\sim}{\boldsymbol{\omega}}_{h,i}^{\text{nom}} + H_{h5,i}\,, && \text{(4-8ab)}\\
&\underset{\sim}{\boldsymbol{\mu}}_{h,i} \ge \mathbf{0}, && \text{(4-8ac)}\\
&x_{h,i}(0) = x_{h,i}(t), \quad \omega_{h,i}^{\text{nom}}(0) = \omega_{h,i}^{\text{nom}}(t), && \text{(4-8ad)}
\end{aligned}\right.$$

$$\begin{array}{c}\text{Grid power}\\ \text{balance and}\\ \text{constraints}\end{array}\left\{\begin{aligned}
&\underset{\sim}{\boldsymbol{P}}_g = L_{g4}\underset{\sim}{\boldsymbol{\omega}}_g, \quad \boldsymbol{\omega}_g = \begin{bmatrix}\boldsymbol{\omega}_g^{\text{con},k}\\ \boldsymbol{\omega}_g^{\text{exo},k}\end{bmatrix}, && \text{(4-8ba)}\\
&\underset{\sim}{\boldsymbol{P}}_{g,\text{imp}} = \underset{\sim}{\boldsymbol{z}}_g, \quad \underset{\sim}{\boldsymbol{P}}_{g,\text{exp}} = \underset{\sim}{\boldsymbol{P}}_g - \underset{\sim}{\boldsymbol{z}}_g, && \text{(4-8bb)}\\
&H_{gv}\underset{\sim}{\boldsymbol{V}}_g \le H_{g4}\underset{\sim}{\boldsymbol{\omega}}_g + H_{g5}, && \text{(4-8bc)}\\
&P_r(0) = P_r(t), \quad P_{\text{pv}}(0) = P_{\text{pv}}(t), && \text{(4-8bd)}
\end{aligned}\right.$$

where matrices/vectors $\Phi_{[\cdot]}$, $\Gamma_{[\cdot]}$, $L_{[\cdot]}$ and $H_{[\cdot]}$ are appropriately defined[2] by iterating the system model over N_p. Notice that in contrast with (3-18a), the explicit DEWH state (4-8aa) and constraint (4-8ab) equations are no longer iteratively defined. They are only dependent on the system inputs and known initial states, $x_{h,i}(0)$, thus removing the need for additional state prediction decision variables. Moreover, if the objective function does not penalise the state (e.g. (4-10)), then the state evolution equations (4-8aa) need not be evaluated because the constraints no longer depend on this evolution.

Soft-constraints

Before discussing soft-constraints, it is useful to introduce here an MPC concept often referred to as ‘recursive feasibility’. In broad terms, it is defined as follows:

Recursive feasibility: an MPC controller is considered recursively feasible if and only if for all initial states, $x(0)$, and all sequences of optimal control inputs, the optimal MPC control problem remains feasible for all time [71].

[2] Detailed descriptions of the evolution matrices for general MLD model (2-5) are presented in Appendix A-2

If recursive feasibility cannot be guaranteed, then it is possible that at certain time instants the MPC controller will not be able to compute a control input. In this case it would be necessary to implement a fall back solution, such as a rule-based control law, which could then supply valid control inputs in place of the MPC controller. To avoid reliance on such a fall back solution, methods exist to help ensure recursive feasibility. The use of soft-constraints represents such a method and is briefly discussed below.

MPC controllers subject to hard-constraints (i.e. must be satisfied), may often lead to optimization problem infeasibility, meaning that no solution is available that satisfies all constraints. This is especially the case when the system under control is subject to unknown disturbances. Consequently, in order to help ensure a recursively feasible solution, designers often replace hard-constraints with soft-constraints which allow some form of constraint violation subject to additional objective penalties [36]. These soft-constraints are typically incorporated into the optimization problem by introducing penalised slack variables, where the size of the variables correspond to the magnitude of the associated constraint violation [72, 73].

Referring to the general MLD model (2-5) presented in the Background chapter; Remark 2.3 indicates that non-negative slack variables $\mu_{[\cdot]}(k) \in \mathbb{R}_{\geq 0}$ can be added to implement the aforementioned soft-constraints. Fortunately, for a grid connected MG the power balance constraint typically does not pose infeasibility issues, provided that one assumes the utility grid is represented by an 'quasi-infinite' bus, which is able to supply/absorb any excess MG demand/generation. By ensuring sufficient bounds on the maximum import/export power of the utility grid, soft-constraints are not required for grid constraints (4-8bc). However, hard-constraints on system states such as minimum DEWH tank temperatures, can easily lead to infeasibility, as the hot water demand $\omega_{h,i}^{\mathrm{nom}}(k)$ may exceed the physical capacity for supply. As a result, for the case-study MG penalized slack variables $\mu_{h,i}(k)$ were included for all DEWH temperature bound state constraints (4-8ab).

The selection of a suitable soft-constraint penalty function represents the final element necessary to implement soft-constraints. The penalty function is added to the EMPC objective to ensure that constraint violations captured in the slack variable $\mu_{h,i}(k)$ are minimized where possible. Without a suitable penalty function the constraints can be violated without consequence, thereby permitting undesired uncontrolled system trajectories. Examples of penalty functions include the use of l_1-norms ($\|\cdot\|_1$), l_∞-norms ($\|\cdot\|_\infty$) or quadratic penalty functions.

The penalty function adopted for the case-study MG is given by:

$$J_{\mathrm{soft},i}(k) = \rho_{h,i}(k) \left\| q_{h,i}^{\mu} \odot \mu_{h,i}(k) \right\|_1 \quad \forall i \in \{1, \ldots, N_h\}, \tag{4-9}$$

where '$\odot$' indicates the Hadamard element-wise product, $\rho_{h,i}(k) \in \mathbb{R}$ is an overall soft-constraint weighting parameter and $q_{h,i}^{\mu} \geq \mathbf{1} \in \mathbb{R}^2$ governs the relative weight between the soft-constraints. In this case, the preference of violating the upper or lower temperature bounds of the DEWH. An l_1-norm was used because the resultant optimization problem can then be solved as a mixed-integer linear program (MILP), for which efficient solvers exist.

The selection of a suitable soft constraint weighing parameters is governed by the theory of 'exact penalty functions'. Broadly speaking, an exact penalty function is obtained when the solution to an optimal control problem subject to soft-constraints produces the same solution as the original hard-constrained problem, if the latter is feasible [72]. Attaining an exact penalty function is desirable as it helps to ensure that constraints are only violated if absolutely necessary. An exact penalty is attained by setting $\rho_{h,i}(k)$ to a sufficiently large value. Determining the minimum required value for an exact penalty weight is far from trivial and remains the subject of continued research (e.g. [72, 74]). The application of such methods is beyond the scope of this thesis. Instead, a heuristic methodology is used as described and simulated in Section 5-4-1.

4-2-3 Objective/cost function

This work investigates the optimal economic control of a co-operative residential community MG (Section 3-1) operating within a traditional macro-grid utility network (i.e. Eskom - South Africa's national electric power utility). Comparable with many global utilities, Eskom currently offers a Time-of-Use (ToU) pricing structure for the majority of residential consumers [75]. For optimal economic performance, in addition to increasing renewable energy source (RES) self-consumption, it is desired that the controllers minimize electricity costs by considering the deterministic time varying energy rates associated with the ToU pricing structure.

Bill minimization

To target bill minimization, the investigated EMPC strategies can be designed to minimize the following operational cost:

$$J_{\text{bill}} = \sum_{k=0}^{N_p-1} l_{e,\text{bill}}(\cdot) = \sum_{k=0}^{N_p-1} \left[c_{g,\text{imp}}(k)P_{g,\text{imp}}(k) + c_{g,\text{exp}}(k)P_{g,\text{exp}}(k)\right] \cdot \alpha_{\text{bill}}, \tag{4-10}$$

with $\alpha_{\text{bill}} = t_s \cdot \left(60^2 \times 10^3\right)^{-1}$, where $c_{g,\text{imp}}(k)$ [R/kWh] is the price paid for importing energy and $c_{g,\text{exp}}(k)$ [R/kWh] is the profit gained by exporting energy back to the grid[3], both of which are time-varying but known. Note that this objective only considers the economics of the interaction with the utility grid. From an economic perspective, it is therefore assumed that additional operational costs for RESs or loads can be neglected. For the case-study MG this is a reasonable assumption as any additional operational costs for both the DEWHs and photovoltaic (PV) generation units are negligible or fixed, and cannot be modified by the chosen control policy. This assumption does not hold for all other possible MG configurations, thus, in some cases it will be necessary to directly consider additional device specific operational costs (e.g. fuel costs for local diesel generators).

Maximizing PV self-consumption

It is possible that the community may only be interested in maximizing PV self-consumption without consideration of the energy bill. One method that has been suggested is to maximize the so called solar fraction [25], which for any time interval $k \in [0, N]$, is defined as [4]:

$$\phi_s(\cdot) = \frac{\sum_{k=0}^{N} \left[\min\left\{0,\ P_l(k) + P_{\text{pv}}(k)\right\} - P_{\text{pv}}(k)\right]}{\sum_{k=0}^{N} P_l(k)}, \tag{4-11}$$

[3] R is the symbol for the 'Rand', which is the local South African currency.

with,

$$P_l(k) = P_r(k) + \sum_{i=1}^{N_h} P_h(k),$$

where by design $\phi_s \in [0, 1]$, indicates the percentage of total MG load, $P_l(k) \in \mathbb{R}_{\geq 0}$, supplied by local PV generation, $P_{\text{pv}}(k) \in \mathbb{R}_{\leq 0}$, over a given time interval. In an MPC framework, maximising the solar fraction could then be targeted by minimizing the MPC cost,

$$J_{\text{solar}} = -\phi_s(\cdot)|_{k \in [0, N_p - 1]}. \tag{4-12}$$

However, from the outset it is clear that optimizing this metric may not necessarily lead to the desired outcome of maximized self-consumption. Under the assumption that exporting power to the grid is permitted, the objective does not have a unique optimum. With the solar fraction capped at 100%, it will not penalise the export of power to the grid as long as the minimum demand levels are met. Alternatively, to avoid the introduction of hard-constraints to restrict export of power to the grid, one may adopt the MPC objective function:

$$J_{\text{self}} = \sum_{k=0}^{N_p - 1} l_{\text{self}}(\cdot) = \sum_{k=0}^{N_p - 1} \|P_{\text{g}}(k)\|_1, \tag{4-13}$$

which attempts to minimize the energy entering or exiting the MG over the prediction horizon, thereby maximizing the local use of PV generation.

Remark 4.3: While using (4-13) to target PV self-consumption directly may help to ensure maximum utilization of local PV generation, it does not guarantee optimal economic operation. For this reason, some works (e.g. [76, 77]) have indirectly targeted increased self-consumption by applying a bill minimization objective, as in (4-10), which favours the use of PV generation. This indirect approach has the added benefit of responding to grid pricing signals when importing external grid energy is unavoidable. Consequently, it was decided that the controllers implemented in this work would primarily make use of the bill minimization cost function (4-10). This was done in the hope that RES self-utilization would increase because it directly contributes to a reduced energy bill when $c_{g,\text{exp}}(k) < c_{g,\text{imp}}(k)$.

Minimizing consumer discomfort

The successful adoption of a DSM scheme almost always relies on the willingness of consumers to participate in the program. Thus, while users may appreciate the cost savings obtained when targeting bill minimization objectives, they will likely reject a program if it does not sufficiently manage consumer comfort. In the case of DEWHs, consumer comfort is traditionally ensured by introducing temperature constraints for the maximum and minimum water temperatures (cf. (3-8)). The final desired user demand temperature can then be managed manually at the point of use or automatically by using a thermostatic mixing valve. This is the approach that was followed for this thesis.

However, another possibility may be to introduce a weighted performance penalty which penalises the deviation from a desired temperature set-point (i.e. *standard* MPC), e.g.:

$$J_{\text{cd}} = \sum_{k=0}^{N_p - 1} l_{cd}(\cdot) = \sum_{k=0}^{N_p - 1} \sum_{i=1}^{N_h} q_{h,i}^{x} \cdot \left\| x_{h,i}(k) - x_{h,i}^{\text{ref}}(k) \right\|_1, \tag{4-14}$$

where $q^x_{h,i}$ is a cost weighing factor.[4] This type of performance cost is most often used for the control of space heating and cooling systems (e.g. [77, 78]), where maintaining a constant temperature helps to ensure consumer comfort. Similar to [77], in future work it may be interesting to investigate whether it would be beneficial to combine such a discomfort cost with an economic objective to determine the relationship of any economic/discomfort trade-offs.

Multi-objective cost function

In the case where the DSM scheme targets multiple management objectives, it then becomes necessary to simultaneously optimize multiple cost functions. Such a problem falls within the scope of multi-objective optimization which can further complicate control problem formulations, especially when attempting to optimize conflicting objectives. The simplest approach to such problems involves the formation of a combined cost function composed of the scalar weighted sum of the conflicting objectives. Through the introduction of user defined weighting factors, designers can control the trade-offs between the objectives [25]. Alternative methods are based on the generation of Pareto-optimal sets, as detailed in [79].

Chosen case-study MG cost function

As mentioned in Remark 4.3, it was decided that the proposed EMPC controllers would all be designed to primarily make use of bill minimization cost function (4-10). Optimizing this cost will result in reduced energy bills while simultaneously enabling the MG target increase RES self-utilization. The overall MG objective for all EMPC controllers is compactly captured in (4-15). It is composed of two costs, the overall economic operating cost (4-10), along soft-constraint penalty terms (4-9):

$$\begin{aligned} J_{\mathrm{MG}}(k,\, \underset{\sim}{\boldsymbol{V}}(k),\, \underset{\sim}{\boldsymbol{\omega}}_g^{\mathrm{exo}}(k)) &= J_{\mathrm{bill}}(k,\, \underset{\sim}{\boldsymbol{V}}(k),\, \underset{\sim}{\boldsymbol{\omega}}_g^{\mathrm{exo}}(k)) + \sum_{i=1}^{N_h} J_{\mathrm{soft,i}}\left(\underset{\sim}{\boldsymbol{V}}_{h,i}(k)\right) \\ &= q_v^\top(k,\, \underset{\sim}{\boldsymbol{\omega}}_g^{\mathrm{exo}}(k)) \cdot \underset{\sim}{\boldsymbol{V}}(k) + q_\omega^\top(k) \cdot \underset{\sim}{\boldsymbol{\omega}}_g^{\mathrm{exo}}(k), \end{aligned} \tag{4-15}$$

with,

$$\boldsymbol{V}(k) = \begin{bmatrix} V_g^\top(k) & V_{h,1}^\top(k) & \cdots & V_{h,N_h}^\top(k) \end{bmatrix}^\top,$$

where $q_v(k,\, \underset{\sim}{\boldsymbol{\omega}}_g^{\mathrm{exo}}(k))$ and $q_\omega(k)$ are appropriately defined time-varying vectors. These can be easily derived based on the cost components of $J_{\mathrm{MG}}(k,\, \underset{\sim}{\boldsymbol{V}}(k),\, \underset{\sim}{\boldsymbol{\omega}}_g^{\mathrm{exo}}(k))$.

4-2-4 Uncertainty

Modelling and control of complex real-world systems is always subject to some form of uncertainty. Optimization-based DSM approaches, such as EMPC, can either be undertaken in a deterministic or stochastic setting. The former ignores uncertainty, which may result in poor

[4] Note that instead of using a l_1-norm, $\|\cdot\|_1$, one could also use l_∞-norm, $\|\cdot\|_\infty$, or a quadratic cost.

performance or solution infeasibility, especially if optimization signals deviate significantly from their expected values.

Uncertainty is introduced due to modelling inaccuracies, measurement noise, and is inherently present in all signal forecasts. Accurately capturing all these uncertainty sources and formulating tractable problem formulations is not a trivial task. Several methods have been proposed to capture uncertainty for robust control (refer to e.g. [25, 36, 73, 80]). Later, in Section 4-3-3, the thesis presents details of stochastic/robust solution frameworks investigated in this work. For simplicity, as presented in [55, 79], the discussed solution frameworks only consider uncertainty in the prediction of exogenous MG disturbances inputs of (4-8). Thus, any device modelling or state measurement uncertainty is ignored.

The actual exogenous input disturbances acting on the MG are captured in $\boldsymbol{\omega}_{h,i}^{\text{nom}}(k)$ for the uncertain DEWH domestic hot water (DHW) demands, and in $\boldsymbol{\omega}_{g}^{\text{exo}}(k)$ for the exogenous uncertain PV generation and residual electrical demand. For further discussion it is useful to decompose these vectors as:

$$\boldsymbol{\omega}_{h,i}^{\text{nom}}(k) = \hat{\boldsymbol{\omega}}_{h,i}^{\text{nom}}(k) + \breve{\boldsymbol{\omega}}_{h,i}^{\text{nom}}(k) \tag{4-16}$$

$$\boldsymbol{\omega}_{g}^{\text{exo}}(k) = \hat{\boldsymbol{\omega}}_{g}^{\text{exo}}(k) + \breve{\boldsymbol{\omega}}_{g}^{\text{exo}}(k), \tag{4-17}$$

where $\hat{\omega}(k)$ is the disturbance prediction[5] and $\breve{\omega}(k)$ is the stochastic prediction error. It is common for $\breve{\omega}(k)$ to be modelled as a continuous/discrete random variable with an assumed, possibly unknown probability distribution [79]. Additionally, to simplify the application of robust solution methodologies, all disturbances are assumed to be bounded as in [70], i.e.:

$$\underline{\omega}(k) \leq \omega(k) \leq \bar{\omega}(k) \quad \forall k, \tag{4-18}$$

where $\underline{\omega}(k)$ and $\bar{\omega}(k)$ denote the minimum and maximum disturbance bounds respectively. Consequently, all disturbance prediction errors, $\breve{\omega}(k)$, are also bounded. This bounding assumption may seem restrictive, but in general it is justified for most practical systems. For the case-study this is clearly the case; DHW demands are bounded by the maximum household water flow rates, PV generation is limited to the installed capacity and residual electrical demand cannot exceed the circuit breaker protection levels.

4-3 EMPC solution frameworks

With the required EMPC components discussed in the previous section, it is now possible to outline the various solution frameworks that were investigated for the application of EMPC. The thesis considers both deterministic frameworks with ignore uncertainty as well as stochastic and robust techniques, which explicitly manage uncertainty.

4-3-1 Performance bound EMPC (PB-EMPC)

In order to provide a simulated 'optimal' performance reference for the investigated EMPC controllers, it is useful to introduce the notion of PB-EMPC. The PB-EMPC problem formulation investigates the application of EMPC with perfect knowledge of all system dynamics

[5] For this work given by the persistence forecast, cf. Section 3-3-2

and future disturbances [81]. The performance bound (PB) concept is not realizable in practice due to unavoidable uncertainty in system modelling and disturbance predictions of real world systems. However, it does allow one to simulate a given controller structure on historical or synthetic disturbance signal predictions to obtain a **theoretical bound** on achievable performance. The PB-EMPC controller may be formulated as:

$$\text{PB-EMPC}: \quad \min_{\{\underset{\sim}{\boldsymbol{V}}_{h,i}\}_{i=1}^{N_h},\, \underset{\sim}{\boldsymbol{V}}_g} \quad J_{\text{PB}} = J_{\text{MG}}(k,\, \underset{\sim}{\boldsymbol{V}}(k),\, \underset{\sim}{\boldsymbol{\omega}}_g^{\text{exo}}(k)) \tag{4-19a}$$

$$\text{s.t.} \quad \text{MG dynamics/constraints (4-8).} \tag{4-19b}$$

4-3-2 Certainty equivalent EMPC (CE-EMPC)

While explicitly incorporating uncertainty into EMPC formulations is appealing and can theoretically lead to increased control performance, or at least a higher probability of solution feasibility, in practice it is often neglected. Instead, researchers and practitioners make the assumption that all uncertain optimization signals are represented by their expected value, resulting in deterministic or so-called certainty equivalent EMPC (CE-EMPC) [81]. Such methods have been effectively applied in literature, by relying on the inherent robustness provided by the receding horizon MPC feedback mechanism [58].

Under the CE framework the EMPC problem is solved by assuming that the disturbances are given by their forecast values, in other words the optimization problem is solved assuming that forecast error, $\breve{\omega}(k) \equiv 0,\ \forall k$. Consequently, $\underset{\sim}{\boldsymbol{\omega}}_{h,i}^{\text{nom}}(k)$ and $\underset{\sim}{\boldsymbol{\omega}}_g^{\text{exo}}(k)$ of the PB-EMPC problem (4-19) are replaced by their expected (i.e. predicted) values:

$$\mathbb{E}[\underset{\sim}{\boldsymbol{\omega}}_{h,i}^{\text{nom}}(k)] \equiv \hat{\underset{\sim}{\boldsymbol{\omega}}}_{h,i}^{\text{nom}}(k) \tag{4-20}$$

$$\mathbb{E}[\underset{\sim}{\boldsymbol{\omega}}_g^{\text{exo}}(k)] \equiv \hat{\underset{\sim}{\boldsymbol{\omega}}}_g^{\text{exo}}(k). \tag{4-21}$$

With this, the CE-EMPC problem formulation is compactly described by the following constrained finite horizon open-loop optimal control problem:

$$\text{CE-EMPC}: \quad \min_{\{\underset{\sim}{\boldsymbol{V}}_{h,i}\}_{i=1}^{N_h},\, \underset{\sim}{\boldsymbol{V}}_g} \quad J_{\text{CE}} = J_{\text{MG}}(k,\, \underset{\sim}{\boldsymbol{V}}(k),\, \hat{\underset{\sim}{\boldsymbol{\omega}}}_g^{\text{exo}}(k)) \tag{4-22a}$$

$$\text{s.t.} \quad \begin{cases} \text{MG dynamics/constraints (4-8), with:} \\ \underset{\sim}{\boldsymbol{\omega}}_{h,i}^{\text{nom}} := \hat{\underset{\sim}{\boldsymbol{\omega}}}_{h,i}^{\text{nom}}, \\ \underset{\sim}{\boldsymbol{\omega}}_g^{\text{exo}} := \hat{\underset{\sim}{\boldsymbol{\omega}}}_g^{\text{exo}}, \end{cases} \tag{4-22b}$$

where the redefinitions, indicated by ':=', in (4-22b) imply that the CE problem makes use of predicted disturbances which include uncertainty.

CE-EMPC has been employed in several works for DSM in a residential MG setting. In [58], the authors applied a MILP based EMPC strategy to a small-scale MG, with experimental results indicating significant economic savings ($\sim 30\%$) over base-line control methods. Kepplinger et al. [23] proposed a controller based on integer linear programming for the optimal economic control of an individual household's switched DEWH, subject to day-ahead real-time electricity pricing and DHW demand forecasts. In [19], Halvagaard et al. present a similar control strategy for individual solar collector hot water heaters with continuously variable supplementary electric heating elements. The work incorporated both solar energy and DHW demand predictions. Other relevant works include [20, 78, 82] which employ CE-EMPC for the economically optimal control of building energy systems.

4-3-3 Overview of stochastic and robust EMPC

In applications where disturbance forecast uncertainty leads to unacceptable performance degradation, or where robust solution feasibility is paramount; system designers may opt to explicitly consider uncertainty within the optimal control problem formulation. For this reason researchers have extended stochastic and robust optimization techniques for application in MPC. Similar to the extensive research effort that has been applied to the CE approaches, MPC incorporating uncertainty has attracted significant research interest. A full and detailed coverage of stochastic and robust MPC is beyond the scope of this thesis. Interested readers are referred to [83, 84] for a detailed coverage of stochastic MPC and optimization under uncertainty, and to [73, 85–87] for robust MPC. Instead, the thesis will provide a brief overview of the topic and highlight the solution frameworks that were formulated for application of EMPC to the case-study MG.

Remark 4.4: The stochastic/robust formulations for the case-study MG were devised by only directly considering uncertainty in the DHW demand of each DEWH, $\underset{\sim}{\boldsymbol{\omega}}_{h,i}^{\text{nom}}(k)$. Thus, the chosen formulations neglect the prediction uncertainty of the disturbances contained in $\underset{\sim}{\boldsymbol{\omega}}_{g}^{\text{exo}}(k)$ (the uncertain PV generation and residual MG demand). Instead, for these disturbances the problems are again optimized assuming certainty equivalence, i.e. $\underset{\sim}{\boldsymbol{\omega}}_{g}^{\text{exo}}(k) \equiv \underset{\sim}{\hat{\boldsymbol{\omega}}}_{g}^{\text{exo}}(k)$. The decision to neglect these uncertainties was made because, for all practically realisable operation conditions, it was assumed that the utility grid could supply any energy imbalance (see Section 3-4-1), therefore ensuring power balance constraints are always satisfied. Conversely, it will later be shown that adopting the certainty equivalence assumption for the DHW demand leads to significant temperature constraint violations, and that these can be successfully mitigated through the application of robust techniques.

4-3-4 Robust min-max EMPC (MM-EMPC)

Broadly speaking, a control system is considered robust if it maintains stable system operation and ensures that performance specifications are met for a specified range of model and disturbance uncertainties [85]. In the case of EMPC for DSM, robust operation can be achieved by ensuring that optimal control problem remains feasible for all possible realisations of the bounded disturbance inputs. To achieve such a robust operation, researchers introduced the notion of min-max MPC (MM-MPC), which optimizes a performance objective assuming the application of a worst-case disturbance realisation [88].

Similar to the formulation presented by Alavi et al. in [55], an *open-loop* robust MM-EMPC problem for economic MG operation may be defined as :

$$\text{MM-EMPC}: \quad \min_{\substack{\{\underset{\sim}{\boldsymbol{V}}_{h,i}\}_{i=1}^{N_h} \\ \underset{\sim}{\boldsymbol{V}}_g^k}} \max_{\{\underset{\sim}{\boldsymbol{\omega}}_{h,i}^{\text{nom}}\}_{i=1}^{N_h}} \quad J_{\text{MM}} = J_{\text{MG}}(k, \underset{\sim}{\boldsymbol{V}}(k), \hat{\underset{\sim}{\boldsymbol{\omega}}}_g^{\text{exo}}(k)) \tag{4-23a}$$

$$\text{s.t.} \quad \begin{cases} \text{MG dynamics/constraints (4-8), with:} \\ \underset{\sim}{\boldsymbol{\omega}}_g^{\text{exo}} := \hat{\underset{\sim}{\boldsymbol{\omega}}}_g^{\text{exo}}, \end{cases} \tag{4-23b}$$

$$\underline{\omega}_{h,i}^{\text{nom},k} \leq \omega_{h,i}^{\text{nom},k} \leq \bar{\omega}_{h,i}^{\text{nom},k} \quad k = 0, \ldots, N_p, \tag{4-23c}$$

where in contrast to the CE-EMPC problem (4-22), the disturbance vector $\underset{\sim}{\boldsymbol{\omega}}_{h,i}^{\text{nom}}(k)$ is no longer assumed to take on its predicted value, but instead is represented by any value within the defined error bounds (4-23c). The formulation minimizes the worst-case performance cost, which is determined by maximizing J_{MM} with respect to the bounded uncertainty. While the ability to manage all uncertain disturbances is desirable, it is commonly accepted that the requirement can be restrictive, and often leads to overly conservative control actions [73].

Remark 4.5: Care has been taken to identify problem (4-23) as a so-called *open-loop* MM-EMPC formulation. In fact, all the stochastic and robust formulations considered in this work are of the *open-loop* variety. The commonly used *open-loop* approach optimizes a single input sequence over the optimization horizon and therefore does not take into account that future control iterations will be undertaken with state feedback updates (i.e. receding horizon) [73]. This *open-loop* characterization was made by Lee et al. in [88], where they describe a *close-loop* alternative which uses dynamic programming to optimize a sequence of input feed-back control laws (or policies) instead of single input sequences. Unfortunately, this *closed-loop* formulation requires the solution of a very high dimensional multi-stage dynamic programming problem which limits its practical applicability. However, simplified sub-optimal *close-loop* approaches have been proposed (e.g. [85, 87]) which make use of parametrised feed-back laws or close-loop predictions. These are implemented by optimizing control correction efforts to a predetermined linear stabilising feedback law [89].

MILP reformulation

Min-max optimization problems are in general difficult to solve, often involving a significantly increased computational complexity compared to their CE counterpart. Fortunately, the structure of the EMPC problems considered in this work allow (4-23) to be recast as a standard MILP program.

First, defining $\forall i \in \{1, \ldots, N_h\}$:

$$\underset{\sim}{\boldsymbol{\omega}}_{h,i,\min}^{\text{nom}}(k) = \begin{bmatrix} \underline{\omega}_{h,i}^{\text{nom}}(k) & \cdots & \underline{\omega}_{h,i}^{\text{nom}}(k+N_p) \end{bmatrix} \tag{4-24a}$$

$$\underset{\sim}{\boldsymbol{\omega}}_{h,i,\max}^{\text{nom}}(k) = \begin{bmatrix} \bar{\omega}_{h,i}^{\text{nom}}(k) & \cdots & \bar{\omega}_{h,i}^{\text{nom}}(k+N_p) \end{bmatrix}, \tag{4-24b}$$

as the minimum and maximum bounds on disturbance $\underset{\sim}{\boldsymbol{\omega}}_{h,i}^{\text{nom}}$ over the prediction horizon. It can be shown that DEWH state constraints (4-8ab) will hold for all disturbances satisfying disturbance bounds (4-23c), provided the following inequalities hold for all DEWH agents $i \in \{1, \ldots, N_h\}$:

$$H_{hv,i}\underset{\sim}{\boldsymbol{V}}_{h,i} \leq H_{hx,i}x_{h,i}(0) + H_{h\omega,i}\underset{\sim}{\boldsymbol{\omega}}^{\text{nom}}_{h,i,\min} + H_{h5,i} \tag{4-25a}$$

$$H_{hv,i}\underset{\sim}{\boldsymbol{V}}_{h,i} \leq H_{hx,i}x_{h,i}(0) + H_{h\omega,i}\underset{\sim}{\boldsymbol{\omega}}^{\text{nom}}_{h,i,\max} + H_{h5,i}. \tag{4-25b}$$

The proof of this result follows in a straight forward manner using the same arguments presented by Alavi F. in [90, Lemma §4.5.1.].

With this, MM-EMPC problem (4-23) is equivalent to:

$$\text{MM-EMPC (MILP)}: \quad \min_{\{\underset{\sim}{\boldsymbol{V}}_{h,i}\}_{i=1}^{N_h},\, \underset{\sim}{\boldsymbol{V}}_g} \quad J_{\text{MM}} = J_{\text{MG}}(k,\, \underset{\sim}{\boldsymbol{V}}(k),\, \hat{\underset{\sim}{\boldsymbol{\omega}}}^{\text{exo}}_g(k)) \tag{4-26a}$$

$$\text{s.t.} \quad \begin{cases} \text{MG dynamics/constraints (4-8), with:} \\ \underset{\sim}{\boldsymbol{\omega}}^{\text{exo}}_g := \hat{\underset{\sim}{\boldsymbol{\omega}}}^{\text{exo}}_g, \\ \text{(4-8ab) replaced by (4-25),} \end{cases} \tag{4-26b}$$

$$\underset{\sim}{\omega}^{\text{nom},k}_{h,i} \leq \omega^{\text{nom},k}_{h,i} \leq \bar{\omega}^{\text{nom},k}_{h,i} \quad k = 0, \ldots, N_p. \tag{4-26c}$$

For the case-study simulations undertaken in Chapter 5, $\underset{\sim}{\boldsymbol{\omega}}^{\text{nom}}_{h,i,\min}(k)$ and $\underset{\sim}{\boldsymbol{\omega}}^{\text{nom}}_{h,i,\max}(k)$ were determined by computing the element-wise minimum and maximum of all 22,000 day-long DHW scenarios generated in Section 3-3-4. They are represented by the upper and lower bounds of the box plot in Figure 3-4. These same scenarios were used for the scenario-based EMPC methods later discussed in Section 4-3-6.

Applications in literature

The application of MM-EMPC for DSM and the optimal economic control of MGs has been quite limited, with most works instead focusing on the related power system unit-commitment problem (e.g. [91, 92]). With that said, Hans et al. [93] proposed an *open-loop* MM-EMPC strategy for the robust operational control of islanded MGs containing loads, energy storage, uncertain RESs, and traditional thermal generation. Where a certainty equivalent approach exhibited constraint violations, the min-max scheme ensured robust operation by explicitly considering load demand and renewable generation uncertainties. Similarly, Alavi et al. [55] presented an *open-loop* MM-EMPC strategy for the robust economic control of grid-connected MGs with fuel-cell generation and battery storage, subject to uncertain residual load demand. In both works the authors were able to recast the initial min-max formulation (4-23) as a standard MILP problem.

4-3-5 Stochastic EMPC (ST-EMPC)

An alternative to the classical notion of robust MPC, targeted through the min-max formulations, is the class of problems denoted as stochastic MPC. Here, instead of considering unknown bounded uncertainties and minimizing the worst-case performance cost, uncertainties are modelled as random variables and the expected value of the cost function is minimized [83].

Stochastic bounded support (STBS) formulation

Under the assumption that the uncertainty realisations fall within a probability distribution with *bounded* support, i.e. $\underset{\sim}{\boldsymbol{\omega}}_{h,i}^{\mathrm{nom}}(k) \in \Omega_{h,i}^{\mathrm{ST}} \subset \mathbb{R}^{n_h^{\omega} \cdot N_p}$, a STBS-EMPC, alternative to (4-23), is formulated as:

$$\text{STBS-EMPC}: \quad \min_{\{\underset{\sim}{\boldsymbol{V}}_{h,i}\}_{i=1}^{N_h},\, \underset{\sim}{\boldsymbol{V}}_g} \quad J_{\mathrm{STBS}} = \mathbb{E}\left[J_{\mathrm{MG}}(k,\, \underset{\sim}{\boldsymbol{V}}(k),\, \hat{\underset{\sim}{\boldsymbol{\omega}}}_g^{\mathrm{exo}}(k))\right] \tag{4-27a}$$

$$\text{s.t.} \quad \begin{cases} \text{MG dynamics/constraints (4-8), with:} \\ \underset{\sim}{\boldsymbol{\omega}}_g^{\mathrm{exo}} := \hat{\underset{\sim}{\boldsymbol{\omega}}}_g^{\mathrm{exo},} \end{cases} \tag{4-27b}$$

$$\forall\, \underset{\sim}{\boldsymbol{\omega}}_{h,i}^{\mathrm{nom}} \in \Omega_{h,i}^{\mathrm{ST}} \subset \mathbb{R}^{n_h^{\omega} \cdot N_p}, \tag{4-27c}$$

where the expected or average cost is minimized subject to constraints which must hold for every possible realization of the uncertain disturbance, $\underset{\sim}{\boldsymbol{\omega}}_{h,i}^{\mathrm{nom}}(k)$. In general, STBS-EMPC formulations belong to the class of 'semi-infinite' programming problems, which consist of a finite number of decision variables and an infinite number of constraints. Except for special cases, problems belonging to this class are in general hard to solve [94]. Fortunately, if $\Omega_{h,i}^{\mathrm{ST}}$ is bounded in a polytopic set, as is implied by (4-18), then the infinite set of constraints can be compactly captured by a finite set. Furthermore, because the work assumes certainty equivalence for exogenous disturbance $\underset{\sim}{\boldsymbol{\omega}}_g^{\mathrm{exo}}(k)$ (cf. Remark 4.4), the cost does not depend on any uncertain variables, thus the expected cost is evaluated as:

$$J_{\mathrm{STBS}} = \mathbb{E}\left[J_{\mathrm{MG}}(k,\, \underset{\sim}{\boldsymbol{V}}(k),\, \hat{\underset{\sim}{\boldsymbol{\omega}}}_g^{\mathrm{exo}}(k))\right] = J_{\mathrm{MG}}(k,\, \underset{\sim}{\boldsymbol{V}}(k),\, \hat{\underset{\sim}{\boldsymbol{\omega}}}_g^{\mathrm{exo}}(k)). \tag{4-28}$$

As a result, for the case-study MG with cost J_{STBS}, the STBS-EMPC formulation (4-27) is equivalent to the MM-EMPC problem (4-23). Both formulations minimize a deterministic cost subject to dynamic constraints which must hold for all realizations (i.e. including the worst-case) of the bounded uncertain disturbance, $\underset{\sim}{\boldsymbol{\omega}}_{h,i}^{\mathrm{nom}}(k)$.

Stochastic chance-constrained (STCC) formulation

The STBS formulation in (4-27) assumes the presence of uncertainties with *bounded* support. Only under this assumption is it possible to provide guarantees of robust constraint fulfilment [94]. In the case that one assumes the presence of disturbances with *unbounded* support, constraint satisfaction can only be guaranteed to hold with a certain probability through the introduction of probabilistic constraints [95]. These so-called chance-constraints can be used replace constraints which dependent on an uncertain disturbance, with a probabilistic counterpart. It is no longer necessary to satisfy these constraints for all possible uncertainty realizations, but rather they need only be satisfied with a specified probability, $(1-\alpha)$. For the case-study MG, a chance-constrained reformulation of the DEWH state constraints (4-8ab) is given by:

$$\mathbb{P}_{\underset{\sim}{\boldsymbol{\omega}}_{h,i}}\left[H_{hv,i}\underset{\sim}{\boldsymbol{V}}_{h,i} \leq H_{hx,i}x_{h,i}(0) + H_{h\omega,i}\underset{\sim}{\boldsymbol{\omega}}_{h,i}^{\mathrm{nom}} + H_{h5,i}\right] \geq 1-\alpha \quad \forall i \in \{1,\ldots,N_h\}, \tag{4-29}$$

where $\mathbb{P}_{\underset{\sim}{\boldsymbol{\omega}}_{h,i}}[\cdot]$ indicates probability that the constraint holds and $\alpha \in (0,1)$ is the admissible constraint violation parameter, indicating the maximum allowed probability that a constraint may be violated [96]. Note that if α could be set to 0, it would imply that the constraints need to be satisfied with certainty, meaning it would again be considered a hard-constraint and would not be solvable for distributions with unbounded support.

Remark 4.6: The fact that chance-constraints need only be satisfied with a specified probability can be exploited even when one assumes the presence of uncertainties with bounded support. By using chance-constraints it is possible to reduce the conservatism of robust techniques, because it is no longer necessary to satisfy constraints for the scenario of a worst-case disturbance realization. This is particularly useful when the worst-case only occurs with very low probability. With that said, this only applies to systems which are able and willing to tolerate some form of constraint violation, otherwise the use of a MM approach may be warranted.

With chance-constraints (4-29), the STCC-EMPC alternative to STBS-EMPC, (4-27), can be formulated as:

$$\text{STCC-EMPC}: \quad \min_{\{\underset{\sim}{\boldsymbol{V}}_{h,i}\}_{i=1}^{N_h},\, \underset{\sim}{\boldsymbol{V}}_g} \quad J_{\mathrm{STCC}} = \mathbb{E}\Big[J_{\mathrm{MG}}(k,\, \underset{\sim}{\boldsymbol{V}}(k),\, \hat{\underset{\sim}{\boldsymbol{\omega}}}_g^{\mathrm{exo}}(k))\Big] \tag{4-30a}$$

$$\begin{aligned} \text{s.t.} \quad & \text{CE constraints (4-22b)},\\ & \text{DEWH chance-constraints (4-29)},\\ & \underset{\sim}{\boldsymbol{\omega}}_{h,i}^{\mathrm{nom}} \in \Omega_{h,i}^{\mathrm{ST}} \subset \mathbb{R}^{n_h^{\omega}\cdot N_p}. \end{aligned} \tag{4-30b}$$

Notice that this particular formulation of STCC-EMPC includes all CE constraints (4-22b), which implies the inclusion of a CE version of the DEWH state constraints (4-8ab). For a pure chance-constrained formulation, these CE DEWH not required and could be fully replaced by chance-constraints (4-29). They remain included here for use in later scenario-based formulations (cf. Section 4-3-7).

In general, STCC-EMPC frameworks requires the solution to a non-trivial, non-convex optimization problems, which are for the most part are intractable to solve. However, through the use of deterministic approximations and scenario-based techniques tractable formulations do exists (e.g. [95, 97–103]). In the next section, the thesis explores one such framework, the so-called scenario-based approach.

4-3-6 Scenario-based EMPC (SB-EMPC): A tractable stochastic approach

To obtain tractable stochastic problem formulations researchers have turned to approximate solutions of the STCC problem, (4-30), by introducing so-called scenario-based MPC [95, 100–103]. Instead of directly considering uncertainties with continuous probability distributions; the approach approximates the stochastic uncertainty distribution, $\Omega_{h,i}^{\mathrm{ST}}$, by randomly extracting a finite set, $\mathcal{S}_{h,i}^{\boldsymbol{\omega}}$, of N_s representative independent and identically distributed uncertainty realizations, i.e. scenarios.

Consider a system where each scenario realization $\underset{\sim}{\boldsymbol{\omega}}_{h,i}^{\mathrm{nom},[\gamma]}(k) \in \mathcal{S}_{h,i}^{\boldsymbol{\omega}}$ with $\gamma = 1, 2, \ldots, N_s$.

Then the SB-EMPC approximation of STCC problem (4-30) can be formulated as:

$$\text{SB-EMPC}: \quad \min_{\{\underset{\sim}{V}_{h,i}\}_{i=1}^{N_h}, \underset{\sim}{V}_g} \quad J_{\text{SB}} = J_{\text{MG}}(k,\, \underset{\sim}{V}(k),\, \hat{\underset{\sim}{\omega}}_g^{\text{exo}}(k)) \tag{4-31a}$$

$$\text{s.t.} \quad \text{CE constraints (4-22b)},$$

$$\underset{\sim}{x}_{h,i}^{[\gamma]} = \Phi_{hx,i} x_{h,i}(0) + \Gamma_{hv,i} \underset{\sim}{V}_{h,i} + \Gamma_{h\omega,i} \underset{\sim}{\omega}_{h,i}^{\text{nom},[\gamma]} + \Gamma_{h5,i}\,, \tag{4-31b}$$

$$H_{hv,i} \underset{\sim}{V}_{h,i} \leq H_{hx,i} x_{h,i}(0) + H_{h\omega,i} \underset{\sim}{\omega}_{h,i}^{\text{nom},[\gamma]} + H_{h5,i}\,, \tag{4-31c}$$

$$\forall\, \underset{\sim}{\omega}_{h,i}^{\text{nom},[\gamma]} \in \mathcal{S}_{h,i}^{\omega} \quad \gamma = 1, \ldots, N_s, \tag{4-31d}$$

with problem constraints holding for all uncertainty scenarios $\gamma = 1, \ldots, N_s$. Note that the scenario-based state evolutions, (4-31b), need not be evaluated as the DEWH states are not penalised in the considered objective function J_{SB}. Moreover, by inspecting the structure of the scenario-based DEWH constraints (4-31c), it is evident that many of these are redundant. In order to reduce the number of constraints passed to the solver, a simplification by Parisio et al. in [103] highlights that for each DEWH agent i, (4-31c) can be replaced by:

$$H_{hv,i} \underset{\sim}{V}_{h,i} \leq H_{hx,i} x_{h,i}(0) + \left[\max_{\gamma=1,\ldots,N_s} H_{h\omega,i} \underset{\sim}{\omega}_{h,i}^{\text{nom},[\gamma]} \right] + H_{h5,i}\,, \tag{4-32}$$

where the max applies element-wise to $H_{h\omega,i} \underset{\sim}{\omega}_{h,i}^{\text{nom},[\gamma]}$.

Determining a sufficient number of scenarios

Intuitively, it is apparent that the extent to which the scenario-based formulation (4-31) sufficiently approximates the original STCC problem (4-30), is related to the number of scenarios considered, N_s. While an increased number of scenarios may lead to an improved approximation of the uncertainty space, it inevitably results in an additional computational burden. Therefore, it is of great interest to select the smallest number of scenarios that ensures the chance-constraints (4-29) will be satisfied with at least probability $1 - \alpha$.

Several works have been published to provide guidance on the selection of a sufficient number of scenarios. In [100], Campi et al. provide a theorem that ensures that a chance-constraint will be satisfied with at least confidence probability level $\beta \in (0, 1)$ provided that the number of scenarios N_s, meets the following inequality:

$$N_s \geq \frac{1}{\alpha}\left(\ln \frac{1}{\beta} + N_d\right), \tag{4-33}$$

where N_d represents the number optimization variables which for EMPC problems grows linearly with the optimization horizon. For example, each DEWH agent's chance-constraint (4-29) would contain $N_d = n_h^u N_h$ input decision variables. In practice it has been found that using (4-33) can be overly conservative when applied to MPC [103, 104]. The result was derived to provide probabilistic violation guarantees for the open-loop optimization problem solved at a single time instant. Thus, conservatism is introduced because it does not consider the close-loop feedback mechanisms provided by the use of a receding horizon approach [105].

Recently, in [104] Schildbach et al. explored a different approach to reduce the aforementioned conservatism. Their work shows that by interpreting chance-constraints as a 'average-in-time', rather than 'pointwise-in-time' it is possible to drastically reduce the theoretically required number of samples. However, in practice unless strict probabilistic guarantees are desired, it can be useful to treat N_s as a tuning variable which allows a trade-off between the close-loop cost and constraint violations [105]. Thus, for the purpose of this work these theoretical bounds are only used as a guide to select the required number of samples.

Scenario generation

To apply SB-EMPC it is necessary to generate N_s disturbance scenarios which hopefully allow for a reasonable approximation of the underlying stochastic uncertainty distribution. Methods for scenario generation and reduction remain an active area of research (e.g. [106–108]). However, to reduce implementation time it was decided that the use of advanced scenario generation methods would not be considered in this work. Consequently, in order to generate representative scenarios for the uncertain water demand, the thesis again made use of the stochastic DHW profile generation software, presented in Section 3-3-4.

To ensure valid results during the simulation study two independent sets of stochastic synthetic DHW demand scenarios were generated. The first set of data represents the actual DHW profiles that were applied to the DEWHs for close-loop simulation. The second independently generated set of data was used to enable the random extraction of scenarios for the solution of the SB-EMPC problems. In essence, the second set of scenarios can be considered as a large database of historical demand data. As mentioned in Section 3-3-4, each daily demand scenario was generated by assuming equal probability distributions for all days of the year. In total, the scenario data set contained 22,000 independent and identically distributed day long demand realizations. Furthermore, note that the second set of scenarios were also used to determine the upper and lower bounds for the MM-EMPC formulation (cf. Section 4-3-4). The distribution of these scenarios is depicted in the bottom plot of Figure 3-4.

Applications in Literature

Research into the application of stochastic and scenario-based MPC continues to expand. Several works have been undertaken to apply stochastic control schemes for the DSM and optimal control of MGs. In [79], Parisio et al. present a two-stage scenario-based stochastic MPC scheme for the optimal economic/environmental control of MGs with uncertain PV generation and energy demand. The strategy was experimentally tested on a small scale grid-connected MG (1 load, 2 battery storage units, 2 PV generators, 1 fuel cell), and showed improved performance over deterministic controllers. Hans et al. [109] apply a scenario-based stochastic MPC control scheme to an *islanded* MG with uncertain load and wind generation. The stochastic approach was compared to a min-max robust counterpart, with the former realising increased economic performance. However, this improvement could only be achieved by accepting several minor constraint violations. Hovgaard et al. [110], Oldewurtel et al. [81] and Gulin et al. [111] apply chance-constrained stochastic MPC schemes to their respective power management application areas. The latter works all assume that uncertainties are modelled by Gaussian distributions, which allow the chance-constraints to be reformulated as deterministic constraints, thus avoiding the need for scenario-based formulations. While this may seem attractive, in practice limiting uncertainties to Gaussian distributions can be extremely restrictive.

4-3-7 Scenario-based reduced horizon EMPC (SBR-EMPC)

The standard SB-EMPC problem (4-31), requires satisfaction of all scenario-based system evolution constraints (4-31c) over the **entire** prediction horizon N_p. In an attempt to reduce the conservatism associated with this requirement a modified approach has been proposed here as an original contribution.

This modified approach, here referred to as 'scenario-based *reduced horizon* EMPC' (SBR-EMPC), no longer requires that the scenario-based system constraints hold over the entire prediction horizon. Instead, these constraints are now only required to hold for a subset of the prediction horizon, $N_{\text{SBR}} < N_p$. Thereafter, for the remainder of the horizon (i.e. $k = N_{\text{SBR}}+1, \ldots, N_p$) only the CE constraints shall remain active. The SBR-EMPC problem is formally proposed here as:

$$\text{SBR-EMPC}: \quad \min_{\{\underset{\sim}{\boldsymbol{V}}_{h,i}\}_{i=1}^{N_h},\, \underset{\sim}{\boldsymbol{V}}_g} \quad J_{\text{SBR}} = J_{\text{MG}}(k,\, \underset{\sim}{\boldsymbol{V}}(k),\, \hat{\underset{\sim}{\boldsymbol{\omega}}}_g^{\text{exo}}(k)) \tag{4-34a}$$

$$\text{s.t.} \quad \text{CE constraints (4-22b)},$$

$$H_{hv,i}\underset{\sim}{\boldsymbol{V}}_{h,i} \leq H_{hx,i}x_{h,i}^0 + H_{h\omega,i}\underset{\sim}{\boldsymbol{\omega}}_{h,i}^{\text{nom},[\gamma]} + H_{h5,i} \Big\}_{k=0}^{N_{\text{SBR}}}, \tag{4-34b}$$

$$\forall\, \underset{\sim}{\boldsymbol{\omega}}_{h,i}^{\text{nom},[\gamma]} \in \mathcal{S}_{h,i}^{\boldsymbol{\omega}} \Big\}_{k=0}^{N_{\text{SBR}}} \quad \gamma = 1, \ldots, N_s, \tag{4-34c}$$

$$N_{\text{SBR}} < N_p, \tag{4-34d}$$

where $\cdot\}_{k=0}^{N_{\text{SBR}}}$ indicates that for the associated constraints; $H_{[\cdot]}$, stacked vectors $\underset{\sim}{\boldsymbol{V}}_{h,i}$ and scenarios $\underset{\sim}{\boldsymbol{\omega}}_{h,i}^{\text{nom},[\gamma]}$, are redefined over reduced horizon N_{SBR} instead of over the prediction horizon N_p. CE constraints (4-22b) are included and remain active for all $k = 0, \ldots, N_p$.

The SBR-EMPC formulation was proposed with the hope that it would allow designers to target increased cost performance when compared with the standard SB approach. By only considering uncertainty for a reduced horizon, it was reasoned that the controller may be able to provide more optimistic input sequences. It was envisaged that the reduced scenario horizon N_{SBR} would act as a tuning parameter to allow a trade-off between reduced cost and constraint violation. It is thought that the risk of constraint violation can be effectively mitigated, provided sufficient controllable input capacity is available over the reduced horizon.

The effectiveness of the proposed modification is tested via simulations on a case-study MG in Chapter 5.

4-4 Optimization methods and complexity considerations

MPC schemes require the formulation of optimal control problems that can be solved efficiently on a real-time basis (i.e. online). To avoid the use of sub-optimal and heuristic optimization methods, which cannot guarantee optimal problem solutions, this thesis limited its focus to problem formulations for which efficient optimal solution methods exist.

For hybrid systems such as the considered residential MG, optimal solution methods are in general only available if one restricts the problem formulation to linear or quadratic cost functions, subject to discrete linear or piecewise affine (PWA) system dynamics. In such cases, the optimal control problem can be cast as a MILP or mixed-integer quadratic programs (MIQPs), which for medium-scale problems can be efficiently solved using a number of commercial and open-source solvers. Consequently, all of the EMPC problems developed in this work have been formulated as MILPs. Nevertheless, it is well known that such MILP and MIQP problems are NP-complete, meaning that in the worst case, the solution time grows exponentially with the problem size [42]. Consequently, for the case-study MG it becomes evident that for an increasing prediction horizon N_p or a large number of agents, N_h, the centralized control strategy eventually cannot be solved to optimality within a single sampling interval. For the purpose of this thesis, these issues are mitigated by only considering MGs of sufficiently small dimension that optimal solutions can be found in a small fraction of the sampling interval.

4-5 Discussion

This chapter presented a detailed overview of EMPC and developed several control problem formulations for the optimal control and DSM of residential MGs. The subject has been extensively covered in current literature and yet it remains an area of continuous active research. Despite significant efforts to advance the field, many research issues remain open. With almost all works exclusively implemented in simulation, the real-world performance of the proposed schemes remains to be proven. Consequently, concerns have been raised that some works appear too focused on mathematical formalisms, resulting in unrealistic simplifying assumptions, with limited applicability to real world scenarios [25]. In conclusion, research investigations which simply attempt to apply, test and evaluate proposed methods on real-world systems, have the potential to deliver significant and valuable academic findings. In the next chapter, the thesis implements and simulates the proposed EMPC controllers on a MG closely modelled on real world community and compares them to the currently used TSRB control method. It is hoped that this study, brings the research a step closer to being applied in reality.

Chapter 5

Case-study: EMPC Applied to a Residential Microgrid

The hybrid system modelling structures relevant to the case-study microgrid (MG) were presented in Chapter 3. Following this, Chapter 4 outlined the economic model predictive control (EMPC) formulations and solution frameworks that were constructed to enable the optimal control of such a MG. In this chapter, the thesis combines all of these components for an illustrative simulation based comparison of the developed controllers. As a point of reference, the EMPC controllers were evaluated against the currently used benchmark thermostatic rule-based (TSRB) control law.

First, Section 5-1 provides a brief overview of the software package that was developed to enable the implementation and simulation of the hybrid MPC/EMPC controllers. Next, Section 5-2 and 5-3 detail the case-study MG and controller parameters used for the simulation set-up. The case-study results for both a single agent and multi-agent cases are then respectively presented in Section 5-4 and 5-5. The chapter closes with the case-study conclusions in Section 5-6.

5-1 Simulation and control software environment

All controllers were implemented and simulated using a custom open-source `Python` based software package, `PyHybridControl`, developed during this thesis. The software makes use of `CVXPY`, a `Python` embedded modelling language for convex optimization [112]. `CVXPY` acts as an interface between `PyHybridControl`'s control problem formulations and a variety of optimization problem solvers (e.g. `Gurobi`, `CPLEX`, `GLPK`, etc.). In this case-study, all optimal control problems were solved using `Gurobi` [113].

`PyHybridControl` was designed using an object-oriented programming framework. This enabled the development of a modular software package that provides users with the flexibility to construct and simulate hybrid MPC/EMPC controllers for general mixed logical dynamical (MLD) systems. In other words, `PyHybridControl` was not only developed for this specific case-study. It was also created to provide researchers with a base framework for future implementation and development of hybrid optimal control.

At this early stage, `PyHybridControl` provides the following main features, it enables users to:

- Generate symbolic and numerical models of hybrid systems using the general MLD model structure defined in (2-5).
- Simulate generic hybrid MLD models.
- Construct independent system agents which can then be combined for multi-agent control.
- Generate and simulate hybrid model predictive control (MPC) controllers with custom convex cost functions.

The `PyHybridControl` source code is distributed under the permissive MIT licence and can be accessed at: https://github.com/michchr/pyhybridcontrol.

5-2 Case-study MG parameters

Table 5-1 outlines the MG parameters used for all simulations undertaken in this case-study chapter. For all cases the controllers were simulated with both $T_{h,i}^{\max} = 65°\text{C}$ and $T_{h,i}^{\max} = 80°\text{C}$. The physical MG on which this case-study is based currently limits $T_{h,i}^{\max}$ to 65°C, a maximum operating limit specified by the DEWH manufacturer. The increased temperature bound is included in this study to test a hypothesis that additional heat storage capacity would allow for greater cost savings. To implement the higher temperature limit in reality will require DEWHs with greater operating ranges along with thermostatic mixing valves to ensure over temperature water is not supplied to the user.

5-2-1 Utility grid Time-of-Use (ToU) pricing and regulations

As mentioned in Section 4-2-3, the case-study MG operates in a location where the local energy utility, Eskom, provides residential customers with a ToU payment structure [75]. Under this structure, the price of electricity in the future is known well in advance and remains constant during given time intervals. Figure 5-1 shows Eskom's ToU price for electricity imports over a two week period. In general, the price curve repeats on a weekly cycle with some modification based on the season of the year or presence of a public holiday[1].

Furthermore, in many locations Eskom currently does not provide feed-in rates for the excess generation of electricity by residential customers. The case-study MG operates under the regulation that energy export to the grid is not permitted. All EMPC controllers were therefore set to optimize the chosen MG objective (4-15) under that assumption that $c_{g,\text{exp}} = 0.00\,\text{R/kWh}$. By not encouraging exports, it was expected that the controllers would increase the self-utilization of local renewable energy source (RES) generation.

[1] For simplicity public holiday prices were neglected in this study.

Table 5-1: Simulation system parameters for the case-study MG containing N_h domestic electric water heater (DEWH) agents $i \in \{1, \ldots, N_h\}$.

Parameter	**Description**	**Value**	**Unit**
	DEWH agent physical parameters		
$A^s_{h,i}$	Surface area of water tank	2.35	$[\mathrm{m}^2]$
C_w	Thermal capacity of water	4181.6	[J/(kg K)]
$m_{h,i}$	Total mass of water in tank	150.0	[kg]
$P^{\mathrm{Nom}}_{h,i}$	Heating element power	3000.0	[W]
$T^{\mathrm{Nom}}_{h,i}$	Nominal hot water withdrawal temperature	45.0	[°C]
$T^{\infty}_{h,i}$	Ambient temperature surrounding tank	25.0	[°C]
$T^{w}_{h,i}$	Tank inlet water temperature	15.0	[°C]
$U_{h,i}$	Standing heat loss co-efficient	0.88	$[\mathrm{W}/(\mathrm{m}^2\,\mathrm{K})]$
	DEWH agent operating parameters		
$T^{\max}_{h,i}$	Maximum tank temperature bound	65.0 or 80.0	[°C]
$T^{\min}_{h,i}$	Minimum tank temperature bound	50.0	[°C]
$\mathbb{E}\left[\omega^{\mathrm{Nom}}_{h,i}\right]$	Long term mean daily hot water demand	200.0	[L/d]
	MG demand and generation parameters		
$P^{\max}_{\mathrm{pv}}$	Maximum PV generation capacity	$2000 \cdot N_h$	[W]
$\mathbb{E}[P_r]$	Long term mean residual MG power demand	$1200 \cdot N_h$	[W]
	Utility grid parameters		
$c_{g,\mathrm{imp}}(k)$	Grid import power price	ToU (Section 5-2-1)	[R/kWh]
$c_{g,\mathrm{exp}}(k)$	Grid export power price	0.00	[R/kWh]
$P^{\max}_{g}$	Maximum grid import power bound	$(1 \times 10^4) \cdot N_h$	[W]
$P^{\min}_{g}$	Maximum grid export power bound	$-(1 \times 10^4) \cdot N_h$	[W]

Remark 5.1: Even though power export is not physically permitted for the case-study MG; for simulation purposes the controllers are allowed to export electricity to the grid, but do so with no cost benefit. In practice this export would be curtailed to zero by lower-level photovoltaic (PV) inverter controls to avoid export to the grid. In other words, $P_{g,\mathrm{exp}}(k)$ represents the available PV generation capacity that is not locally utilized and that needs to be curtailed. The simulated export power is used to compute the PV generation self-utilization. Moreover, note that the PV generation capacity of 2000W per household (cf. Table 5-1) was deliberately set higher than necessary. If this was not done, it would not have been possible to evaluate whether controllers improved self-utilization because the base MG load would always utilize all available capacity. In practice, designers would need to consider the level of self-utilization that can be achieved for a given controller when determining the economically optimal sizing of PV generation.

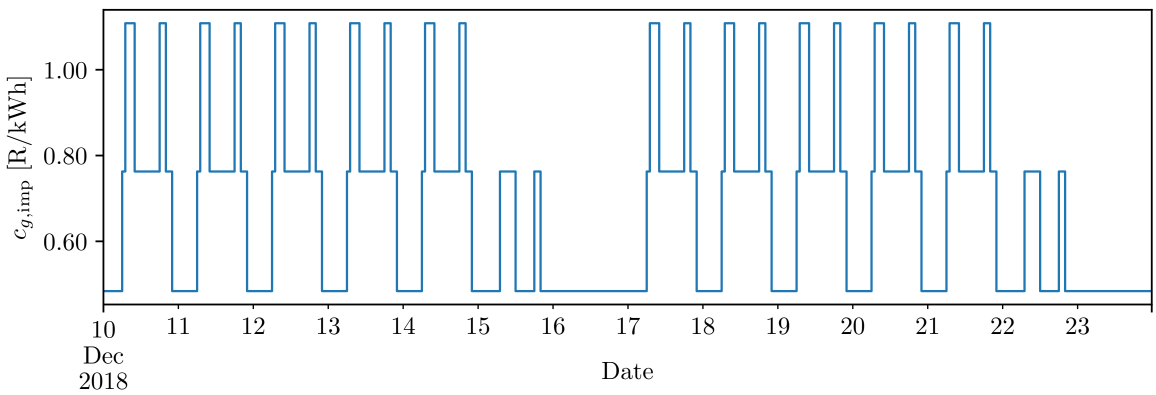

Figure 5-1: Eskom's ToU electricity import price provided to residential customers in South Africa [75]

5-2-2 Simulation data and scenarios

To enable the simulation of the case-study MG, it was necessary to make use of various data sources to emulate the uncontrollable exogenous inputs. For both the PV generation and MG residual demand, the simulations make use of actual historical data obtained from Solar Africa®, as outlined in Section 3-3-3. For the simulation of applied domestic hot water (DHW) profiles the case-study relies on the '*DHWcalc*' synthetic demand generation software package, discussed in Section 3-3-4. The generation of stochastic scenarios for the scenario-based controllers was also made using this software, with the exact methodology discussed in Section 4-3-6.

5-3 Case-study controllers: parameters and performance metrics

This section lists the considered controllers and details the user defined control or 'tuning' parameters that are available to modify system performance. It concludes by defining the close-loop performance metrics that were used to compare the considered controllers.

5-3-1 Economic model predictive controllers (EMPCs)

With reference to Chapter 4, the case-study implemented and evaluated the following EMPC controllers:

- **PB-EMPC** (Performance bound) - given by problem (4-19)
- **CE-EMPC** (Certainty equivalent) - given by problem (4-22)
- **MM-EMPC** (Min-max) - given by problem (4-23)
- **SB-EMPC** (Scenario-based) - given by problem (4-31)
- **SBR-EMPC** (Scenario-based reduced) - given by problem (4-34).

All EMPC controllers were optimized subject to MG objective (4-15). Furthermore, while they all utilize linearised DEWH MLD model (3-9) for control action computation; a discretized version of the linear parameter-varying (LPV) DEWH model (3-3) was used for close-loop simulation (cf. Section 3-2-2).

EMPC parameters

Given the physical system parameters in Table 5-1, the above mentioned EMPC controller formulations, and the chosen MG cost function (4-15); the only remaining 'tunable' EMPC control parameters are (where applicable):

- N_p - prediction horizon for each controller.
- $q^{\mu}_{h,i}$ - the soft constraint penalty weights for DEWH temperature bounds.
- N_{SBR} - reduced scenario horizon (for SBR-EMPC controller).
- N_s - number of stochastic scenarios (for SB controller types).
- t_s - discrete sampling time.

This illustrative simulation study provides a preliminary investigation of the effects of varying some of these parameters, while others remain fixed. The fixed parameters are shown in Table 5-2.

Table 5-2: Fixed EMPC controller parameters.

Parameter	Value
t_s	15 min
N_s	20

The sampling time t_s was fixed to 15 minutes as this provides a sufficiently high sampling frequency to capture the DEWH dynamics while not requiring excessively large prediction horizons. Moreover, the maximum available input switching frequency is given by the sampling time. If this is too high it can lead to the premature failure of actuation hardware. While excessive switching can be mitigated by adding additional switching constraints, this leads to increased problem complexity. For the chosen sampling time, excessive switching frequency does not pose an issue.

The investigated scenario-based controllers also make use of a fixed number of scenarios, N_s. The literature for selecting a suitable number of scenarios was presented in Section 4-3-6. However, as mentioned therein, the theoretically suggested required number of samples have often been found to be conservative in practice. By treating N_s as a tuning parameter, it was found that $N_s = 20$, provided sufficiently robust operation while still allowing the work to highlight a cost/constraint violation trade-off.

5-3-2 Thermostatic rule-based (TSRB) benchmark controller

A thermostatic rule-based controller is simulated as a performance benchmark against which the EMPC controllers can be compared. The thermostatic control law for each DEWH agent, presented in (3-7) is restated below:

TSRB :

$$u_{h,i}(k) = \begin{cases} 1, & \text{if } x_{h,i}(k) \leq T_{h,i}^{\text{on}} \text{ (heating element on)} \\ 0, & \text{if } x_{h,i}(k) \geq T_{h,i}^{\text{off}} \text{ (heating element off)} \\ u_{h,i}(k-1), & \text{if } T_{h,i}^{\text{on}} < x_{h,i}(k) < T_{h,i}^{\text{off}} \text{ (maintain previous input).} \end{cases}$$

Thermostatic controller parameters

Table 5-3: TSRB controller set points.

Parameter	Value
$T_{h,i}^{\text{off}}$	$T_{h,i}^{\max} - 4\,°\text{C}$
$T_{h,i}^{\text{on}}$	$T_{h,i}^{\max} - 12\,°\text{C}$

For the simulation study $T_{h,i}^{\text{on}}$ and $T_{h,i}^{\text{off}}$ were set as shown in Table 5-3.

5-3-3 Closed-loop performance metrics

Many metrics can be used in order to compare the performance of the different controllers. The metrics considered during this study are briefly outlined below. Each metric is evaluated over the entire simulation duration, N_t. All close-loop performance metrics stated in this chapter are computed over a simulation period of 3 weeks.

Total electricity bill

The primary metric considered is the closed-loop economic performance, $J_{\text{bill}}^{\text{cl}}$. This cost represents the actual energy bill that would need to be paid by the residential community. Therefore, it excludes any soft-constraint penalty costs. The close-loop electricity bill is derived from (4-10) with $c_{g,\text{exp}}(k) \equiv 0$:

$$J_{\text{bill}}^{\text{cl}} = \sum_{k=0}^{N_t} \left[c_{g,\text{imp}}(k) P_{g,\text{imp}}(k) \right] \cdot \alpha_{\text{bill}}. \tag{5-1}$$

DEWH temperature bound violations

The energy bill cannot be considered in isolation. If this were the case, the optimal solution would be to switch-off all devices and use no electricity. To ensure that consumer comfort is maintained, minimum energy requirements must be met. For the case-study MG these requirements are assured by maintaining the DEWH temperatures within certain bounds. If the tank temperatures drop too low, users will not have access to hot water. A metric to capture this performance is the sum total violation of temperature constraints over the simulation horizon:

$$\begin{bmatrix} T_{\text{vio}}^{\text{over}} \\ T_{\text{vio}}^{\text{under}} \end{bmatrix} = \sum_{k=0}^{N_p} \sum_{i=1}^{N_h} \mu_{h,i}(k), \tag{5-2}$$

where $T_{\text{vio}}^{\text{over}}$ and $T_{\text{vio}}^{\text{under}}$ are the summation of temperature violations over $T_{h,i}^{\max}$ and below $T_{h,i}^{\min}$ respectively. These are computed using the DEWH slack variables, $\mu_{h,i}(k)$.

RES self-consumption

The final considered metric is the self-consumption of local RES generation, in this case PV. Because MG export is prohibited in the case-study (see Remark 5.1), it is desired that the self-consumption be as high as possible. Self-consumption, $\nu_{\text{self}}^{\text{cl}} \in [0, 1]$, is computed as the fraction of local generation not exported to the grid:

$$\nu_{\text{self}}^{\text{cl}} = \frac{\sum_{k=0}^{N_t} P_{\text{pv}}(k) - \sum_{k=0}^{N_t} P_{g,\text{exp}}(k)}{\sum_{k=0}^{N_t} P_{\text{pv}}(k)}. \tag{5-3}$$

5-4 Single agent case

In this section, the thesis investigates the application of a suite of controllers for a MG containing a single DEWH, i.e. $N_h = 1$. By considering only one agent, this allowed for more rapid testing and simplified analysis. An assumption is made that performance trade-offs observed for the single agent case will likely manifest in a similar manner for a multi-agent case. For the single agent case, simulations are run to illustrate the effects of varying the control parameters not listed in Table 5-2. Furthermore, as mentioned in Section 5-2, the simulations are run for two different DEWH upper temperature bounds.

5-4-1 Varying temperature bound soft-constraint penalties

To limit the remaining number of free control parameters, it was further decided to fix the temperature bound soft-constraint penalties. The fixed penalty weights were determined after performing the following guiding simulation.

All the EMPC controllers investigated make use of soft-constraint penalty function (4-9), restated below[2]:

$$J_{\text{soft},i}(k) = \rho_{h,i}(k) \left\| q_{h,i}^{\mu} \odot \mu_{h,i}(k) \right\|_1 \quad \forall i \in \{1, \ldots, N_h\},$$

[2] '$\odot$' indicates the Hadamard element-wise product.

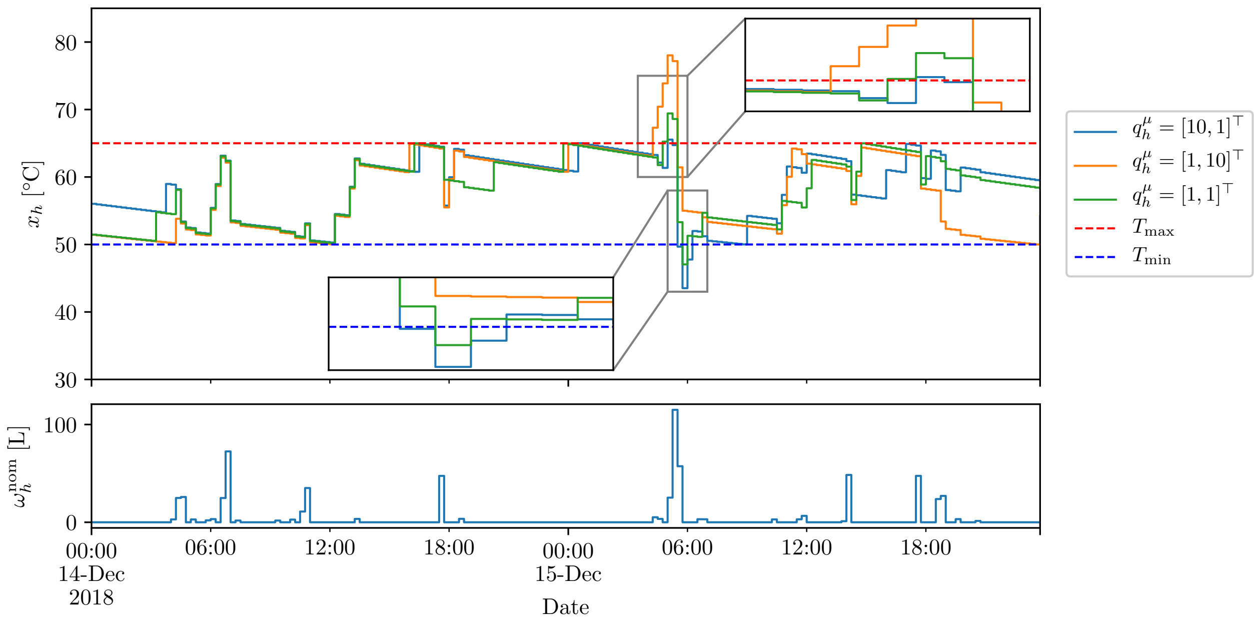

Figure 5-2: Single agent: closed-loop simulation of PB-EMPC controller to demonstrate the effects of various relative soft-constraint penalties q_h^μ. Top plot: temperature trajectories; Bottom plot: actual applied DHW demand profile.

In an attempt to ensure that this penalty function was exact, the following heuristic was used to set the over-all weighting parameter $\rho_{h,i}(k)$:

$$\rho_{h,i}(k) = \sum_{k=0}^{N_p-1} \Big[\alpha_{\text{bill}} P_{h,i}^{\text{nom}} \cdot c_{g,\text{imp}}(k)\Big], \tag{5-4}$$

with $\alpha_{\text{bill}} = t_s \cdot \left(60^2 \times 10^3\right)^{-1}$. The idea behind this heuristic, is that $\rho_{h,i}(k)$ will always be greater that the maximum open-loop economic cost per agent, if the combined sum violation of any agent's temperature bounds exceeds an amount greater than 1°C over the prediction horizon.

Table 5-4: Parameter cases for the relative soft-constraint penalty q_h^μ.

Parameter	Case	Description
q_h^μ	$[1\ 1]^\top$	Equal weight on upper and lower bound violation
	$[10\ 1]^\top$	Increased weight on upper bound violation
	$[1\ 10]^\top$	Increased weight on lower bound violation

Using penalty function (4-9) with $\rho_{h,i}(k)$ governed by (5-4), the EMPC controllers were simulated with the relative weighting factor q_h^μ shown in Table 5-4. For clarity, these parameters were only simulated using the PB-EMPC controller with prediction horizon, $N_p = 48$. The resultant output trajectories for the varying relative penalties are shown in Figure 5-2. From the plot it can be seen that at approximately 06:00 on 15th December the bounds needed to be violated due to a large DHW demand disturbance ω_h^{nom}. Given that the tank capacity is only 150L, this violation could not be avoided. However, as expected it can be seen that the relative penalties exhibit their intended effect. With equal weights the violation is shared approximately equally between the upper and lower bounds. Alternatively, by applying additional weight to the upper or lower bound, one is able to shift the violation to the opposite bound.

The upper temperature bounds are normally dictated by physical limitations which ensure safe operation as well as reducing the risk of over-temperature water being supplied to users. Therefore, it was decided that an increased penalty would be applied to the upper bound. Consequently, for all subsequent simulations $q_{h,i}^{\mu}$ was fixed at:

$$q_{h,i}^{\mu} = \begin{bmatrix}10 & 1\end{bmatrix}^{\top}. \tag{5-5}$$

5-4-2 Controller performance comparison

With the majority of EMPC controller parameters fixed, it was possible to perform a single agent simulation campaign to compare the controllers and investigate the impacts of changing prediction and reduced scenario horizons, N_p and N_{SBR}, respectively. The horizons and maximum temperature bounds were varied as shown in Table 5-5.

Table 5-5: Varying parameter cases for single agent EMPC simulations.

Parameter	Cases	Description
N_p	$\{12, 24, 48\}$	3, 6 or 12 hour control prediction horizon
N_{SBR}	$\{4, 6, 8\}$	1, 1.5 or 2 hour reduced scenario horizon for SBR controller (see Section 4-3-7)
$T_h^{\max}$	$\{65°\text{C}, 80°\text{C}\}$	Maximum temperature bounds

The controllers were all simulated with a simulation duration of 3 weeks ($N_t = 2016$ steps). For each varied parameter the controllers were simulated with 10 different DHW demand profiles, with the final results presented as an average of these. Note that the same 10 demand profiles were applied to each controller. The mean control problem solution times per time step across all EMPC controllers are shown in Table 5-6. These times are negligible compared to the 15min sampling time.

The performance metrics outlined in Section 5-3-3 were evaluated and plotted in Figure 5-3 and Figure 5-4. For the energy bill savings and self-consumption metrics the results are presented as a percentage increase/decrease relative to the performance of the associated thermostatic rule-based (TSRB) controller. As previously mentioned, the simulations were undertaken for two different maximum DEWH temperature bounds, $T_h^{\max} = 65$ or 80°C, with the latter implying increased heat storage capacity. Before discussing the results, it is important to note that the savings indicated in the plots for $T_h^{\max} = 80$°C are with respect to a TSRB controller with increased set-points (i.e. as per Table 5-3). Due to increased thermal losses with the higher set-point, the absolute costs of the controller also increase.

Consequently, care must be taken when interpreting the savings achieved with the higher temperature bound. The same applies to the multi-agent case.

Table 5-6: Single agent mean computation times across all EMPC controllers.

Prediction horizon N_p	**Mean solver time per step**
12	2.1ms
24	5.7ms
48	52.7ms

5-4-3 Results discussion

The following discussion relates to the single agent controller performance results presented in Figure 5-3 and Figure 5-4. As expected, in all cases the PB-EMPC controller outperforms all other controllers. However, this performance is **not attainable in practice** as it assumes perfect knowledge of all disturbances and can only be viewed as representing a theoretical limit on performance. Hence, it is not discussed further. In almost all cases the EMPC controllers outperform the TSRB controller in terms of cost savings, particularly when considering the increased temperature bound. Furthermore, with the exception of CE-EMPC and other minor cases, the EMPC controllers result in reduced constraint violations.

In terms of cost savings, CE-EMPC provides the greatest realizable savings of 4% and 9% for the respective considered temperature bounds. However, as the controller does not directly account for disturbance uncertainty, it attains by far the greatest temperature constraint violations (note the log scale). These violations may not be acceptable in practice. In Figure 5-5, examples of the magnitude of these violations are shown for the multi-agent case.

It was observed that MM-EMPC attains the worst cost performance, this was to be expected as it represents the most conservative approach to EMPC. In terms of constraint violations, MM-EMPC in general performs very well. It does exhibit some over-temperature violations, but inspection of the data finds that these violations are minor at any time instant. It is thought that these violations are due to the extreme nature of the disturbance cases considered by the MM approach. They force the controller to find a compromised state of violation between the upper and lower temperature bounds. Overall the controller exhibits the lowest realizable under temperature violations.

The SB-EMPC controller achieves modest cost savings. Interestingly, these savings are largest for the shortest prediction horizon. It is reasoned that larger horizons require the controller to consider increased uncertainty which may lead to the unnecessary expansion of state trajectories over the prediction horizon. A method to combat this expansion is presented by Alavi F. in [90]. By using an affine disturbance feedback policy parametrization, his work showed significantly increased cost performance when compared with the '*open-loop*' EMPC approach. The application of such a feedback parametrization is suggested as a possible area for future work.

In this work, a heuristic to tackle the loss of performance by the standard SB-EMPC approach, was to implement the proposed SBR-EMPC controller. For a minor increase in constraint

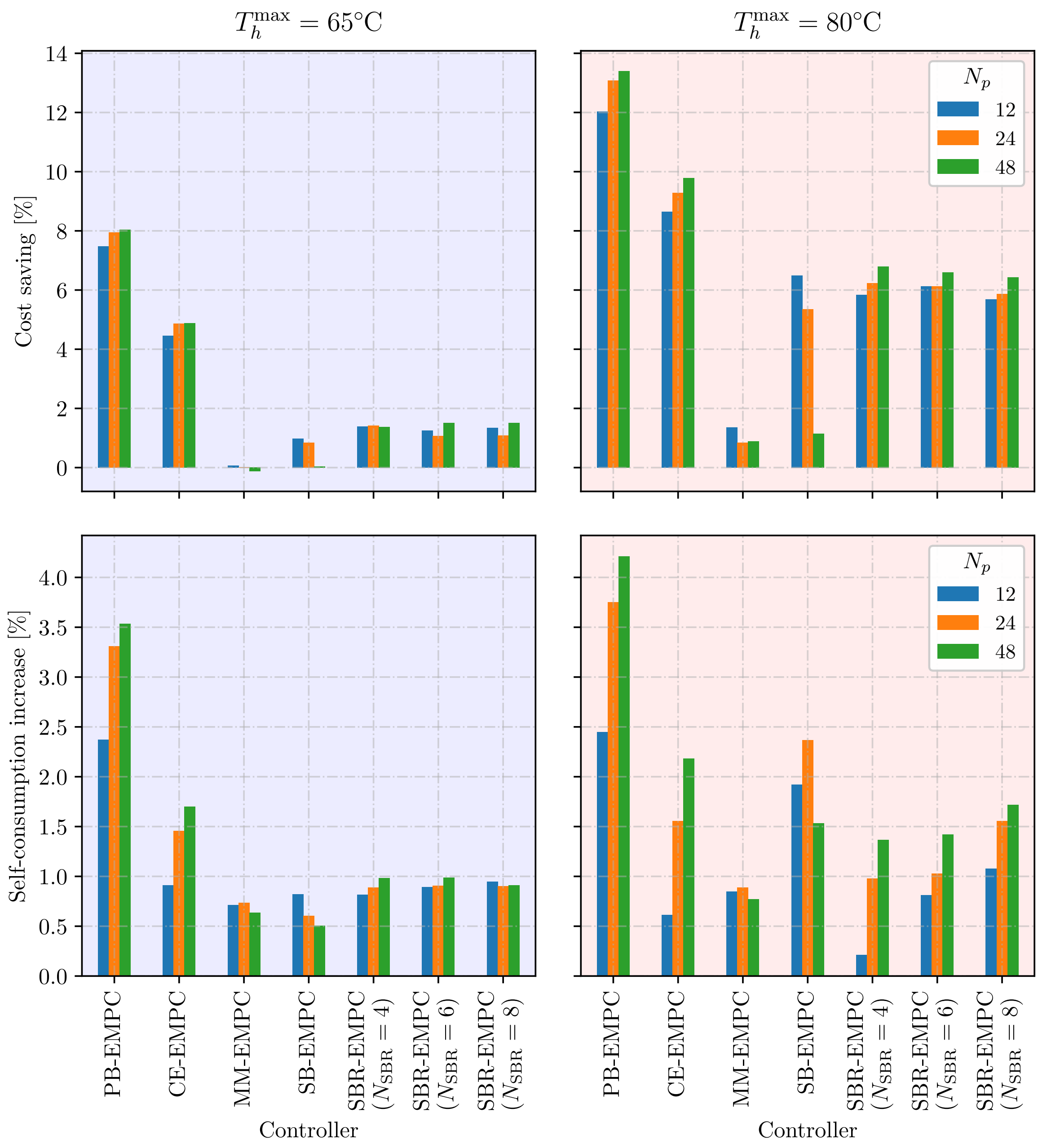

Figure 5-3: Single agent: closed-loop performance comparison of the simulated EMPC controllers relative to the associated thermostatic rule-based (TSRB) controller (i.e. $T_h^{\max}$ is set as indicated). Performance is compared for various prediction horizons, N_p, and reduced scenario horizons, N_{SBR} (for the SBR controller). Each metric is obtained as the average of 10 simulations over a simulation horizon of 3 weeks ($N_t = 2016$ steps), each with different actual DHW demand profiles. Top row: cost savings relative to TSRB; Bottom row: increase in self-consumption relative to TSRB; Left column: $T_h^{\max} = 65°\mathrm{C}$, Right column: $T_h^{\max} = 80°\mathrm{C}$.

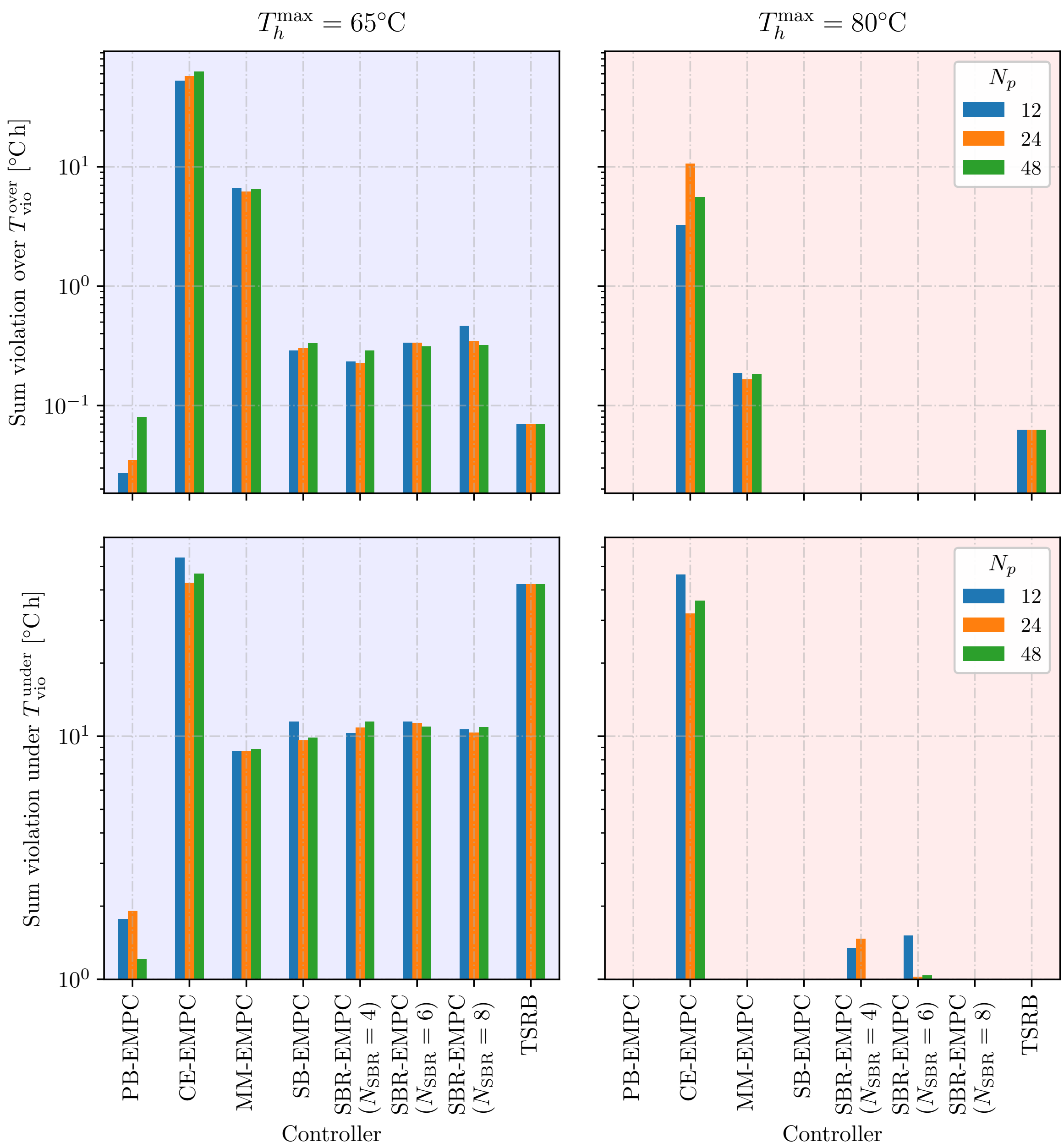

Figure 5-4: Single agent: comparison of the simulated EMPC controller's constraint violations in closed-loop when compared with the associated thermostatic rule-based (TSRB) controller (i.e. $T_h^{\max}$ is set as indicated). Sum total violations are compared for various prediction horizons, N_p, and reduced scenario horizons, N_{SBR} (for the SBR controller). Each metric is obtained as the average of 10 simulations over a simulation horizon of 3 weeks ($N_t = 2016$ steps), each with different actual DHW demand profiles. Top row: sum violation over $T_h^{\max}$; Bottom row: sum violation under $T_h^{\min}$; Left column: $T_h^{\max} = 65°\mathrm{C}$; Right column: $T_h^{\max} = 80°\mathrm{C}$.

violations, the cost performance of SB-EMPC was improved (if only marginally) by making use of a reduced uncertainty scenario horizon. It was found that shorter reduced scenario horizons, N_{SBR}, in general provided marginal cost improvements, although sometimes with the trade-off of increased constraint violations.

As a final point of discussion, it is noted that the EMPC controllers all make some marginal improvement in the level of self-consumption of PV generation when compared to the TSRB controller. However, with a realizable increase of at most 1-2%, it has to be questioned whether the current setup would provide sufficient justification to increase the capacity of local PV generation. Especially given that exporting power to the grid is not permitted.

5-5 Multi-agent case

Applying EMPC for the demand side management (DSM) of a multi-agent MG represents the overarching objective of this thesis. After successfully simulating the controllers in a single agent setting, application to a multi-agent case followed in a straight forward manner. To maintain acceptable simulation times, a case-study MG with $N_h = 20$ agents was considered. All fixed parameters used for the single agent case remained fixed at the same, constant values. The only change in parameters was an increase in PV generation and residual MG power demand, as well as the maximum and minimum utility grid power bounds. These parameters are all scaled linearly with N_h as outlined in Table 5-1.

5-5-1 Controller performance comparison

For the multi-agent case a limited set of simulations were undertaken. The parameters used for the multi-agent simulations are shown in Table 5-7. All parameters not explicitly noted remain fixed as indicated in previous sections.

Table 5-7: Parameter cases for multi-agent EMPC simulations.

Parameter	**Cases**	**Description**
N_h	20	Number of DEWHs/households
N_p	48	12 hour control prediction horizon
N_{SBR}	8	2 hour reduced scenario horizon for SBR controller (cf. Section 4-3-7)
$T_{h,i}^{\max}$	$\{65°\mathrm{C}, 80°\mathrm{C}\}$	Maximum temperature bounds

As with the single agent case, all controllers were simulated over a simulation horizon of 3 weeks ($N_t = 2016$ steps). For both simulation cases the same actual DHW demand disturbances were applied, along with the same PV generation and residual demand profiles. The state trajectories for all agents corresponding to cases $T_{h,i}^{\max} = 65°\mathrm{C}$ and $T_{h,i}^{\max} = 80°\mathrm{C}$, are plotted in Figure 5-5 and Figure 5-6 respectively. The corresponding close-loop performance metrics for both cases, computed over the entire simulation horizon, can be found in Table 5-8.

5-5-2 Results discussion

Table 5-8: Multi-agent $N_h = 20$: closed-loop performance comparison of the simulated EMPC controllers relative to the associated thermostatic rule-based (TSRB) controller (i.e. $T_h^{\max}$ is set as indicated). Performance metrics are computed over a 3 week simulation horizon ($N_t = 2016$ steps).

	PB	**CE**	**MM**	**SB**	**SBR**	**TSRB**
$N_p = 48$, $N_{\text{SBR}} = 8$, and thermal upper bound $T_{h,i}^{\max} = 65$°C						
Total bill $J_{\text{bill}}^{\text{cl}}$ [R]	5688.45	6080.36	6419.07	6407.83	6328.54	6485.39
Cost savings [%]	12.29	6.25	1.02	1.20	2.42	-
Self-consumption $\nu_{\text{self}}^{\text{cl}}$	0.84	0.77	0.75	0.74	0.74	0.72
Self-consumption increase [%]	12.64	5.51	3.01	2.46	2.90	-
Violation over $T_{\text{vio}}^{\text{over}}$ [°C h]	1.76	1013.18	82.40	8.63	7.41	0.97
Violation under $T_{\text{vio}}^{\text{under}}$ [°C h]	37.20	819.90	369.26	265.60	233.99	874.28
Mean solver time per step [s]	2.41	1.44	0.28	2.67	1.19	-
$N_p = 48$, $N_{\text{SBR}} = 8$, and thermal upper bound $T_{h,i}^{\max} = 80$°C						
Total bill $J_{\text{bill}}^{\text{cl}}$ [R]	5434.45	5907.28	6571.54	6411.11	6147.72	6746.48
Cost savings [%]	19.45	12.44	2.59	4.97	8.88	-
Self-consumption $\nu_{\text{self}}^{\text{cl}}$	0.92	0.83	0.76	0.79	0.80	0.72
Self-consumption increase [%]	19.33	10.68	3.84	6.68	7.32	-
Violation over $T_{\text{vio}}^{\text{over}}$ [°C h]	0.09	142.40	7.46	1.43	0.00	0.91
Violation under $T_{\text{vio}}^{\text{under}}$ [°C h]	0.00	497.71	12.45	9.42	18.51	11.67
Mean solver time per step [s]	1.62	0.98	0.34	11.99	0.71	-

This discussion is based on the multi-agent simulation results presented in Figures 5-5 and 5-6, and Table 5-8. It is noted that a majority of the discussion points made for the single agent case in Section 5-4-3 are equally applicable for the multi-agent case. To minimize repetition they will not be restated here. Further discussion will focus on differences or points not previously addressed.

In general, for the multi-agent case it appears that all controllers achieve marginally improved cost and self-consumption performance when compared with the single agent case. This is likely due to the increased available decision space, now that all agents are able to share access to a larger pool of PV generation capacity. However, it could also be due to the differences in DHW demand profiles between the single and multi-agent cases. Furthermore, the cost performance of the scenario-based controllers is based on random sampling which means that the performance itself is also a random variable. Thus, the observation is not conclusive and would require further testing.

The CE-EMPC controller retains the greatest physically realizable cost and self-consumption improvement. However, the temperature state-trajectory plots clearly indicate that there are significant constraint violations associated with a controller which does not explicitly consider

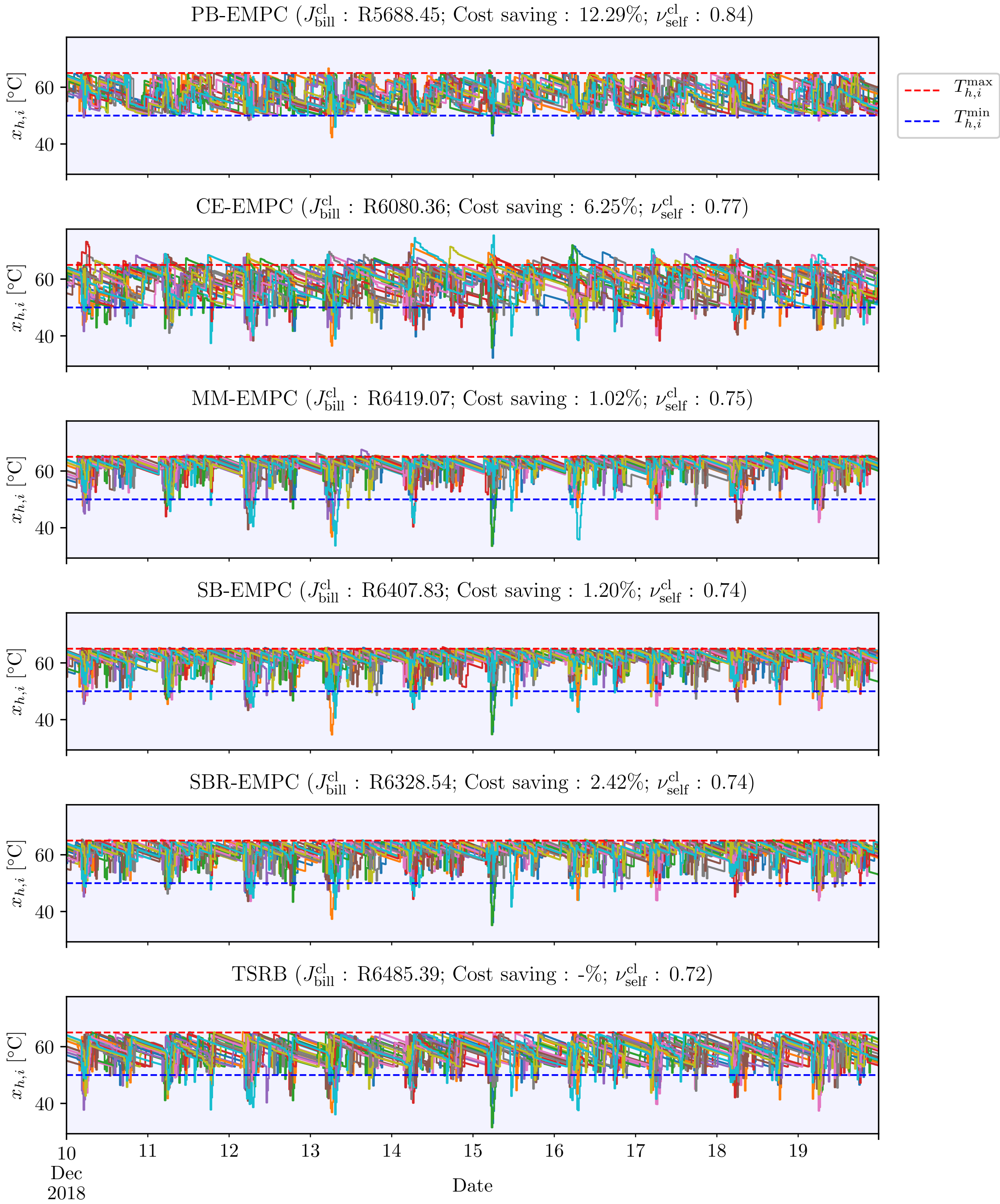

Figure 5-5: Multi-agent $N_h = 20$: simulation of DEWH state trajectories for the various EMPC controllers as compared to a TSRB controller. Performance metrics are computed over a 3 week simulation horizon ($N_t = 2016$ steps). Only 10 days shown in plot for clarity. Parameters: $N_p = 48$, $N_{\mathsf{SBR}} = 8$, $T^{\max}_{h,i} = 65$°C. Corresponding performance metrics given in upper half of Table 5-8.

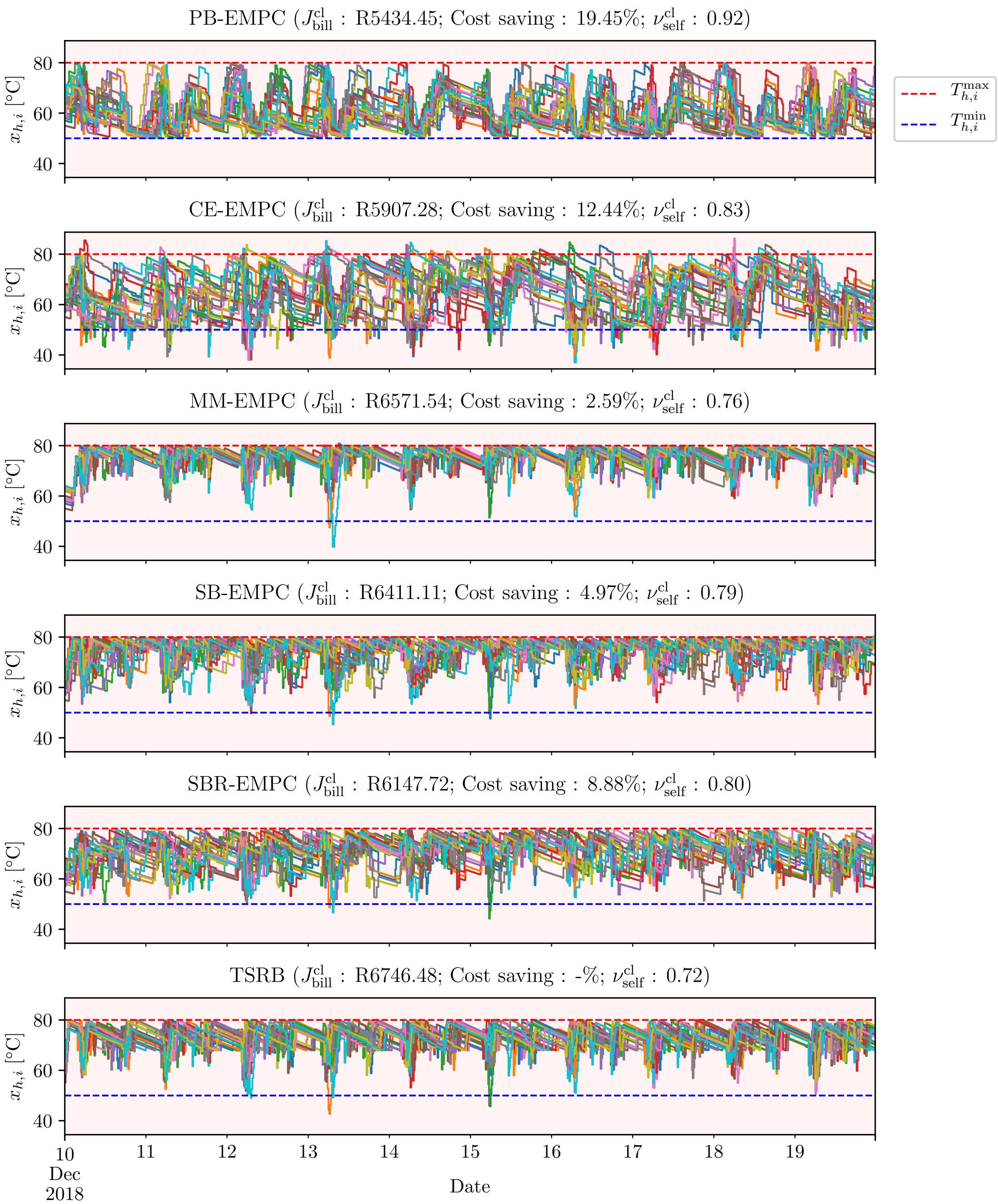

Figure 5-6: Multi-agent $N_h = 20$: simulation of DEWH state trajectories for the various EMPC controllers as compared to a TSRB controller. Performance metrics are computed over a 3 week simulation horizon ($N_t = 2016$ steps). Only 10 days shown in plot for clarity. Parameters: $N_p = 48$, $N_{\text{SBR}} = 8$, $T^{\text{max}}_{h,i} = 80°\text{C}$. Corresponding performance metrics given in lower half of Table 5-8.

uncertainty. Conversely, while all stochastic and robust control variants continue to only show a marginally increased cost and self-consumption performance when compared to the TSRB controller; when $T_{h,i}^{\max} = 65°\text{C}$, all controllers outperform the benchmark with significantly reduced lower bound constraint violations.

When comparing the SB-EMPC and SBR-EMPC controllers, it is clear that given a prediction horizon of $N_p = 48$, the reduced scenario-horizon leads to significantly increased performance across almost all metrics. However, for the single agent case, SB-EMPC exhibited increased performance for lower prediction horizons (e.g. $N_p = 12$ in Figure 5-3). Thus, the increased performance of SBR-EMPC may not be as significant when applied with a lower prediction horizon. Related to this comparison, an interesting observation can be made based on Figure 5-6. The state-trajectories for the SBR-EMPC controller are seen to make far greater use of the available feasible operating region than the SB-EMPC controller. This mode of operation more closely matches the PB case and likely leads to reduced costs, because water is not kept at unnecessarily high temperatures.

As a final note, it is useful to briefly discuss the computation times of the associated multi-agent controllers. For the multi-agent case it was found that solutions were not converging in reasonable time. To reduce solution computation times, the "MIP gap" termination tolerance was increased from 10^{-4} to 10^{-2}. In addition to this, a computational time limit of 20s was set for each solution step. Consequently, the problems were not always solved to optimality. The times shown in Table 5-8 correspond to the increased termination tolerance and were subject to the solution time limit. Even with the relaxed termination conditions, it is clear that solution times have in general increased significantly compared to the single agent case. The growth in computation times was to be expected and highlights that with an increasing number of agents the problem will eventually not be solvable within a single sampling instance. To combat this increasing complexity, researchers have turned to alternative solution frameworks such as distributed optimization. Distributed techniques allow certain large scale problems to be decomposed into smaller sub-problems which, when solved in parallel, can lead to reduced computation times. While distributed frameworks are beyond the scope of this thesis, they present an interesting direction for future work.

5-6 Case-study conclusions

In this chapter the thesis presented the results obtained when applying the range of EMPC controllers formulated in Chapter 4 to the case-study residential MG. Each of the proposed controllers was simulated subject to various control parameters and compared against the currently used TSRB control strategy. Overall, it can be concluded that the EMPC controllers are able to outperform the TSRB controller both in terms of energy costs and RES self-consumption. However, while CE-EMPC was able to obtain the greatest cost savings of all physically realisable controllers, it did so subject to significant constraint violations, as clearly demonstrated in Figures 5-5 and 5-6. These constraint violations are likely not tolerable in practice as they present conditions where either consumer comfort or safe system operation is not maintained. Consequently, from a holistic perspective SB-EMPC and SBR-EMPC present the best performing controllers, by effectively managing a trade-off between cost and constraint violations. Moreover, for the multi-agent case the proposed SBR-EMPC controller was shown to outperform standard SB-EMPC, even if only marginally. However, the single-agent case highlighted that the performance of the standard SB-EMPC controller is highly dependent on the prediction horizon N_p. Therefore, it is not possible to conclude that SBR-EMPC unequivocally outperforms SB-EMPC.

Finally, under the assumption that CE-EMPC is excluded due to unacceptable constraint violations, the best performing multi-agent controller for $T_{h,i}^{\max} = 65°\text{C}$, is SBR-EMPC. However, for this particular case-study MG it only achieves a marginal cost improvement of 2.42% and a self-consumption increase of 2.90%. Therefore, it remains debatable whether the implementation of such a controller would present a valid economic business case.

Chapter 6

Conclusions and Future Work

6-1 Summary

The purpose of this thesis was to explore the use of demand side management (DSM) schemes to optimize the economic and sustainable operation of a case-study residential microgrid (MG). To realise these objectives, the work developed, implemented and tested the performance of several state-of-the-art economic model predictive controllers (EMPCs). To validate the benefits of the proposed controllers, the work evaluated their performance against a benchmark rule-based controller which represents the currently utilized control methodology. The investigation and development process undertaken in this work is briefly summarized as follows.

EMPC controllers require the use of a case specific system model. The model is required for the prediction of future state evolutions which, when optimized subject to a given objective, may be used to determine state dependent optimal control input sequences. Consequently, as detailed in Chapter 3, the first thesis objective was to develop a residential MG model suitable for system control. All system modelling was based on a specific case-study residential community, where each household contains a controllable domestic electric water heater (DEWH) and all users share access to a communal roof-top photovoltaic (PV) supply. To ensure tractable optimal control problem formulations, it was decided that the work would make use of simple mixed logical dynamical (MLD) models for all case-study MG components. The use of the MLD modelling framework enabled the development of control problem formulations which could be solved using mixed-integer linear programming (MILP), for which increasingly efficient solvers exist.

By making use of an overall MG MLD system model (3-18), Chapter 4 detailed the investigated EMPC control problem formulations. All the controllers were formulated to optimize an economic objective which simultaneously targeted reduced energy bills, while also encouraging the self-utilization of local renewable energy source (RES) generation. In an ideal world, it would be possible to formulate controllers which are able to perfectly predict the system evolution along with the impact of any disturbances acting on the system. This would allow designers to implement high performance optimal controllers without considering uncertainty, i.e. certainty equivalent EMPC (CE-EMPC). Unfortunately, reality dictates that all predictions are subject to uncertainty and in the case of domestic hot water (DHW) demand, the uncertainty at an individual household level is significant. Consequently, the work investigated the implementation of stochastic and robust EMPC frameworks, which explicitly manage uncertainty. As a primary focus, the work formulated stochastic scenario-based EMPC controllers which attempt to approximate solutions of stochastic chance-constrained (STCC) control problems that are generally intractable to solve. Moreover, in order to ensure recursive solution feasibility, the investigated controllers all make use of soft-constraints which allow for some constraint violation, subject to an objective penalty. Soft-constraints were required even in the case of perfect predictions because it was not possible to guarantee that user demand would not exceed the maximum DHW storage capacity of a DEWH.

Lastly, in Chapter 5 the thesis presented an illustrative MG application case-study to evaluate the performance of the investigated controllers. The simulations were all undertaken by making use of the open-source, `Python` based, software package developed as part of this thesis. Final conclusions and recommendations resulting from the thesis work are outlined in the following section.

6-2 Conclusions and recommendations

Through an illustrative case-study it was shown that all developed EMPC controllers were, in most cases, able to outperform the currently used benchmark thermostatic rule-based (TSRB) strategy. Performance improvements were realised across three close-loop metrics, including lower energy bills, increased RES self-consumption, and reduced DEWH temperature constraint violations. The results clearly indicate that while CE-EMPC was able to produce the greatest cost savings and self-consumption improvements, of all physically realizable controllers; it did so while permitting significant and likely unacceptable temperature bound constraint violations. Therefore, even though the robust and stochastic formulations provide lower cost performance, they drastically reduce the realised constraint violations, and likely represent the most suitable choice when considered in a holistic sense. In particular, the newly proposed 'scenario-based *reduced horizon* EMPC' (SBR-EMPC) controller showed the greatest robust performance across all considered metrics; albeit only marginally when compared to the traditional SB-EMPC controller.

With that said, it remains clear that all physically realisable EMPC controllers considered in this work, still exhibit a significant performance gap when compared to the **theoretical** performance bound EMPC (PB-EMPC) formulation. While this gap can never be completely eliminated due to the inherent uncertainty associated with real-world predictions, it is expected that additional improvements are still achievable. These include the development of improved forecasting and scenario generation/removal methods, along with structural changes to the controller such as the possible implementation of disturbance feedback as implemented in [90]. Moreover, the current physical specifications of the case-study MG are likely not optimally designed for the attainment of an optimal DSM scheme. For example, it is possible that higher capacity DEWH units may allow for increased savings. However, this remains to be proven as larger tanks may also lead to increased standing heat losses, thus requiring improved insulation.

To conclude, the thesis returns its attention to the specific South African residential community on which the case-study MG was formulated. Presently, each household only has access to a 150L DEWH with a maximum operating temperature bound of $T_{h,i}^{\max} = 65°\text{C}$. Under these conditions, and assuming that the CE-EMPC controller is excluded due to excessive constraint violations, it would be recommended that the community implement the SBR-EMPC controller. However, as indicated in Table 5-8 for $T_{h,i}^{\max} = 65°\text{C}$, SBR-EMPC achieved only marginal performance improvements, when compared to the currently used TSRB controller. Therefore, it remains debatable whether an energy bill saving of 2.42% and self-utilization increase of 2.90%, would warrant the significant complexity associated with the implementation of the developed controller in its current state. Consequently, while EMPC for the DSM of residential MGs shows great promise, it can be concluded that the optimal control of MGs still presents a complex, multi-faceted problem with considerable scope for improvement.

6-3 Future work

The final section of this thesis presents a collection of possible opportunities that were identified for further consideration and future work:

1. **System modelling and validation**:

   The dynamic system models developed for this thesis were all generated subject to various simplifying assumptions (e.g. constant ambient and DEWH inlet temperatures, etc.), with all system parameters selected based on manufacturers' design specifications. To ensure that the results generated in this work accurately represent the actual performance that could be achieved in physical application, further work is required to validate the relevant system models to ensure that they adequately capture the real-world system dynamics. As a specific example, this work neglected DEWH thermal stratification effects along with other non-linear fluid dynamics. It would be prudent to investigate any impacts this has on performance. Even though more sophisticated models (e.g. [23, 34]) may not be suitable for optimization based controllers, they could provide useful insights in close-loop simulation. That said, the ultimate test would be to apply the controllers via physical experimentation.

2. **Forecasting and scenario generation**:

   Related to improved system modelling, this thesis only made use of rudimentary forecasting (i.e. persistence forecast) and scenario generation methods. Through the development of more accurate forecasting techniques with reduced errors and uncertainty, it is highly likely that the performance of the EMPC controllers could be further improved. As for scenario generation, future work should be undertaken to generate more realistic scenarios based on actual historical data (e.g. [79, 106, 107]). Moreover, recent studies (e.g. [104, 108, 114]) have also highlighted that performance of scenario-based EMPC may be improved through the application of suitable scenario removal/reduction algorithms. The use of such algorithms may further enhance the business case for applying scenario-based EMPC to the case-study MG.

3. **‘Closed-loop’ EMPC**:

   As discussed in Remark 4.5, all stochastic and robust EMPC methods investigated in this thesis were of the so-called ‘open-loop’ variety. This means that the controllers only optimize a single open-loop input sequence over the control horizon, instead of optimizing over a closed-loop feedback policy. Consequently, the open-loop approach does not capture the true nature of receding horizon control because it fails to consider that future model predictive control (MPC) iterations will have access to additional measurement information. While complete closed-loop approaches are often intractable, researchers have shown that the use of parametrised feedback laws can help to reduce the often conservative performance of open-loop methods. By extending the EMPC formulations developed in this work, increased performance could be attained through the inclusion of feedback mechanisms such as the disturbance feedback approach applied in [90].

4. **EMPC scalability**:

   The EMPC controllers developed in this work were only implemented and tested on small to medium-scale residential MGs. Moreover, all control actions were exclusively determined using a centralised control topology. These centralised topologies require all sensor and state information to be collected and transmitted to a central location, to enable globally optimal decision by a single computing agent. As discussed in Section 4-4, for the case-study MG it becomes evident that for an increasing prediction horizon N_p or a large number of agents, N_h, the centralized control strategy eventually cannot be solved to optimality within a single sampling interval. To address this issue researchers have turned to distributed and multi-level hierarchical control topologies. Distributed techniques allow certain large scale problems to be decomposed into smaller sub-problems which, when solved in parallel, can lead to reduced computation times. Examples of these techniques include methods such as dual decomposition or the alternating direction method of multipliers (ADMM). To combat scalability issues, future work may look to extend the centralised methods using similar techniques to those explored in, e.g. [90, 115].

5. **Continued open-source software development**:

   A final recommendation is made for future work to continue the development of open-source collaborative software packages for the implementation of future proposed methods. While research on the mathematical formulations and fundamental theoretical development of MPC and EMPC continue to progress, it is important that work continues to make these techniques more accessible for real-world application. The development of these packages would also significantly reduce the re-work required when attempting to implement improvements, as well as allowing for validation of published results.

Appendix A

Detailed System Matrices

A-1 Discrete DEWH MLD model details

The discrete linearized domestic electric water heater (DEWH) mixed logical dynamical (MLD) model given in (3-9), is rewritten below with full descriptions of the system matrices:

$$\begin{aligned} x_{h,i}(k+1) &= A_{h,i}x_{h,i}(k) + B_{h1,i}u_{h,i}(k) + B_{h4,i}\omega_{h,i}^{\text{nom}}(k) + b_{h5,i} \\ y_{h,i}(k) &= x_{h,i}(k) \\ E_{h1,i}x_{h,i}(k) &\leq f_{h5,i} + \Psi_{h,i}\mu(k), \end{aligned}$$

with,

$$A_{h,i} = e^{\bar{A}^c_{h,i}t_s}, \quad B_{h1,i} = \Upsilon_{h,i}\bar{B}^c_{h1,i}, \quad B_{h4,i} = \Upsilon_{h,i}\bar{B}^c_{h4,i}, \quad b_{h5,i} = \Upsilon_{h,i}\bar{b}^c_{h5,i},$$
$$E_{h,i} = I^{2\times 2}, \quad f_{h5,i} = \begin{bmatrix} T^{\max}_{h,i} \\ T^{\min}_{h,i} \end{bmatrix}, \quad Psi_{h,i} = I^{2\times 2},$$

and,

$$\Upsilon_{h,i} = \bar{A}^c_{h,i}{}^{-1}\left(e^{\bar{A}^c_{h,i}t_s} - 1\right).$$

A-2 Explicit MLD model evolution

Given the general MLD model (2-5), restated bellow:

$$\begin{aligned} x(k+1) &= Ax(k) + B_1u(k) + B_2\delta(k) + B_3z(k) + B_4\omega(k) + b_5 \\ y(k) &= Cx(k) + D_1u(k) + D_2\delta(k) + D_3z(k) + D_4\omega(k) + d_5 \\ &\quad Ex(k) + F_1u(k) + F_2\delta(k) + F_3z(k) + F_4\omega(k) + Gy(k) \leq f_5 + \Psi\mu(k), \end{aligned}$$

the system evolution in the prediction horizon N_p can be explicitly computed as:

$$\begin{aligned}
\underset{\sim}{\boldsymbol{x}}(k) &= \Phi_x x(0) + \Gamma_v \underset{\sim}{\boldsymbol{V}}(k) + \Gamma_\omega \underset{\sim}{\boldsymbol{\omega}}(k) + \Gamma_5 \\
\underset{\sim}{\boldsymbol{y}}(k) &= L_x x(0) + L_v \underset{\sim}{\boldsymbol{V}}(k) + L_\omega \underset{\sim}{\boldsymbol{\omega}}(k) + L_5 \\
H_v \underset{\sim}{\boldsymbol{V}}(k) &\leq H_x x(0) + H_\omega \underset{\sim}{\boldsymbol{\omega}}(k) + H_5,
\end{aligned}$$

with $V(k) = \begin{bmatrix} u^\top(k) & \delta^\top(k) & z^\top(k) & \mu^\top(k) \end{bmatrix}^\top \in \mathbb{R}^{n^v}$, and,

$$\underset{\sim}{\boldsymbol{x}}(k) = \begin{bmatrix} x(k) \\ x(k+1) \\ \vdots \\ x(k+N_p) \end{bmatrix}, \quad \underset{\sim}{\boldsymbol{V}}(k) = \begin{bmatrix} V(k) \\ V(k+1) \\ \vdots \\ V(k+N_p) \end{bmatrix}, \quad \underset{\sim}{\boldsymbol{\omega}}(k) = \begin{bmatrix} \omega(k) \\ \omega(k+1) \\ \vdots \\ \omega(k+N_p) \end{bmatrix},$$

where the state evolution matrices are defined by:

$$\Phi_x = \begin{bmatrix} A^0 \\ A^1 \\ \vdots \\ A^{N_p} \end{bmatrix}, \quad \Gamma_v = \begin{bmatrix} \mathbf{0} & \mathbf{0} & \mathbf{0} & \cdots & \mathbf{0}^{n^x \times n^v} \\ AB_v & B_v & \mathbf{0} & \cdots & \mathbf{0} \\ \vdots & \vdots & \vdots & \ddots & \vdots \\ A^{N_p-1}B_v & A^{N_p-2}B_v & A^{N_p-3}B_v & \cdots & \mathbf{0} \end{bmatrix},$$

$$B_v = \begin{bmatrix} B_1 & B_2 & B_3 & \mathbf{0}^{n_x \times n_\mu} \end{bmatrix},$$

$$\Gamma_\omega = \begin{bmatrix} \mathbf{0} & \mathbf{0} & \mathbf{0} & \cdots & \mathbf{0}^{n^x \times n^\omega} \\ AB_4 & B_4 & \mathbf{0} & \cdots & \mathbf{0} \\ \vdots & \vdots & \vdots & \ddots & \vdots \\ A^{N_p-1}B_4 & A^{N_p-2}B_4 & A^{N_p-3}B_4 & \cdots & \mathbf{0} \end{bmatrix},$$

$$\Gamma_5 = \begin{bmatrix} \mathbf{0}^{n^x \times 1} \\ b_5 \\ Ab_5 + b_5 \\ \vdots \\ A^{N_p-1}b_5 + A^{N_p-2}b_5 + \cdots + b_5 \end{bmatrix},$$

the output evolution matrices are:

$$L_x = \underset{\sim}{C}\Phi_x, \quad L_v = \underset{\sim}{C}\Gamma_v + \underset{\sim}{D}_v, \quad L_\omega = \underset{\sim}{C}\Gamma_\omega + \underset{\sim}{D}_4, \quad L_5 = \underset{\sim}{C}\Gamma_5 + \underset{\sim}{d}_5,$$

with,

$$
\underset{\sim}{C} = \begin{bmatrix} C & \mathbf{0} & \mathbf{0} & \cdots & \mathbf{0} \\ \mathbf{0} & C & \mathbf{0} & \cdots & \mathbf{0} \\ \vdots & \vdots & \vdots & \ddots & \vdots \\ \mathbf{0} & \mathbf{0} & \mathbf{0} & \cdots & C \end{bmatrix}, \quad \underset{\sim}{D}_v = \begin{bmatrix} D_v & \mathbf{0} & \mathbf{0} & \cdots & \mathbf{0} \\ \mathbf{0} & D_v & \mathbf{0} & \cdots & \mathbf{0} \\ \vdots & \vdots & \vdots & \ddots & \vdots \\ \mathbf{0} & \mathbf{0} & \mathbf{0} & \cdots & D_v \end{bmatrix},
$$

$$
D_v = \begin{bmatrix} D_1 & D_2 & D_3 & \mathbf{0}^{n_y \times n_\mu} \end{bmatrix},
$$

$$
\underset{\sim}{D}_4 = \begin{bmatrix} D_4 & \mathbf{0} & \mathbf{0} & \cdots & \mathbf{0} \\ \mathbf{0} & D_4 & \mathbf{0} & \cdots & \mathbf{0} \\ s & & & & \\ \mathbf{0} & \mathbf{0} & \mathbf{0} & \cdots & D_4 \end{bmatrix}, \quad \underset{\sim}{d}_5 = \begin{bmatrix} d_5 \\ d_5 \\ \vdots \\ d_5 \end{bmatrix},
$$

and the constraint evolution matrices are:

$$
\begin{aligned}
H_x &= -(\underset{\sim}{E}\Phi_x + \underset{\sim}{G}L_x), \quad H_v = \underset{\sim}{E}\Gamma_v + \underset{\sim}{F}_v + \underset{\sim}{G}L_v, \\
H_\omega &= -(\underset{\sim}{E}\Gamma_\omega + \underset{\sim}{F}_4 + \underset{\sim}{G}L_\omega), \quad H_5 = \underset{\sim}{f}_5 - (\underset{\sim}{E}\Gamma_5 + \underset{\sim}{G}L_5),
\end{aligned}
$$

with,

$$
\underset{\sim}{E} = \begin{bmatrix} E & \mathbf{0} & \mathbf{0} & \cdots & \mathbf{0} \\ \mathbf{0} & E & \mathbf{0} & \cdots & \mathbf{0} \\ \vdots & \vdots & \vdots & \ddots & \vdots \\ \mathbf{0} & \mathbf{0} & \mathbf{0} & \cdots & E \end{bmatrix}, \quad \underset{\sim}{G} = \begin{bmatrix} G & \mathbf{0} & \mathbf{0} & \cdots & \mathbf{0} \\ \mathbf{0} & G & \mathbf{0} & \cdots & \mathbf{0} \\ \vdots & \vdots & \vdots & \ddots & \vdots \\ \mathbf{0} & \mathbf{0} & \mathbf{0} & \cdots & G \end{bmatrix},
$$

$$
\underset{\sim}{F}_v = \begin{bmatrix} F_v & \mathbf{0} & \mathbf{0} & \cdots & \mathbf{0} \\ \mathbf{0} & F_v & \mathbf{0} & \cdots & \mathbf{0} \\ \vdots & \vdots & \vdots & \ddots & \vdots \\ \mathbf{0} & \mathbf{0} & \mathbf{0} & \cdots & F_v \end{bmatrix}, \quad F_v = \begin{bmatrix} F_1 & F_2 & F_3 & -\Psi \end{bmatrix},
$$

$$
\underset{\sim}{F}_4 = \begin{bmatrix} F_4 & \mathbf{0} & \mathbf{0} & \cdots & \mathbf{0} \\ \mathbf{0} & F_4 & \mathbf{0} & \cdots & \mathbf{0} \\ \vdots & \vdots & \vdots & \ddots & \vdots \\ \mathbf{0} & \mathbf{0} & \mathbf{0} & \cdots & F_4 \end{bmatrix}, \quad \underset{\sim}{f}_5 = \begin{bmatrix} f_5 \\ f_5 \\ \vdots \\ f_5 \end{bmatrix}.
$$

Bibliography

[1] P. Palensky and D. Dietrich, "Demand Side Management: Demand Response, Intelligent Energy Systems, and Smart Loads," *IEEE Transactions on Industrial Informatics*, vol. 7, pp. 381–388, Aug. 2011.

[2] I. Atzeni, L. G. Ordóñez, G. Scutari, D. P. Palomar, and J. R. Fonollosa, "Demand-Side Management via Distributed Energy Generation and Storage Optimization," *IEEE Transactions on Smart Grid*, vol. 4, pp. 866–876, Jun. 2013.

[3] M. A. Eltawil and Z. Zhao, "Grid-connected photovoltaic power systems: Technical and potential problems—A review," *Renewable and Sustainable Energy Reviews*, vol. 14, pp. 112–129, Jan. 2010.

[4] J. Widén, E. Wäckelgård, and P. D. Lund, "Options for improving the load matching capability of distributed photovoltaics: Methodology and application to high-latitude data," *Solar Energy*, vol. 83, pp. 1953–1966, Nov. 2009.

[5] R. Luthander, J. Widén, D. Nilsson, and J. Palm, "Photovoltaic self-consumption in buildings: A review," *Applied Energy*, vol. 142, pp. 80–94, Mar. 2015.

[6] R. Deng, Z. Yang, M. Y. Chow, and J. Chen, "A Survey on Demand Response in Smart Grids: Mathematical Models and Approaches," *IEEE Transactions on Industrial Informatics*, vol. 11, pp. 570–582, Jun. 2015.

[7] P. D. Lund, J. Lindgren, J. Mikkola, and J. Salpakari, "Review of energy system flexibility measures to enable high levels of variable renewable electricity," *Renewable and Sustainable Energy Reviews*, vol. 45, pp. 785–807, May 2015.

[8] X. Fang, S. Misra, G. Xue, and D. Yang, "Smart Grid - The New and Improved Power Grid: A Survey," *IEEE Communications Surveys Tutorials*, vol. 14, pp. 944–980, 2012.

[9] H. Farhangi, "The path of the smart grid," *IEEE Power and Energy Magazine*, vol. 8, pp. 18–28, Jan. 2010.

[10] H. Gharavi and R. Ghafurian, "Smart Grid: The Electric Energy System of the Future," *Proceedings of the IEEE*, vol. 99, pp. 917–921, Jun. 2011.

[11] G. M. Masters, *Renewable and Efficient Electric Power Systems.* Hoboken, NJ: John Wiley & Sons, 2004.

[12] A. H. Mohsenian-Rad, V. W. S. Wong, J. Jatskevich, R. Schober, and A. Leon-Garcia, "Autonomous Demand-Side Management Based on Game-Theoretic Energy Consumption Scheduling for the Future Smart Grid," *IEEE Transactions on Smart Grid*, vol. 1, pp. 320–331, Dec. 2010.

[13] R. H. Lasseter, "MicroGrids," in *2002 IEEE Power Engineering Society Winter Meeting Conference*, vol. 1, 2002, pp. 305–308.

[14] F. Katiraei, R. Iravani, N. Hatziargyriou, and A. Dimeas, "Microgrids management," *IEEE Power and Energy Magazine*, vol. 6, pp. 54–65, May 2008.

[15] A. Bidram and A. Davoudi, "Hierarchical Structure of Microgrids Control System," *IEEE Transactions on Smart Grid*, vol. 3, pp. 1963–1976, Dec. 2012.

[16] J. B. Rawlings, D. Angeli, and C. N. Bates, "Fundamentals of economic model predictive control," in *2012 IEEE 51st IEEE Conference on Decision and Control (CDC)*, Dec. 2012, pp. 3851–3861.

[17] M. Ellis, H. Durand, and P. D. Christofides, "A tutorial review of economic model predictive control methods," *Journal of Process Control*, vol. 24, pp. 1156–1178, Aug. 2014.

[18] F. Sossan, A. M. Kosek, S. Martinenas, M. Marinelli, and H. Bindner, "Scheduling of domestic water heater power demand for maximizing PV self-consumption using model predictive control," in *IEEE PES ISGT Europe 2013*, Oct. 2013, pp. 1–5.

[19] R. Halvgaard, P. Bacher, B. Perers, E. Andersen, S. Furbo, J. B. Jørgensen, N. K. Poulsen, and H. Madsen, "Model Predictive Control for a Smart Solar Tank Based on Weather and Consumption Forecasts," *Energy Procedia*, vol. 30, pp. 270–278, Jan. 2012.

[20] R. Halvgaard, N. K. Poulsen, H. Madsen, and J. B. Jørgensen, "Economic Model Predictive Control for building climate control in a Smart Grid," in *2012 IEEE PES Innovative Smart Grid Technologies (ISGT)*, Jan. 2012, pp. 1–6.

[21] F. Ruelens, B. J. Claessens, S. Vandael, S. Iacovella, P. Vingerhoets, and R. Belmans, "Demand response of a heterogeneous cluster of electric water heaters using batch reinforcement learning," in *2014 Power Systems Computation Conference*, Aug. 2014, pp. 1–7.

[22] S. Sichilalu, T. Mathaba, and X. Xia, "Optimal control of a wind–PV-hybrid powered heat pump water heater," *Applied Energy*, vol. 185, pp. 1173–1184, Jan. 2017.

[23] P. Kepplinger, G. Huber, and J. Petrasch, "Autonomous optimal control for demand side management with resistive domestic hot water heaters using linear optimization," *Energy and Buildings*, vol. 100, pp. 50–55, Aug. 2015.

[24] P. Siano, "Demand response and smart grids—A survey," *Renewable and Sustainable Energy Reviews*, vol. 30, pp. 461–478, Feb. 2014.

[25] A. Barbato and A. Capone, "Optimization Models and Methods for Demand-Side Management of Residential Users: A Survey," *Energies*, vol. 7, pp. 5787–5824, Sep. 2014.

[26] J. S. Vardakas, N. Zorba, and C. V. Verikoukis, "A Survey on Demand Response Programs in Smart Grids: Pricing Methods and Optimization Algorithms," *IEEE Communications Surveys Tutorials*, vol. 17, pp. 152–178, 2015.

[27] NERC, "2011 Demand Response Availability Report," North American Electric Reliability Corporation, Atlanta, GA, Tech. Rep., Mar. 2013. [Online]. Available: https://www.nerc.com/docs/pc/dadswg/2011%20DADS%20Report.pdf

[28] P. Samadi, A. H. Mohsenian-Rad, R. Schober, V. W. S. Wong, and J. Jatskevich, "Optimal Real-Time Pricing Algorithm Based on Utility Maximization for Smart Grid," in *2010 First IEEE International Conference on Smart Grid Communications*, Oct. 2010, pp. 415–420.

[29] M. H. Albadi and E. F. El-Saadany, "Demand Response in Electricity Markets: An Overview," in *2007 IEEE Power Engineering Society General Meeting*, Jun. 2007, pp. 1–5.

[30] F. Borrelli, *Constrained Optimal Control of Linear and Hybrid Systems.* Springer, 2003, vol. 290.

[31] D. Fischer and H. Madani, "On heat pumps in smart grids: A review," *Renewable and Sustainable Energy Reviews*, vol. 70, pp. 342–357, Apr. 2017.

[32] P. H. Shaikh, N. B. M. Nor, P. Nallagownden, I. Elamvazuthi, and T. Ibrahim, "A review on optimized control systems for building energy and comfort management of smart sustainable buildings," *Renewable and Sustainable Energy Reviews*, vol. 34, pp. 409–429, Jun. 2014.

[33] W. Saad, Z. Han, H. V. Poor, and T. Basar, "Game-Theoretic Methods for the Smart Grid: An Overview of Microgrid Systems, Demand-Side Management, and Smart Grid Communications," *IEEE Signal Processing Magazine*, vol. 29, pp. 86–105, Sep. 2012.

[34] M. Negnevitsky and K. Wong, "Demand-Side Management Evaluation Tool," *IEEE Transactions on Power Systems*, vol. 30, pp. 212–222, Jan. 2015.

[35] S. J. Qin and T. A. Badgwell, "A survey of industrial model predictive control technology," *Control Engineering Practice*, vol. 11, pp. 733–764, Jul. 2003.

[36] D. Q. Mayne, J. B. Rawlings, C. V. Rao, and P. O. M. Scokaert, "Constrained model predictive control: Stability and optimality," *Automatica*, vol. 36, pp. 789–814, Jun. 2000.

[37] I. Atzeni, L. G. Ordóñez, G. Scutari, D. P. Palomar, and J. R. Fonollosa, "Noncooperative and Cooperative Optimization of Distributed Energy Generation and Storage in the Demand-Side of the Smart Grid," *IEEE Transactions on Signal Processing*, vol. 61, pp. 2454–2472, May 2013.

[38] S. Mei, W. Wei, and F. Liu, "On engineering game theory with its application in power systems," *Control Theory Technol.*, vol. 15, pp. 1–12, Feb. 2017.

[39] T. Başar and G. J. Olsder, *Dynamic Noncooperative Game Theory*, 2nd ed. Philadelphia: SIAM, 1999.

[40] C. G. Cassandras and S. Lafortune, *Introduction to Discrete Event Systems*, 2nd ed. New York, NY: Springer, 2008.

[41] B. De Schutter, W. Heemels, J. Lunze, and C. Prieur, "Survey of modeling, analysis, and control of hybrid systems," *Handbook of Hybrid Systems Control–Theory, Tools, Applications*, pp. 31–55, 2009.

[42] A. Bemporad and M. Morari, "Control of systems integrating logic, dynamics, and constraints," *Automatica*, vol. 35, pp. 407–427, Mar. 1999.

[43] K. J. Åström and B. Wittenmark, *Computer-Controlled Systems: Theory and Design*. Courier Corporation, 2013.

[44] E. Sontag, "Nonlinear regulation: The piecewise linear approach," *IEEE Transactions on Automatic Control*, vol. 26, pp. 346–358, Apr. 1981.

[45] M. Morari, M. Baotic, and F. Borrelli, "Hybrid Systems Modeling and Control," *European Journal of Control*, vol. 9, pp. 177–189, Jan. 2003.

[46] W. P. M. H. Heemels, B. De Schutter, and A. Bemporad, "Equivalence of hybrid dynamical models," *Automatica*, vol. 37, pp. 1085–1091, Jul. 2001.

[47] A. Bemporad, G. Ferrari-Trecate, and M. Morari, "Observability and controllability of piecewise affine and hybrid systems," *IEEE Transactions on Automatic Control*, vol. 45, pp. 1864–1876, Oct. 2000.

[48] K. K. Wong, "Evaluation tool for demand-side management of domestic hot water load," Master's Thesis, University of Tasmania, Dec. 2014. [Online]. Available: https://eprints.utas.edu.au/21720/

[49] P. G. Rousseau, J. P. Strauss, and G. P. Greyvenstein, "Demand side management for water heating installations in South African commercial buildings," *Int. J. Energy Res.*, vol. 25, pp. 291–317, Mar. 2001.

[50] J. C. Laurent and R. P. Malhame, "A physically-based computer model of aggregate electric water heating loads," *IEEE Transactions on Power Systems*, vol. 9, pp. 1209–1217, Aug. 1994.

[51] T. Schütz, R. Streblow, and D. Müller, "A comparison of thermal energy storage models for building energy system optimization," *Energy and Buildings*, vol. 93, pp. 23–31, Apr. 2015.

[52] A. Campos Celador, M. Odriozola, and J. M. Sala, "Implications of the modelling of stratified hot water storage tanks in the simulation of CHP plants," *Energy Conversion and Management*, vol. 52, pp. 3018–3026, Aug. 2011.

[53] J. S. Shamma, "Analysis and design of gain scheduled control systems," PhD Thesis, Massachusetts Institute of Technology, 1988.

[54] K. Deng, Y. Sun, A. Chakraborty, Y. Lu, J. Brouwer, and P. G. Mehta, "Optimal scheduling of chiller plant with thermal energy storage using mixed integer linear programming," in *2013 American Control Conference*, Jun. 2013, pp. 2958–2963.

[55] F. Alavi, N. van de Wouw, and B. D. Schutter, "Min-max control of fuel-cell-car-based smart energy systems," in *2016 European Control Conference (ECC)*, Jun. 2016, pp. 1223–1228.

[56] M. Carrion and J. M. Arroyo, "A computationally efficient mixed-integer linear formulation for the thermal unit commitment problem," *IEEE Transactions on Power Systems*, vol. 21, pp. 1371–1378, Aug. 2006.

[57] G. Morales-España, J. M. Latorre, and A. Ramos, "Tight and Compact MILP Formulation for the Thermal Unit Commitment Problem," *IEEE Transactions on Power Systems*, vol. 28, pp. 4897–4908, Nov. 2013.

[58] A. Parisio, E. Rikos, and L. Glielmo, "A Model Predictive Control Approach to Microgrid Operation Optimization," *IEEE Transactions on Control Systems Technology*, vol. 22, pp. 1813–1827, Sep. 2014.

[59] M. Q. Raza and A. Khosravi, "A review on artificial intelligence based load demand forecasting techniques for smart grid and buildings," *Renewable and Sustainable Energy Reviews*, vol. 50, pp. 1352–1372, Oct. 2015.

[60] J. Antonanzas, N. Osorio, R. Escobar, R. Urraca, F. J. Martinez-de-Pison, and F. Antonanzas-Torres, "Review of photovoltaic power forecasting," *Solar Energy*, vol. 136, pp. 78–111, Oct. 2016.

[61] A. R. Khan, A. Mahmood, A. Safdar, Z. A. Khan, and N. A. Khan, "Load forecasting, dynamic pricing and DSM in smart grid: A review," *Renewable and Sustainable Energy Reviews*, vol. 54, pp. 1311–1322, Feb. 2016.

[62] C. Wan, J. Zhao, Y. Song, Z. Xu, J. Lin, and Z. Hu, "Photovoltaic and solar power forecasting for smart grid energy management," *CSEE Journal of Power and Energy Systems*, vol. 1, pp. 38–46, Dec. 2015.

[63] R. H. Inman, H. T. C. Pedro, and C. F. M. Coimbra, "Solar forecasting methods for renewable energy integration," *Progress in Energy and Combustion Science*, vol. 39, pp. 535–576, Dec. 2013.

[64] L. Suganthi and A. A. Samuel, "Energy models for demand forecasting—A review," *Renewable and Sustainable Energy Reviews*, vol. 16, pp. 1223–1240, Feb. 2012.

[65] L. Gelažanskas and K. A. A. Gamage, "Forecasting Hot Water Consumption in Residential Houses," *Energies*, vol. 8, pp. 12 702–12 717, Nov. 2015.

[66] C. Chen, S. Duan, T. Cai, B. Liu, and G. Hu, "Smart energy management system for optimal microgrid economic operation," *IET Renewable Power Generation*, vol. 5, pp. 258–267, May 2011.

[67] B. Zhao, X. Zhang, J. Chen, C. Wang, and L. Guo, "Operation Optimization of Standalone Microgrids Considering Lifetime Characteristics of Battery Energy Storage System," *IEEE Transactions on Sustainable Energy*, vol. 4, pp. 934–943, Oct. 2013.

[68] U. Jordan and K. Vajen, "DHWcalc: Program to generate domestic hot water profiles with statistical means for user defined conditions," in *ISES Solar World Congress*, 2005, pp. 1–6.

[69] D. Angeli, R. Amrit, and J. B. Rawlings, "On Average Performance and Stability of Economic Model Predictive Control," *IEEE Transactions on Automatic Control*, vol. 57, pp. 1615–1626, Jul. 2012.

[70] F. Alavi, E. Park Lee, N. van de Wouw, B. De Schutter, and Z. Lukszo, "Fuel cell cars in a microgrid for synergies between hydrogen and electricity networks," *Applied Energy*, vol. 192, pp. 296–304, Apr. 2017.

[71] J. Löfberg, "Oops! I cannot do it again: Testing for recursive feasibility in MPC," *Automatica*, vol. 48, pp. 550–555, Mar. 2012.

[72] E. C. Kerrigan and J. M. Maciejowski, “Soft constraints and exact penalty functions in model predictive control,” 2000.

[73] A. Bemporad and M. Morari, “Robust model predictive control: A survey,” in *Robustness in Identification and Control.* Springer, London, 1999, pp. 207–226.

[74] M. Hovd and F. Stoican, “On the design of exact penalty functions for MPC using mixed integer programming,” *Computers & Chemical Engineering*, vol. 70, pp. 104–113, Nov. 2014.

[75] Eskom Holdings SOC Ltd, “Eskom 2018/19 Tariffs and charges,” 2018. [Online]. Available: http://www.eskom.co.za

[76] J. Salpakari and P. Lund, “Optimal and rule-based control strategies for energy flexibility in buildings with PV,” *Applied Energy*, vol. 161, pp. 425–436, Jan. 2016.

[77] Y. Zong, L. Mihet-Popa, D. Kullmann, A. Thavlov, O. Gehrke, and H. W. Bindner, “Model Predictive Controller for Active Demand Side Management with PV self-consumption in an intelligent building,” in *2012 3rd IEEE PES Innovative Smart Grid Technologies Europe (ISGT Europe)*, Oct. 2012, pp. 1–8.

[78] K. J. Kircher and K. M. Zhang, “Model predictive control of thermal storage for demand response,” in *2015 American Control Conference (ACC)*, Jul. 2015, pp. 956–961.

[79] A. Parisio, E. Rikos, and L. Glielmo, “Stochastic model predictive control for economic/environmental operation management of microgrids: An experimental case study,” *Journal of Process Control*, vol. 43, pp. 24–37, Jul. 2016.

[80] S. L. Janak, X. Lin, and C. A. Floudas, “A new robust optimization approach for scheduling under uncertainty: II. Uncertainty with known probability distribution,” *Computers & Chemical Engineering*, vol. 31, pp. 171–195, Jan. 2007.

[81] F. Oldewurtel, A. Parisio, C. N. Jones, D. Gyalistras, M. Gwerder, V. Stauch, B. Lehmann, and M. Morari, “Use of model predictive control and weather forecasts for energy efficient building climate control,” *Energy and Buildings*, vol. 45, pp. 15–27, Feb. 2012.

[82] Y. Ma, A. Kelman, A. Daly, and F. Borrelli, “Predictive Control for Energy Efficient Buildings with Thermal Storage: Modeling, Stimulation, and Experiments,” *IEEE Control Systems*, vol. 32, pp. 44–64, Feb. 2012.

[83] D. M. de la Penad, A. Bemporad, and T. Alamo, “Stochastic Programming Applied to Model Predictive Control,” in *Proceedings of the 44th IEEE Conference on Decision and Control*, Dec. 2005, pp. 1361–1366.

[84] N. V. Sahinidis, “Optimization under uncertainty: State-of-the-art and opportunities,” *Computers & Chemical Engineering*, vol. 28, pp. 971–983, Jun. 2004.

[85] A. Bemporad, F. Borrelli, and M. Morari, “Min-max control of constrained uncertain discrete-time linear systems,” *IEEE Transactions on Automatic Control*, vol. 48, pp. 1600–1606, Sep. 2003.

[86] D. Q. Mayne, M. M. Seron, and S. V. Raković, “Robust model predictive control of constrained linear systems with bounded disturbances,” *Automatica*, vol. 41, pp. 219–224, Feb. 2005.

[87] J. Löfberg, *Minimax Approaches to Robust Model Predictive Control.* Linköping University Electronic Press, 2003, vol. 812.

[88] J. H. Lee and Z. Yu, "Worst-case formulations of model predictive control for systems with bounded parameters," *Automatica*, vol. 33, pp. 763–781, May 1997.

[89] D. M. de la Peña, T. Alamo, D. R. Ramírez, and E. F. Camacho, "Min-max model predictive control as a quadratic program," *IFAC Proceedings*, vol. 38, pp. 263–268, Jan. 2005.

[90] F. Alavi, "Model Predictive Control of Fuel-Cell-Car-Based Smart Energy Systems in the Presence of Uncertainty," PhD Thesis, Delft University of Technology, 2019. [Online]. Available: http://resolver.tudelft.nl/uuid:7c2e1f22-2d40-4974-8be5-be4cec493941

[91] D. Bertsimas, E. Litvinov, X. A. Sun, J. Zhao, and T. Zheng, "Adaptive Robust Optimization for the Security Constrained Unit Commitment Problem," *IEEE Transactions on Power Systems*, vol. 28, pp. 52–63, Feb. 2013.

[92] R. Jiang, J. Wang, M. Zhang, and Y. Guan, "Two-Stage Minimax Regret Robust Unit Commitment," *IEEE Transactions on Power Systems*, vol. 28, pp. 2271–2282, Aug. 2013.

[93] C. A. Hans, V. Nenchev, J. Raisch, and C. Reincke-Collon, "Minimax Model Predictive Operation Control of Microgrids," *IFAC Proceedings Volumes*, vol. 47, pp. 10 287–10 292, Jan. 2014.

[94] L. Deori, S. Garatti, and M. Prandini, "Computational approaches to robust Model Predictive Control: A comparative analysis," *IFAC Proceedings Volumes*, vol. 47, pp. 10 820–10 825, Jan. 2014.

[95] M. Prandini, S. Garatti, and J. Lygeros, "A randomized approach to stochastic model predictive control," in *2012 IEEE 51st Annual Conference on Decision and Control (CDC).* IEEE, 2012, pp. 7315–7320.

[96] A. T. Schwarm and M. Nikolaou, "Chance-constrained model predictive control," *AIChE Journal*, vol. 45, pp. 1743–1752, 1999.

[97] F. Oldewurtel, C. N. Jones, and M. Morari, "A tractable approximation of chance constrained stochastic MPC based on affine disturbance feedback," in *2008 47th IEEE Conference on Decision and Control*, Dec. 2008, pp. 4731–4736.

[98] J. Matuško and F. Borrelli, "Scenario-based approach to stochastic linear predictive control," in *2012 IEEE 51st IEEE Conference on Decision and Control (CDC).* IEEE, 2012, pp. 5194–5199.

[99] V. Rostampour and T. Keviczky, "Robust randomized model predictive control for energy balance in smart thermal grids," in *2016 European Control Conference (ECC)*, Jun. 2016, pp. 1201–1208.

[100] M. C. Campi, S. Garatti, and M. Prandini, "The scenario approach for systems and control design," *Annual Reviews in Control*, vol. 33, pp. 149–157, Dec. 2009.

[101] D. Bernardini and A. Bemporad, "Scenario-based model predictive control of stochastic constrained linear systems," in *Proceedings of the 48h IEEE Conference on Decision and Control (CDC) Held Jointly with 2009 28th Chinese Control Conference.* IEEE, 2009, pp. 6333–6338.

[102] G. C. Calafiore and L. Fagiano, "Robust model predictive control via scenario optimization," *IEEE Transactions on Automatic Control*, vol. 58, pp. 219–224, 2013.

[103] A. Parisio, D. Varagnolo, M. Molinari, G. Pattarello, L. Fabietti, and K. H. Johansson, "Implementation of a Scenario-based MPC for HVAC Systems: An Experimental Case Study," *IFAC Proceedings Volumes*, vol. 47, pp. 599–605, Jan. 2014.

[104] G. Schildbach, L. Fagiano, C. Frei, and M. Morari, "The scenario approach for Stochastic Model Predictive Control with bounds on closed-loop constraint violations," *Automatica*, vol. 50, pp. 3009–3018, Dec. 2014.

[105] X. Zhang, G. Schildbach, D. Sturzenegger, and M. Morari, "Scenario-based MPC for energy-efficient building climate control under weather and occupancy uncertainty," in *2013 European Control Conference (ECC)*, Jul. 2013, pp. 1029–1034.

[106] M. Kaut and S. W. Wallace, *Evaluation of Scenario-Generation Methods for Stochastic Programming*. Humboldt-Universität zu Berlin, Mathematisch-Naturwissenschaftliche Fakultät II, Institut für Mathematik, 2003.

[107] G. Papaefthymiou and B. Klockl, "MCMC for Wind Power Simulation," *IEEE Transactions on Energy Conversion*, vol. 23, pp. 234–240, Mar. 2008.

[108] H. Heitsch and W. Römisch, "Scenario reduction algorithms in stochastic programming," *Computational optimization and applications*, vol. 24, pp. 187–206, 2003.

[109] C. A. Hans, P. Sopasakis, A. Bemporad, J. Raisch, and C. Reincke-Collon, "Scenario-based model predictive operation control of islanded microgrids," in *54th IEEE Conference on Decision and Control (CDC)*. IEEE, 2015, pp. 3272–3277.

[110] T. G. Hovgaard, L. F. S. Larsen, and J. B. Jørgensen, "Robust economic MPC for a power management scenario with uncertainties," in *2011 50th IEEE Conference on Decision and Control and European Control Conference*, Dec. 2011, pp. 1515–1520.

[111] M. Gulin, J. Matuško, and M. Vašak, "Stochastic model predictive control for optimal economic operation of a residential DC microgrid," in *2015 IEEE International Conference on Industrial Technology (ICIT)*, Mar. 2015, pp. 505–510.

[112] S. Diamond and S. Boyd, "CVXPY: A Python-embedded modeling language for convex optimization," *The Journal of Machine Learning Research*, vol. 17, pp. 2909–2913, 2016.

[113] Gurobi Optimization LLC, "Gurobi Optimizer Reference Manual," 2019. [Online]. Available: https://www.gurobi.com/

[114] N. Growe-Kuska, H. Heitsch, and W. Romisch, "Scenario reduction and scenario tree construction for power management problems," in *2003 IEEE Bologna Power Tech Conference Proceedings*, vol. 3. IEEE, 2003.

[115] V. Rostampour Samarin, "Distributed Data-Driven Decision Making in Uncertain Networked Systems with Applications in Smart Energy Systems," PhD Thesis, Delft University of Technology, 2018. [Online]. Available: http://resolver.tudelft.nl/uuid:b620d797-9e41-4ea4-8fd2-6375aab609a9

Glossary

List of Acronyms

AI	artificial intelligence
ANN	artificial neural network
CE	certainty equivalent
CPP	Critical-peak pricing
DA-RTP	Day-Ahead Real-Time pricing
DER	distributed energy resource
DEWH	domestic electric water heater
DG	distributed generation
DHW	domestic hot water
DLC	direct load control
DR	demand response
DS	distributed storage
DSM	demand side management
EMPC	economic model predictive control
EMS	energy management system
FM	fully mixed
ICT	information and communication technology
LPV	linear parameter-varying
LQG	linear-quadratic-Gaussian
MG	microgrid
MILP	mixed-integer linear program
MIQP	mixed-integer quadratic program
MLD	mixed logical dynamical
MM	min-max
MPC	model predictive control
NWP	Numerical Weather Prediction
PAR	peak-to-average ratio
PB	performance bound
PCC	point of common coupling
PID	proportional-integral-derivative
PV	photovoltaic
PWA	piecewise affine
RES	renewable energy source
RHC	receding-horizon control
RTO	real-time optimization
RTP	Real-Time pricing
SB	scenario-based
SBR	scenario-based reduced (utilizes reduced scenario horizon)

SG	smart grid	**TES**	thermal energy storage
ST	stochastic	**ToU**	Time-of-Use
STBS	stochastic bounded support	**TSRB**	thermostatic rule-based
STCC	stochastic chance-constrained	**ZOH**	zero-order hold

List of Symbols

A_{pv}	PV array surface area	$[\mathrm{m}^2]$
$A^s_{h,i}$	Surface area of the DEWH tank	$[\mathrm{m}^2]$
C_w	Thermal capacity of water	$[\mathrm{J/(kg\,K)}]$
$G_c(k)$	Incident solar irradiance acting on the PV array	$[\mathrm{W/m}^2]$
N_{SBR}	Reduced scenario horizon for SBR-EMPC	
N_h	Number of DEWHs in the MG	
N_p	MPC/EMPC prediction horizon	
N_s	Number of stochastic scenarios	
N_t	Closed-loop simulation horizon (i.e. duration of simulation)	
$P_{\mathrm{pv}}(k)$	Aggregate microgrid (MG) photovoltaic (PV) generation power	[W]
$P_{g,\mathrm{exp}}(k)$	Power exported from the utility grid	[W]
$P_{g,\mathrm{imp}}(k)$	Power imported from the utility grid.	[W]
$P_g(k)$	Power imported/exported from/to the utility grid	[W]
$P_{h,i}(k)$	Electrical input power for DEWH	[W]
$P^{\mathrm{nom}}_{h,i}$	Nominal electric power of the DEWH resistive heating element	[W]
$P_r(k)$	Aggregate residual (uncontrollable) electrical power demand in the MG	[W]
$\dot{Q}_j$	Heat flow rate attributed to component j	[W]
$T^{\mathrm{STC}}_{\mathrm{pv}}$	PV cell array reference temperature under standard test conditions	[°C]
T^c_{pv}	PV array solar cell operating temperature	[°C]
$T_{h,i}(t)$	Average water temperature in the DEWH	[°C]
$T^{\infty}_{h,i}$	Ambient temperature surrounding the DEWH	[°C]
$T^{\mathrm{nom}}_{h,i}$	Nominal DEWH tank and hot-water demand withdrawal temperature	[°C]
$T^w_{h,i}$	DEWH inlet water temperature	[°C]
$\mathcal{U}$	Feasible input constraint set	
$U_{h,i}$	Standing heat loss rate across the DEWH tank insulation	$[\mathrm{W/(m^2\,K)}]$
Ω	Disturbance set	
$\mathcal{X}$	Feasible state constraint set	
$\mathcal{Y}$	Feasible output constraint set	

α_{pv}	PV array power temperature co-efficient	
$c_{g,\text{exp}}(k)$	Price in South African Rand for exporting electric energy (profit)	[R/kWh]
$c_{g,\text{imp}}(k)$	Price in South African Rand of importing electric energy (cost)	[R/kWh]
$\delta(k)$	General MLD binary auxiliary variable/s	
$\delta_g(k)$	Grid MLD model binary auxiliary variable	
$\eta_{\text{pv}}(k)$	Conversion efficiency of the PV cell array	[%]
k	Discrete time instance	
$\mu_{h,i}(k)$	DEWH temperature constraint slack variables	[°C]
$m_{h,i}$	Total mass of water in the DEWH tank	[kg]
t_s	Discrete control system sampling time	[s]
$u(k)$	General system input/s	
$u_{h,i}(k)$	DEWH on-off binary switching input	
$\boldsymbol{\omega}_g(k)$	Stacked vector of grid device powers	[W]
$\boldsymbol{\omega}_g^{\text{con}}(k)$	Stacked vector of controllable grid device powers	[W]
$\boldsymbol{\omega}_g^{\text{exo}}(k)$	Stacked vector of exogenous uncontrollable grid device powers	[W]
$\omega(k)$	General system disturbance/s	
$\omega_{h,i}(k)$	DEWH hot water demand	[L/s]
$\omega_{h,i}^{\text{nom}}(k)$	Scaled DEWH hot water demand at nominal temperature $T_{h,i}^{\text{nom}}$	[L/s]
$x(k)$	General system state/s	
$x_{h,i}(k)$	Average water temperature in the DEWH, equivalent to $T_{h,i}(k)$	[°C]
$y(k)$	General system output/s	
$z(k)$	General MLD continous auxiliary variable/s	
$z_g(k)$	Grid MLD model continuous auxiliary variable	[W]